11-13-2013 12:00 AM

Transforming growth factor-beta receptor signalling is modulated by integrin-linked kinase

Stellar H. Boo, *The University of Western Ontario*

Supervisor: Dr. Lina Dagnino, *The University of Western Ontario*

A thesis submitted in partial fulfillment of the requirements for the Master of Science degree in Physiology

TRANSFORMING GROWTH FACTOR-BETA RECEPTOR SIGNALLING IS MODULATED BY INTEGRIN-LINKED KINASE

(Thesis format: Monograph)

by

Stellar H. Boo

Graduate Program in Physiology

A thesis submitted in partial fulfillment
of the requirements for the degree of
Master of Science

The School of Graduate and Postdoctoral Studies
The University of Western Ontario
London, Ontario, Canada

Abstract

Transforming growth factor-beta 1 (TGF-β1) modulates regeneration after injury through induction of fibroblast proliferation, migration, and differentiation into myofibroblasts. Induction of myofibroblast differentiation by TGF-β1 requires expression of integrin-linked kinase (ILK). I now show that ILK interacts with TGF-β receptor type II (TβRII) in primary dermal fibroblasts. Further, colocalization of ILK and TβRII can be observed at the cell membrane and in intracellular vesicles. The association of TβRII and ILK does not require TGF-β1 stimulation, kinase activity of TGF-β1 receptor type I or TβRII, and it does not involve interactions between ILK and focal adhesion-associated proteins. When this interaction is abolished by targeted inactivation of the *Ilk* gene, TβR signalling is diminished, as demonstrated by decreased phosphorylated SMAD2 levels in response to TGF-β1 treatment. This can be restored by exogenous expression of human ILK or by inhibition of TβRII degradatory pathway. Thus, ILK is essential for normal TβR signalling.

Keywords

Transforming growth factor-beta 1, Transforming growth factor-beta receptor signaling, SMAD, Integrin-linked kinase, Dermal fibroblast, Epidermal keratinocyte, Myofibroblast, Wound repair, Fibrosis

Co-Authorship Statement

Observations made in Figure 3. 1. have been previously identified by Linda Vi and observations made in Figure 3. 9. B has been published (Vi et al. 2011). Experiments for Appendices A, B, and C were performed with the assistance of Linda Vi, during my fourth year undergraduate thesis. All other experiments were performed by me during my graduate degree.

Acknowledgments

First, I would like to thank Dr. Lina Dagnino for her guidance during my time in her lab. I have learned A LOT since I started working in Dagnino lab as an undergraduate research student and I've gained so much research skills under her supervision. Her helpful suggestions, patience, and understanding were crucial in making my research experience pleasant.

I would also like to thank all of my committee members, Dr. John Di Guglielmo, Dr. James Hammond (former GSR), and Dr. Thomas Drysdale, for their helpful suggestions and feedback. At every committee meetings, they suggested new ideas and experiments to be done for my research, as well as constructive feedback and discussion on my data – I wouldn't be writing this if it weren't for them.

Next, I would like to thank my second family – present and former members of the Dagnino lab. I would like to thank Linda Vi for introducing me to the world of research. She had (and still has) such passion, which made me so interested in research and she motivated me to pursue a graduate degree. Thank you for your enthusiasm, wise words, and iced coffees. But I am glad there were no more midnight cell-scraping sessions after you left. I would like to thank Tames Irvine for being a big brother I've always wished I had (until I met him, of course). He put up with my whining during lengthy weekends in the lab, anger at missing reagents, and sadness at splotchy blots. He did many of my "chop-chops" for me, which was the best thing anyone could do for me and always enjoyed my baked goods. I would like to thank Randeep Singh who also helped me with "chop-chops" because she is a MACHINE. She always had helpful suggestions and feedback on my data, presentations, and thesis,

which was also the best thing anyone could do for me. I would like to thank Brad Jackson and Michelle Im for making the lab fun, since I was almost always in such a gloomy and sassy mood towards the end. I would also like to thank Ernie Ho, Samar Sayedyahossein, and Alena Rudkouskaya for great discussions and giving me the dermis of their pups. I would also like to thank members of the Di Guglielmo lab. Sarah Coyne (McLean) helped me a lot when I first started working on TGF-beta pathway and she always had cute stories of her cats and her dog. Ciric To was always so supportive and fun to talk to. Adrian Gunaratne and Eddie Chan were always so happy to lend me reagents and antibodies when our lab ran out.

And finally, I would like to thank my family for their endless support. Thank you for your love and encouragement. Words cannot describe my thanks for faith you had in me throughout my time in graduate school. Thank you.

Table of Contents

List of Tables

List of Figures

List of Abbreviations

Abbreviations	Full Name
ADAM12	Disintegrin and metalloproteinase 12
Ad-βgal	Adenovirus encoding β-galactosidase
Ad-Cre	Adenovirus encoding cre-recombinase
Ad-hILK	Adenovirus encoding human wild-type ILK
ALK5	Activin-linked kinase 5
ANOVA	Analysis of variance
α-SMA	Alpha-smooth muscle actin
βgal	β-galactosidase
CASK	Calcium/calmodulin-dependent serine protein kinase
Cav-1	Caveolin 1
DLG5	Discs large homolog 5
DMEM-RS	Dulbecco's modified Eagle's medium with reduced serum
DMSO	Dimethylsulfoxide
DTT	Dithiothreitol
ECM	Extracellular matrix
EDTA	Ethylenediaminetetraacetic acid
EGF	Epidermal growth factor
ELMO2	Engulfment and cell motility 2

EMEM	Eagle’s minimum essential medium
EMT	Epithelial-to-mesenchymal transition
FAK	Focal adhesion kinase
FBS	Fetal bovine serum
GAPDH	Glyceraldehyde 3-phosphodehydrogenase
GFP	Green fluorescent protein
GST	Glutathione S-transferase
HA	Hemagglutinin
HEK	Human embryonic kidney
HRP	Horse radish peroxidase
IgG	Immunoglobulin G
ILK	Integrin-linked kinase
IMDF	Immortalized mouse dermal fibroblasts
IP	Immunoprecipitation
kDa	Kilodalton
LAP	Latency-associated peptide
LLC	Large latent complex
LTBP	Latent TGF-β binding protein
MAPK	Mitogen-activated protein kinase
MG132	Z-Leu-Leu-Leu-al

MMP	Matrix metalloproteinase
MOI	Multiplicity of infection
PAI-1	Plasminogen activator inhibitor-1
PBS	Phosphate-buffered saline
PEI	Polyethyleneimine
PFA	Paraformaldehyde
PH	Pleckstrin homology
PINCH	Particularly interesting new cysteine-histidine rich protein
PKB	Protein kinase B
PLL	Poly-L-lysine
PMSF	Phenylmethylsulfonylfluoride
pSMAD	Phosphorylated SMAD
PVDF	Polyvinylidenefluoride
RIPA	Radioimmunoprecipation assay
SARA	SMAD anchor for receptor activation
SDS-PAGE	Sodium dodecyl sulfate polyacrylamide gel electrophoresis
SEM	Standard error of mean
SERPINE-1	Serine proteinase inhibitor 1
SLC	Small latent complex
SMAD	Mothers against decapentaplegic homolog

Smurf	SMAD ubiquitin regulatory factor
TAK-1	TGF-β-activated kinase 1
TβR	Transforming growth factor-β receptor
TBS-T	Tris-buffered saline with Tween
TBS-TM	Tris-buffered saline with Tween and skim milk
TGF-β1	Transforming growth factor-β1
Ub	Ubiquitin
WT	Wild-type

List of Appendices

Chapter 1 – Introduction

1.1 Transforming growth factor-beta

The transforming growth factor beta (TGF-β) signalling pathway is involved in myriad biological, developmental, and pathological processes. The three mammalian isoforms of TGF-β (TGF-β1, 2, and 3) are implicated in embryonic development, tumour formation, hematopoiesis, regulation of the immune response, fibrosis, and wound healing (reviewed in Prud'homme & Piccirillo 2000). At the cellular level, TGF-β regulates proliferation and differentiation of diverse cell types (reviewed in Wahl 1994). However, the functions of these three cytokine isoforms do not completely overlap *in vivo*, as gene-inactivation studies have shown (reviewed in Dünker & Krieglstein 2000).

1.1.1 Transforming growth factor-β1

Transforming growth factor-β1 is a member of the TGF-β superfamily, which is characterized by the presence of a cysteine-knot structure. TGF-β1 is secreted as an inactive homodimer, which consists of a TGF-β dimer associated with the N-terminal latency-associated peptide (LAP). This is termed small latent complex (SLC). In the SLC, TGF-β and LAP are non-covalently linked. The SLC binds to latent TGF-β binding protein (LTBP) *via* disulfide bonds, forming the large latent complex (LLC). Association with LTBP is crucial for the incorporation of TGF-β into the extracellular matrix (ECM) (Miyazono K et al. 1991). In the ECM, the LLC can be cleaved by integrin αvβ6, matrix metalloproteinases, and/or low pH levels, to form the active TGF-β1 homodimer, which

can then interact with and activate TGF-β receptors on the cell surface (Münger et al. 1999, Yu & Stamenkovic 2000, Pircher et al. 1986) (Figure 1.1).

1.2 Wound healing

The skin protects the body against harmful environmental agents and possesses an exceptional capacity for tissue and regeneration after injury. Upon cutaneous injury, TGF-β1 is released into the wound site to initiate wound healing (reviewed in Hinz 2007).

The skin is composed by two main layers: the epidermis and the dermis. The epidermis is a stratified squamous epithelium formed by keratinocytes at various stages of differentiation. The epidermis attaches to a basement membrane, which links it to the dermis. The latter is mainly composed of fibroblasts and various ECM substrates, including collagens (reviewed in Martin 1997).

When the skin is wounded, healing processes are initiated by various growth factors and cytokines. Wound healing occurs through several consecutive, but overlapping phases, which include clot formation, inflammation, regeneration, and remodelling.

Shortly after injury, a fibrin clot is formed to temporarily cover the wound. The clot is composed of fibrin fibres and platelets, which degranulate, releasing cytokines and growth factors. These cytokines and growth factors, including TGF-β1, act as chemotactic signals to attract inflammatory cells, and activate keratinocytes and fibroblasts adjacent to the wound. In this manner, re-epithelialization is initiated, which is

Figure 1. 1. TGF-β1 activation

The inactive form of TGF-β1 is in complex with latency associated peptides (LAP) to form a small latent complex (SLC) within the cell. This associates with latent TGF-β1 binding protein (LTBP) to form a large latent complex (LLC). The latent form of TGF-β1is secreted by the cell and the activation of TGF-β1 requires its release from LAP, mediated by proteases or acidic conditions (Miyazono K et al. 1991, Yu and Stamenkovic 2000, Pircher et al. 1986, Finnson et al. 2013).

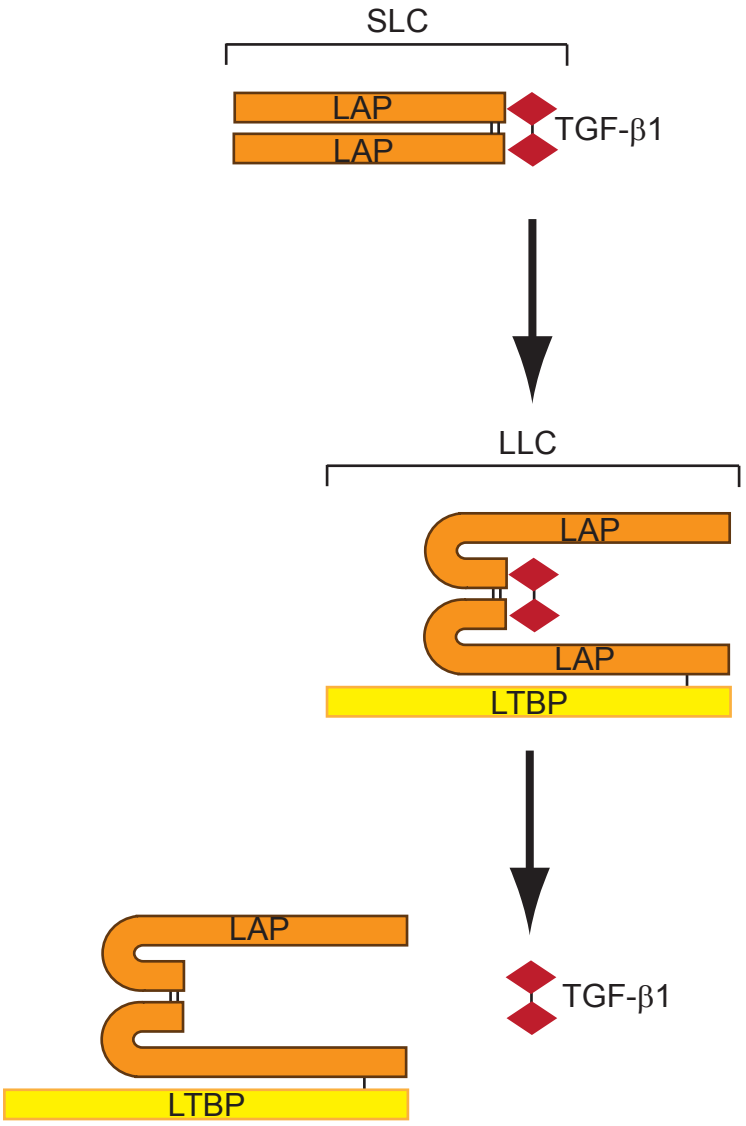
SLC
LAP
LAP
TGF-β1
LLC
LAP
LAP
LTBP
LAP
LTBP
TGF-β1

subsequently followed by tissue contraction, and angiogenesis (reviewed in Martin 1997). The second healing stage, which involves inflammatory responses, starts with the recruitment of neutrophils and monocytes to the wound site from circulating blood. These inflammatory cells clear the wound of contaminating microorganisms, and release pro-inflammatory cytokines that further activate keratinocytes and fibroblasts (reviewed in Martin 1997).

In the epidermis, keratinocytes are activated to proliferate and migrate during the re-epithelialization/regeneration phase (reviewed in Singer & Clark 1999). The existing cell-cell adhesions at the wound margins are disassembled, and new cell-ECM contacts are formed, *via* rearrangement of adhesion complexes, such as those containing integrins. This rearrangement assists migration of keratinocytes into the wound site. Once keratinocytes cover the denuded wound, re-epithelialization is complete (reviewed in Singer & Clark 1999).

Dermal fibroblasts around the wound site are also activated to proliferate and migrate into the wound. Activated fibroblasts initially become proto-myofibroblasts. These cells exhibit actin stress fibres and develop limited contractile properties in response to mechanical stimuli and inflammation (reviewed in Tomasek et al. 2002). Growth factors, such as TGF-β1, together with mechanical tension, and additional signals from the ECM, induce differentiation of proto-myofibroblasts into myofibroblasts, characterized by expression of α-smooth muscle actin (α-SMA). Myofibroblasts exhibit high contractile properties, and thus assist in wound contraction and closure (reviewed in Tomasek et al. 2002).

The last phase of healing is remodelling, during which tissue function and appearance are partially or completely restored. Keratinocytes differentiate to form a stratified epidermal layer during this phase. In the dermis, angiogenesis takes place, to form a new capillary network, and ECM is remodelled to reconstruct skin structures through the regulated synthesis and degradation of collagen (reviewed in Martin 1997).

TGF-β1 is one of many growth factors released following cutaneous injury, and it promotes production of various ECM proteins, as well as wound closure. Thus, TGF-β1 is a key modulator of tissue regeneration after wounding. This cytokine also participates in maintaining skin homeostasis (reviewed in Hinz 2007).

1.3 Transforming growth factor-β receptors

TGF-β signals are transduced by TGF-β receptors (TβR). There are three kinds of TGF-β receptors in mammals: Type I (TβRI), type II (TβRII), and type III (TβRIII) (reviewed in Shi & Massagué 2003).

TβRII is a transmembrane serine-threonine kinase, and is thought to be constitutively active (Wrana et al. 1994). TβRII can be found at the cell membrane as a monomer, homo-oligomer, or hetero-oligomer associated with TβRI (Henis et al. 1994, Rechtman et al. 2009). The formation of TβRI-TβRII complexes can occur in the presence or absence of TGF-β1 (Henis et al. 1994, Gilboa et al. 1998, Rechtman et al. 2009). However, TGF-β1 enhances the formation of tetraheteromeric species containing two TβRI and two TβRII moieties (Rechtman et al. 2009).

TβRI, also known as activin-linked kinase 5 (ALK5), is structurally similar to TβRII. However, due to its shorter extracellular domain, TβRI is unable to bind to TGF-β (Bierie & Moses 2006). TβRI can also be found at the cell membrane as a homodimer in the presence or absence of TGF-β1 (Gilboa et al. 1998, Rechtman et al. 2009).

TβRIII, also termed betaglycan, has a short intracellular domain, and does not possess any known enzymatic activity. It functions to bind to TGF-β ligands and present them to TβRII, thus modulating this signalling pathway (Lopez-Casillas et al. 1993).

1.3.1 Canonical TβR signalling

The canonical TGF-β signalling pathway involves phosphorylation and activation of SMAD transcription factors (Miyazono et al. 2000). Canonical TβR signalling begins when ligand-bound TβRII transphosphorylates and activates TβRI. Active TβRI then phosphorylates the receptor-regulated SMAD transcription factors (SMAD2 and/or SMAD3). Once SMAD2 and SMAD3 are phosphorylated, they are able to recruit SMAD4, a common-mediator SMAD. The SMAD2/4 and/or SMAD3/4 complexes translocate into the nucleus, where they interact with other transcription factors and transcriptional regulators to increase transcription of target genes. These target genes include those involved in ECM remodelling, cytoskeleton organization, and acquisition of a contractile phenotype, such as α-SMA (reviewed in Hinz 2007). These events are crucial for myofibroblast differentiation and wound contraction (Figure 1.2).

Figure 1. 2. The canonical TGF-β1 signalling pathway

The canonical TGF-β1 signalling pathway starts with ligand binding to TβRII, which recruits and activates TβRI. Activated TβRI in the TβRI-TβRII complex phosphorylates SMAD2/3, resulting in recruitment of SMAD4 and formation of SMAD2/4 and SMAD3/4 complexes. The SMAD complexes translocate to the nucleus and cause changes in gene transcription, such as increases in α-smooth muscle actin (α-SMA) in dermal fibroblasts (reviewed in Hinz 2007).

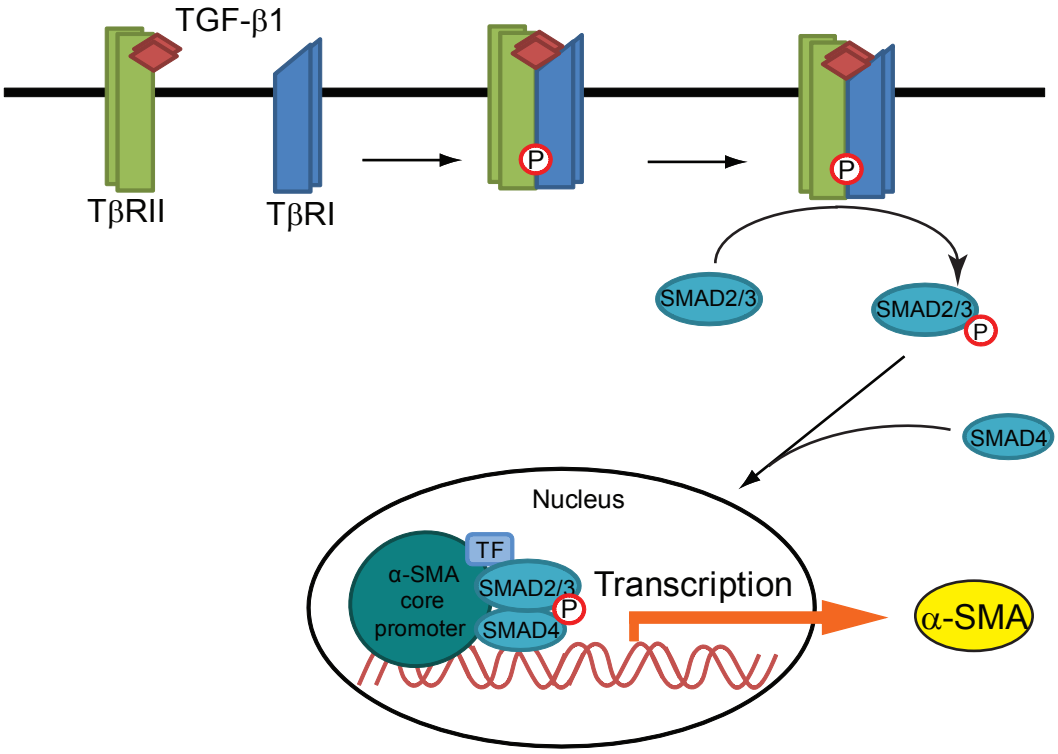
TGF-β1
TβRII
TβRI
P
P
SMAD2/3
SMAD2/3
P
SMAD4
Nucleus
TF
α-SMA
core
promoter
SMAD2/3
P
SMAD4
Transcription
α-SMA

1.3.2 Non-canonical TβR signalling

In addition to SMAD-mediated signalling, TGF-β also activates several non-canonical pathways. For example, TGF-β1 can activate Ras, Raf, and the mitogen-activated protein kinase (MAPK) downstream cascades, resulting in ERK stimulation. Activated ERK can regulate the transcription of many genes, such as type I collagen in fibroblasts (Mucsi et al. 1996). TGF-β1 can also activate the JNK/p38 MAPK pathway, through TGF-β-activated kinase 1(TAK-1) stimulation (Edlund et al. 2003), leading to epithelial-to-mesenchymal transition (EMT) and apoptosis in epithelial cells (Yu et al. 2002).

1.3.3 TGF-β receptor endocytosis

Following ligand binding, TβRI-TβRII complexes are internalized mainly *via* caveolae- or clathrin-mediated endocytosis (Di Guglielmo et al. 2003) (Figure 1.3).

Caveolae-mediated endocytosis requires formation of lipid rafts (Simons & Toomre 2000). Lipid rafts are microdomains of the plasma membrane rich in cholesterol (Simons & Toomre 2000). Internalization of TβRs through lipid raft/caveolin-positive vesicles results in the recruitment of inhibitory SMAD7 and of the SMAD ubiquitin regulatory factor Smurf. This recruitment, in turn, leads to ubiquitination of the receptor complex and its subsequent degradation by proteasomes and/or lysosomes (Kavsak et al. 2000, Di Guglielmo et al. 2003, Le Roy & Wrana 2005).

In contrast, internalization of TGF-β receptor complexes *via* clathrin-coated pits forms early endosome antigen 1 (EEA-1)-positive vesicles. These vesicles become early

endosomes and contain complexes composed of SMAD2 and/or SMAD3 associated with another protein termed SMAD anchor for receptor activation (SARA) (Tsukazaki et al. 1998). In the early endosomes, TβR complexes are sorted and subsequently directed to recycling endosomes. This process also results in amplification of TβR signalling (Runyan et al. 2005). As a next step, TβR complexes can recycle to the cell membrane or be targeted to late endosomes, and then to lysosomes, where they are degraded (Le Roy & Wrana 2005) (Figure 1.3).

1.4 TβR signalling and skin regeneration

TGF-β1 inhibits proliferation and DNA synthesis in epidermal keratinocytes (Matsumoto et al. 1990). However, it also induces expression of integrins necessary for keratinocyte migration and re-epithelialization (Gailit et al. 1994).

In the wounded dermis, TGF-β1 triggers fibroblast proliferation and subsequent migration into the site of injury (reviewed in Hinz 2007). TGF-β1 is also necessary to initiate the production of a collagen-rich matrix and it induces differentiation of fibroblasts into myofibroblasts (Desmoulière et al. 1993, reviewed in Desmoulière et al. 2005, Hinz 2007). If TGF-β1 signalling in mouse fibroblasts is abolished *via* inactivation of the gene that encodes TβRII, abnormal wound healing is observed. Specifically, decreased dermal contraction and increased rates of re-epithelialization occur under these conditions (Martinez-Ferrer et al. 2010).

Figure 1. 3. TβR complex internalization via caveolin and clathrin

Complexes containing TGF-β and TβRs can be internalized via clathrin-dependent or caveolin-dependent endocytosis. TβR complexes internalized via lipid-rafts/caveolae are ubiquitinated and targeted for proteasomal or lysosomal degradation. TβR degradation can be inhibited using MG132, a proteasomal inhibitor, or nystatin, a cholesterol sequestering agent that inhibits formation of lipid-rafts. TβR complexes endocytosed via clathrin-dependent mechanisms are able to transduce further downstream signalling, and can be recycled back to the cell membrane, or degraded by the lysosomes (Di Guglielmo et al. 2003).

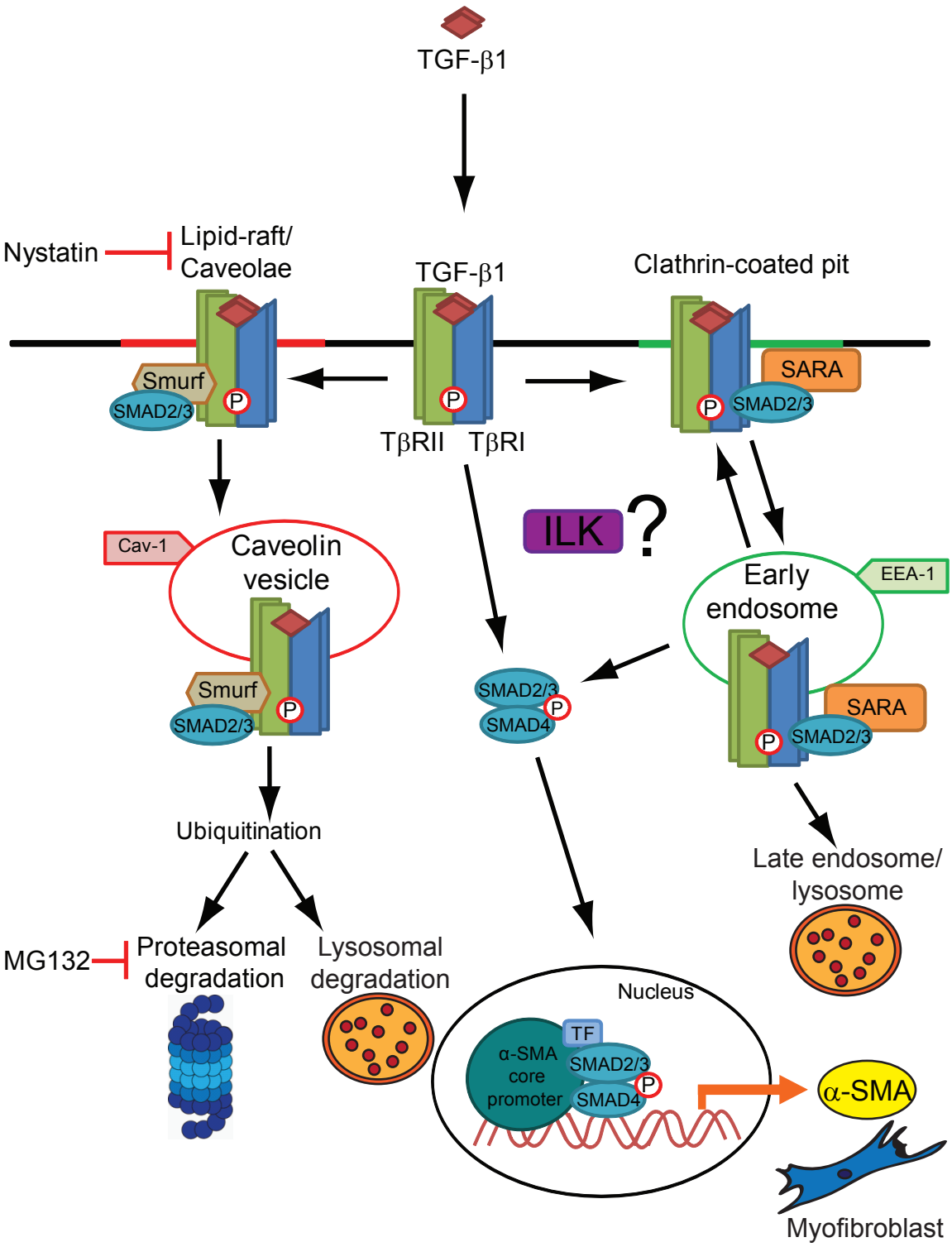
TGF-β1
Nystatin
Lipid-raft/
Caveolae
TGF-β1
Clathrin-coated pit
Smurf
SMAD2/3
P
TβRII
TβRI
SARA
SMAD2/3
ILK
?
Cav-1
Caveolin
vesicle
Smurf
SMAD2/3
Early
endosome
EEA-1
SMAD2/3
SMAD4
SARA
SMAD2/3
Ubiquitination
Late endosome/
lysosome
MG132
Proteasomal
degradation
Lysosomal
degradation
Nucleus
α-SMA
core
promoter
TF
SMAD2/3
SMAD4
α-SMA
Myofibroblast

1.4.1 SMAD proteins in skin homeostasis

Several mouse models using targeted gene inactivation or overexpression have been generated to determine the contribution of SMAD proteins to skin function (reviewed in Flanders 2004).

For example, epidermis-restricted overexpression of SMAD2 in transgenic mice results in increased expression of SMAD4 and TGF-β1. These mutant mice display skin thickening, sparse hair, and abnormal pinna formation, due to the presence of hypertrophic cartilage, demonstrating the importance of proper regulation of SMAD2 levels during development (Ito et al. 2001). *Smad2* gene inactivation results in embryonic lethality in mice, due to impaired mesoderm formation, gastrulation, and establishment of the anterior-posterior axis (reviewed in Flanders 2004). In contrast, *Smad3* gene inactivation produced mice which exhibited degenerative joint disease and chronic infections, due to defects in the immune system (Yang et al. 1999, Yang et al. 2001). Interestingly, SMAD3-deficient mice showed accelerated cutaneous wound healing, due to more rapid re-epithelialization and reduced accumulation of ECM in granulation tissue (Ashcroft et al. 1999).

SMAD4 is the only common-mediator SMAD, and inactivation of the gene that encodes this protein leads to embryonic lethality due to abnormal gastrulation and endoderm formation (Sirard et al. 1998). Keratinocyte-specific *Smad4* gene inactivation in mice, using a Cre-LoxP approach, showed increased basal keratinocyte proliferation, accompanied with increased levels of Akt phosphorylation and accelerated re-

epithelization after wounding. In these animals, epidermal hyperplasia and spontaneous formation of skin tumours after wound repair was also reported (Yang et al. 2012, Yang et al. 2005, Qiao et al. 2006). Furthermore, these mice also showed progressive hair loss due to impaired hair follicle cycling (Yang et al. 2005, Qiao et al. 2006).

In vitro experiments have shown that there are two sets of TGF-β target genes: SMAD4-dependent (e.g. *SERPINE1*, also known as *PAI*-1) and SMAD4-independent (e.g. *SMAD7*) (Levy & Hill 2005). Loss of SMAD4 expression in HaCaT cells, a spontaneously-immortalized human keratinocyte cell line, resulted in attenuation of TGF-β1-induced cell cycle arrest and migration. In contrast, loss of SMAD4 expression in the pancreatic tumour cell line Colo-357 still led to EMT, as evidenced by the upregulation of the mesenchymal marker vimentin (Levy & Hill 2005). Thus, loss of SMAD4 expression may promote tumourigenesis by attenuation of TGF-β1-induced inhibition of keratinocyte proliferation without impairment of other responses to TGF-β1 involved in tumour progression, such as EMT (Levy & Hill 2005).

Although SMAD2, 3, and 4 are constitutively expressed in the epidermis, the level of the inhibitory SMAD7 is generally low, and it increases with TGF-β1 treatment (He et al. 2001). Keratinocyte-restricted over-expression of SMAD7 in transgenic mice resulted in keratinocyte proliferation, tumour progression, aberrant hair follicle morphogenesis, and defects in the corneal epithelium (He et al. 2002).

Few studies have examined the effects of overexpression or gene inactivation of different SMAD proteins on the dermis. Overexpression of SMAD3 in fibroblasts enhances collagen gel contraction (an *in vitro* assay that mimics wound contraction) (Sumiyoshi et

al. 2003). Conversely, SMAD3-deficient mouse embryonic fibroblasts show diminished capacity for collagen gel contraction, indicating that wound contraction may be positively modulated by SMAD3 (Liu et al. 2003). SMAD3 deficiency also results in reduced fibrosis and decreased collagen deposition, due to reduced TGF-β autoinduction by inflammatory cells and reduced fibroblast recruitment to the wound site (Flanders et al. 2002). Regenerated dermis from mice with *Smad3* gene inactivation contained less myofibroblasts and scar tissue than that from normal mice, under conditions in which fibrosis was induced by radiation (Flanders et al. 2002). These observations signify that SMAD3 fulfills important pro-fibrotic functions in the skin.

1.4.2 Pathological consequences associated with aberrant TβR signalling

A large body of work has now established that insufficient or excessive TβR signalling is associated, respectively, with abnormal wound healing and numerous fibrotic conditions, including hypertrophic scarring and keloid formation in the skin (Tuan & Nichter 1998, Tredget 1999). For example, rats that were subcutaneously implanted with osmotic minipumps filled with TGF-β1 developed granulation tissue with abundant myofibroblasts after wounding, suggesting that TGF-β1 may play a role in scarring through the prolonged activation of these cells (Desmoulière et al. 1993). In keloid fibroblasts, high levels of TGF-β production, increased TβRI and TβRII expression, and elevated levels of phosphorylated SMAD3 are observed, indicating that increased TGF-β signalling is associated with formation of keloids and fibrosis (Chin et al. 2000). Keloid fibroblasts also display decreased mRNA levels of inhibitory SMADs, compared to

fibroblasts from non-fibrotic scars or from normal skin. In keloid fibroblasts, the low transcription and protein levels of inhibitory SMAD, may prolong or augment TGF-β signalling, contributing to the formation of excessive scarring through over-production of ECM (Yu et al. 2006).

TGF-β signalling is necessary, but not sufficient, for the induction of myofibroblast differentiation (reviewed in Hinz 2010). Myofibroblast differentiation also requires mechanotransduction, that is, transduction of mechanical signals from the ECM into intracellular signals (reviewed in Hinz 2010) (Figure 1.4). Mechanical stimuli are transduced by integrins (reviewed in Hinz 2010) (Figure 1.5). In the context of the dermis, integrins play a role in myofibroblast differentiation by mediating the transition of fibroblasts to proto-myofibroblasts containing stress fibres, which subsequently differentiate into myofibroblasts with additional mechanical stress and with TGF-β1 stimulation (reviewed in Hinz 2010).

1.5 Integrins

Integrins are a major class of cell surface proteins that participate in cell-cell and cell-ECM communication (reviewed in Hinz 2010). There are 18 α and 8 β subunits known in mammalian cells, which form 24 different heterodimers composed of one α and one β subunit. The α subunit in each αβ dimer determines ligand-binding affinities (reviewed in Margadant et al. 2010).

In intact epidermis, the most abundant integrins are α2β1, α3β1, and α6β4 (reviewed in Watt 2002). The expression of these integrins is confined to basal keratinocytes. Integrins

Figure 1. 4. Myofibroblast differentiation

Dermal and other fibroblasts are induced to differentiate into proto-myofibroblasts by mechanical stimuli. Proto-myofibroblasts contain stress fibres but does not express α-smooth muscle actin (α-SMA). With added stimulation by TGF-β1, proto-myofibroblasts differentiate into contractile myofibroblasts, which express α-SMA and aid in closure of the wound (reviewed in Hinz 2010).

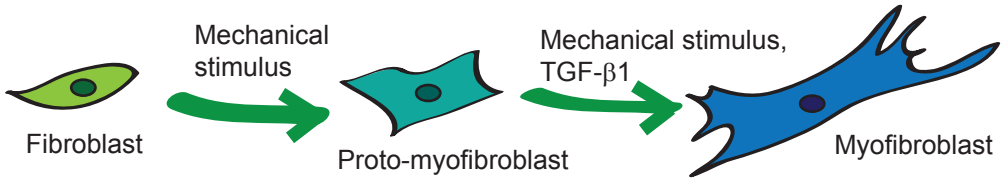
Mechanical
stimulus
Mechanical stimulus,
TGF-β1
Fibroblast
Proto-myofibroblast
Myofibroblast

Figure 1. 5. Integrin-mediated mechanotransduction

Heterodimeric integrins at focal adhesions transduce ECM signals into intracellular signals. ILK has been shown to colocalize to the focal adhesions and interact with various proteins (reviewed in Wickström et al. 2010a). Integrin mediated signal transduction and TGF β1 stimulation are both required for myofibroblast differentiation.

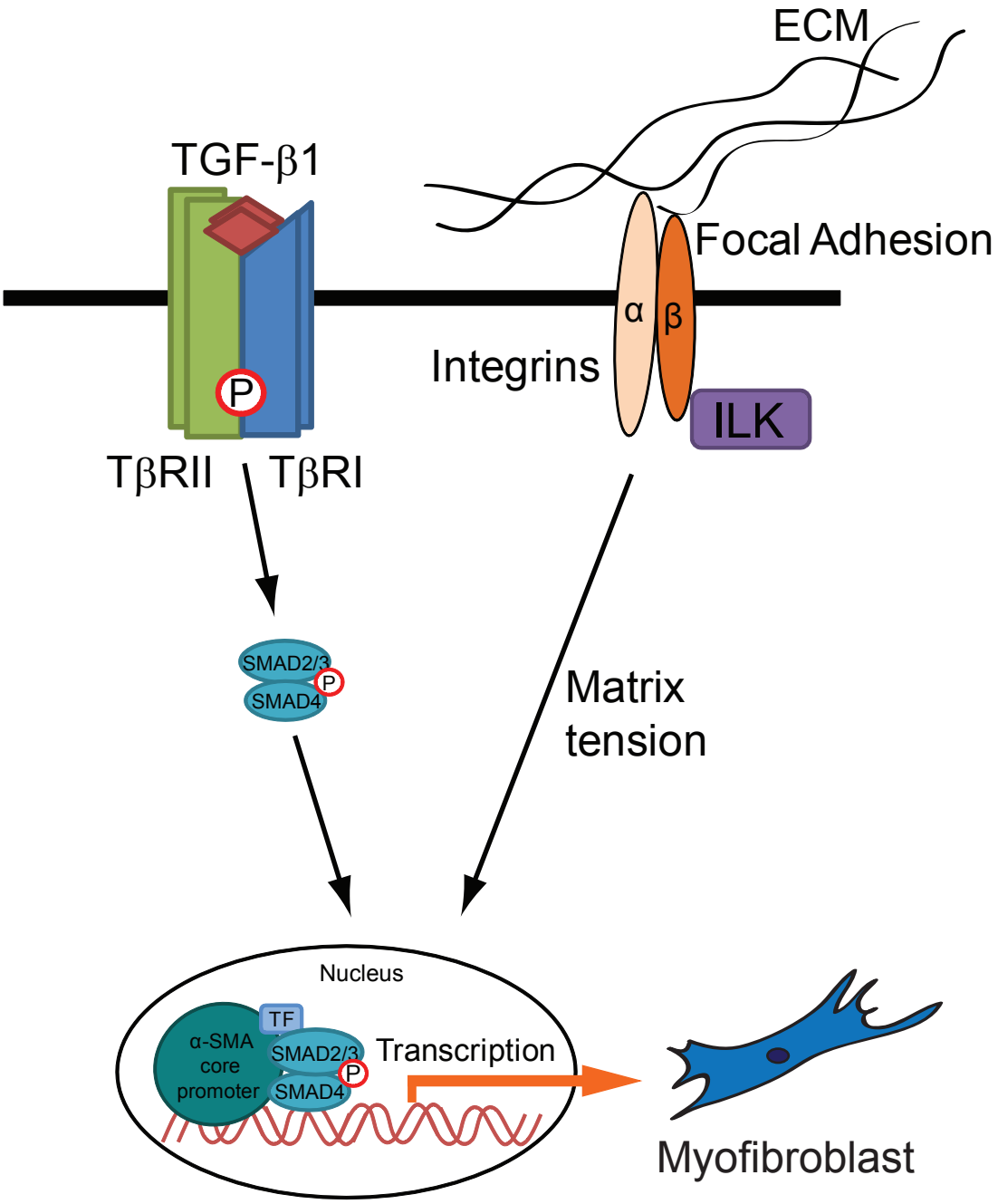
ECM
TGF-β1
Focal Adhesion
α
β
Integrins
ILK
P
TβRII
TβRI
SMAD2/3
P
SMAD4
Matrix
tension
Nucleus
TF
α-SMA
core
promoter
SMAD2/3
P
SMAD4
Transcription
Myofibroblast

mediate attachment of these cells to the underlying basement membrane (reviewed in Watt 2002). Integrins are down-regulated in the differentiated keratinocytes of the suprabasal layers, and are up-regulated in motile keratinocytes at wound sites or in several skin disorders, including psoriasis and carcinomas (reviewed in Margadant et al. 2010). In epidermal keratinocytes, integrins promote focal adhesion kinase (FAK) signalling and Rac1 activation, leading to keratinocyte spreading, polarization, and subsequent migration into the wound (Choma et al. 2007). Keratinocyte-restricted inactivation of the *Itgb1* gene, which encodes for integrin β1, results in abnormal hair follicle morphogenesis and severe blistering due to abnormal basement membrane assembly (Brakebusch et al. 2000, Raghavan et al. 2000), as well as delays in keratinocyte migration to wound sites (Grose et al. 2002). In addition, epidermis-restricted β1 integrin gene inactivation results in perinatal death due to abnormal epidermal barrier formation, leading to dehydration (Raghavan et al. 2000).

Integrins α1β1, α2β1, and α5β1 are expressed in dermal fibroblasts (reviewed in Silver et al. 2003). Myofibroblasts express those same integrins, in addition to αvβ5, αvβ3, and αvβ8. The latter three integrin contribute to latent TGF-β1 activation by binding to LAP and causing a conformational change when mechanical stimuli are applied by ECM stretch or cell contraction (reviewed in Hinz 2010). Integrins play important roles in focal adhesion formation, signal transduction, cell adhesion, and migration. The majority of integrin complexes link the ECM to the actin cytoskeleton, thus transducing mechanical stimuli (Geiger et al. 2009).

Integrin β1 can also play a role in activation of latent TGF-β (Liu et al. 2010). For example, in mink lung epithelial cells co-cultured with integrin β1-expressing fibroblasts, the plasminogen activator inhibitor-1 (PAI-1) promoter activity is activated (Liu et al. 2010). PAI-1 is a TGF-β target gene. Conversely, integrin-β1-deficient fibroblasts were unable to induce PAI-1 promoter activation in those cells (Liu et al. 2010). Loss of β1 integrin expression reduces myofibroblast formation and fibroblast proliferation, adhesion and spreading on ECM (Liu et al. 2010). Fibroblast-restricted *Itgb1* gene inactivation leads to poor wound healing due in part, to poor α-SMA stress fibre formation and impaired myofibroblast differentiation (Liu et al .2010). Integrin β1 is also required for normal Rac1 activation and generation of reactive oxygen species in dermal fibroblasts, which are important for the production of type I collagen and α-SMA (Liu & Leask 2013, Liu et al. 2009). Other integrin heterodimers, including α11β1, αvβ1, αvβ3, αvβ5, αvβ6, αvβ8, α8β1, α5β1, and α3β1 have been shown to play a role in TGF-β1 signalling during myofibroblast differentiation (Carraceodo et al. 2010, reviewed in Margadant & Sonnenberg 2010).

1.6 Interactions between integrins and TGF-β1

Given that integrins and TGF-β are required for myofibroblast differentiation, it is not surprising that a crosstalk exists between these two pathways. Many studies have shown that integrins modulate the TGF-β pathway and, reciprocally, that TGF-β can modulate expression and activation of integrins and integrin-associated proteins (reviewed in Margadant & Sonnenberg 2010).

The LAPs of inactive TGF-β1 complexes contain arginine-glycine-aspartic acid (RGD) sequences that are bound by integrin β1 (Münger et al. 1998). Integrin αvβ1 recognizes and binds to this sequence, which suggests a potential role for integrin αvβ1 in modulating the localization of TGF-β1 at the cell surface (Münger et al. 1998). Other studies have shown a significant role for integrin complexes in the modulation of TGF-β1 activation and, indirectly, by regulating the expression of TβRI, TβRII, and SMAD7 (reviewed in Margadant & Sonnenberg 2010). For example, integrin α3-deficient mice show increased SMAD7 expression, along with decreased pSMAD2 levels and delayed re-epithelialization, indicating that integrin α3 plays an important role in regulating TβR signalling (Reynolds et al. 2008).

Integrin αvβ6 expression increases in epidermal keratinocytes at wound edges (Breuss et al. 1995). Integrins αvβ6 and αvβ8 bind to latent TGF-β1, by interacting with LAP, and they also activate TGF-β1 in lung epithelial cells (Münger et al. 1999, Mu et al. 2002). When the RGD amino acid sequence in LAP is mutated to RGE, integrins αvβ6 and αvβ8 cannot bind to the latent form of this mutant TGF-β1, resulting in attenuated integrin-mediated TGF-β1 activation. Mice that express this mutant exhibit phenotypes similar to those of TGF-β1-null mice (Yang et al. 2007).

Interestingly, although integrin β3-null mice show decreased keratinocyte proliferation, they also exhibit enhanced wound healing rates because of enhanced infiltration of dermal fibroblasts into the wound site (Reynolds et al. 2005). Elevated levels of TGF-β1, TβRI and TβRII are observed in integrin β3-null mice, resulting in enhanced TGF-β1 signalling and wound closure rates. This finding suggests that TGF-β1 signalling is

suppressed by αvβ3 integrins. Finally, induction of suprabasal epidermal expression of integrin α6β4, which is normally localized to basal keratinocytes, also results in aberrant TGF-β1 signalling, leading to abrogation of TGF-β-mediated growth inhibition (Owens et al. 2003).

TGF-β can modulate the expression of various types of integrins. For example, TGF-β1 stimulation in epidermal keratinocytes leads to increased expressions of α5β1, αvβ4, and α2β1 integrins, decreased expression of α3β1 integrin, and de novo expression of αvβ6 integrin, all of which are similar to integrin expression patterns at the wound edge (Zambruno et al. 1995).

In fibroblasts, integrin αvβ5 has been shown to promote myofibroblast differentiation by stimulating TGF-β1 autocrine signalling (Asano et al. 2006a, b). Fibroblast-restricted loss of integrin β1 also leads to reduced activation of TGF-β1, resulting in delayed wound healing (Liu et al. 2010). This evidence shows that under abnormal skin conditions, including wounded skin, integrin expression is altered, leading to changes in TGF-β signalling. Consistent with this concept, pharmacological inhibition of TGF-β1 signalling in mouse embryo fibroblasts interfered with α11 integrin up-regulation in response to mechanical strain (Carracedo et al. 2010). These observations suggest that, without TGF-β1 signalling, mechanical stimuli cannot be properly transduced. In addition, fibroblast-specific inactivation of the *Tgfbr2* gene resulted in reduced levels of α1, α2, and β1 integrins (Martinez-Ferrer et al. 2010).

1.7 Integrin-linked kinase (ILK)

Integrins do not have catalytic activity and signals generated by their activation are transduced by various proteins that bind to their cytoplasmic domains. These proteins include FAK and integrin-linked kinase (ILK) (reviewed in Margadant et al. 2010).

Integrin-linked kinase was first described as a serine-threonine kinase, which binds directly to β1 integrins to transduce ECM signals (Hannigan et al. 1996). It is a ubiquitous pseudokinase with scaffolding properties and an apparent molecular weight of 51 kDa (Fukuda et al. 2011). ILK contains three main domains: five N-terminal ankyrin repeats, a pleckstrin-homology-like domain, and a C-terminal kinase-like domain (Figure 1.6) (Chiswell et al. 2008).

The ankyrin repeat region is responsible for its interaction with Particularly Interesting New Cysteine-Histidine protein (PINCH) (Tu et al. 1999, Chiswell et al. 2008). The central region resembles a pleckstrin-homology domain, based on its amino acid sequence, but is unable to bind phosphatidylinositol 3,4,5-trisphosphate (Fukuda et al. 2009). The kinase-like domain at the C-terminus interacts with paxillin and α-, β-, and γ-parvins (reviewed in Qin & Wu 2012). The interaction between ILK and α-parvin occurs at focal adhesions, and regulates cell adhesion and actin cytoskeleton organization (Tu et al. 2001). ILK colocalizes with β-parvin, also known as affixin, at focal adhesions, and they regulate cell adhesion (Yamaji et al. 2001). Lastly, γ-parvins, which are expressed in hematopoietic cell types, interact with ILK, although the biological significance of this interaction is still unclear (Chu et al. 2006).

Figure 1. 6. ILK protein domains

ILK has 452 amino acids and three distinct domains, based on sequence homology. The first N-terminal 174 amino acids include 5 ankyrin repeats. Amino acid residues 180-212 form a pleckstrin homology-like domain (PH), and amino acid residuces 193-447 exhibit some homology to protein kinases (Chiswell et al. 2008).

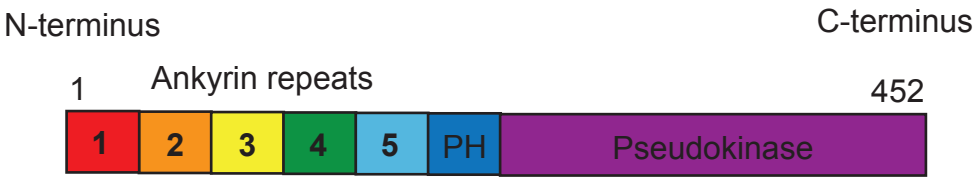
N-terminus
C-terminus
1
Ankyrin repeats
452
1
2
3
4
5
PH
Pseudokinase

1.7.1 ILK as a pseudokinase

There are numerous reports providing evidence for and against the idea that ILK possesses kinase activity.

The amino acid sequence of ILK shows a fairly large degree of homology to serine/threonine kinases. The kinase domain of ILK possesses ATP-binding lysine residue and an APE motif, which are conserved residues in other serine-threonine kinases. Mutation of the ATP-binding lysine has been associated with decreased enzymatic activity (Maydan et al. 2010). Although ILK lacks other motifs conserved in kinases, such as DFG and HRD motifs, not all kinases possess them. For example, calcium/calmodulin-dependent serine protein kinase (CASK) lacks the canonical DFG motif, which is indispensable for kinase function, as it is required for Mg^{2+} binding, and yet CASK can phosphorylate its substrates without Mg^{2+} (Mukherjee et al. 2008). Haspin, another protein kinase, also lacks in DFG and APE motifs, but is still catalytically functional (Eswaran et al. 2009).

It has been reported that ILK can phosphorylate myelin basic protein, and the cytoplasmic domain of β1 integrin (Hannigan et al. 1996), β-parvin (affixin) (Yamaji et al. 2001), 17 kDa protein kinase C-dependent phosphatase inhibitor, and phosphatase homoenzyme inhibitor-1 *in vitro* (Deng et al. 2002). In addition, purified ILK was reported to directly phosphorylate protein kinase B (PKB/Akt) (Persad et al. 2001). A point mutant ILK E359K showed suppressed kinase activity in some, but not other studies (Persad et al. 2001).

More recently, a thorough study was conducted to determine whether ILK is a *bona fide* kinase (Maydan et al. 2010). In this study, highly purified recombinant glutathione S-transferase (GST)-ILK was reportedly isolated and purified from insect cells with no detectable contaminating kinases, as shown by mass spectrometric analysis. The purified GST-ILK showed autophosphorylation and phosphorylation of the 20-kDa regulatory myosin light chain, as well as glycogen synthase kinase-3 peptide in a Mn^{2+}-dependent manner, with phosphorylation kinetics reportedly comparable to other kinases (Maydan et al. 2010). In this study, no data on Akt phosphorylation were included. Together, all these observations have led several groups to propose that ILK is a *bona fide* serine-threonine kinase.

On the other hand, ILK lacks many key motifs that are conserved in other kinases. There are three conserved motifs: a VAIK motif to orient ATP in the ATP-binding pocket, an HRD motif for proton transfer, and a DFG motif to bind Mg^{2+} and for alignment of β- and γ-phosphates of ATP in the ATP-binding pocket (Boudeau et al. 2006). ILK does not possess DFG and HRD motifs, and although ILK binds to ATP, it cannot hydrolyze it to ADP, since the putative catalytic loop of ILK is distant from the bound ATP (Fukuda et al. 2009).

Other *in vitro* studies have shown that purified recombinant ILK is unable to phosphorylate previously identified substrates, including myelin basic protein and cytoplasmic tail of β integrin (Fukuda et al. 2009). It has also been shown that ILK deficiency or expression of mutant ILK lacking its "kinase" activity (ILK E359K) has negligible effects on phosphorylation of its proposed substrates, such as PKB/Akt and

GSK-3β in many cell types. For example, ILK-deficient immortalized kidney fibroblasts show lack of cell spreading, focal adhesion formation, and stress fibre formation, which can be restored by ILK E359K (Sakai et al. 2003), suggesting that the "kinase" activity of ILK either does not exist, or that it is dispensable. These cells also show comparable levels of PKB/Akt and GSK-3β phosphorylation to those observed in ILK-expressing cells (Sakai et al. 2003). Similarly, ILK-deficient chondrocytes show defects in cell adhesion, spreading, focal adhesions, and stress fibre formation, indicative of its role in actin organization. In these cells, PKB/Akt and GSK-3β phosphorylation was unaffected (Grashoff et al. 2003). *In vitro* kinase assays using ILK E359K immunoprecipitates from HeLa cells show comparable kinase activity to those of wild-type ILK immunoprecipitates (Nikolopoulos & Turner 2002).

In vivo experiments have also shown that an intact "kinase" domain in ILK is dispensable for normal function. In *Drosophila melanogaster*, embryos that expressed ILK E359K showed similar phenotypes to those that expressed wild-type ILK. In this system, human ILK E359K rescued embryonic lethality caused by the lack of functional endogenous ILK (Zervas et al. 2001). In *Caenorhabditis elegans*, abnormal muscle assembly in the absence of ILK was restored by introduction of human ILK E359K, indicative of the dispensable "kinase" activity of ILK *in vivo* (Mackinnon et al. 2002).

In a very elegant study, Lange et al. generated several knock-in mouse strains with point mutations in the *Ilk* gene that had previously been reported to affect kinase activity *in vitro* (Lange et al. 2009). Mice expressing ILK S343A, previously shown by other groups to lack kinase activity in *in vitro* kinase assays, or ILK S343D, shown to exhibit

hyperactive kinase function, displayed a normal phenotype. This indicates that the proposed kinase activity of ILK observed in *in vitro* studies is not required for normal development (Lange et al. 2009). Epidermal keratinocytes from these mice showed normal adhesion, spreading, actin cytoskeleton formation, and focal adhesion formation (Lange et al. 2009). In addition, phosphorylation of previously identified substrates of ILK – Akt1 and Gsk3β – was not affected *in vivo* by expression of these ILK mutants (Lange et al. 2009). Mice expressing other ILK mutants previously reported to lack kinase activity, including ILK K220A or ILK K220M, displayed normal skin phenotypes and phosphorylation of Akt1 and Gsk3β, contrary to previous reports (Lange et al. 2009). These observations are consistent with the notion that ILK is a pseudokinase.

1.7.2 ILK as a scaffold protein

ILK fulfills important biological functions through its scaffolding properties. For example, mutation of E359 to K abrogates the interaction between ILK and α-parvin or paxillin. This ILK mutant cannot localize to focal adhesions and interferes with cell adhesion and migration (Wu & Dedhar 2001, Nikolopoulos & Turner 2002). Knock-in mice expressing ILK K220A exhibited renal agenesis, similar to that observed in α-parvin-deficient mice (Lange et al. 2009). Upon further examination of ILK K220A, it was discovered that the interaction between ILK K220A and α-parvin was significantly decreased relative to wild-type ILK, which likely caused severe impairment in kidney development (Lange et al. 2009). Others have also shown that ILK K220M causes impaired kidney development owing to its disrupted structural integrity (Fukuda et al. 2011). ILK also functions as an adaptor protein in complexes with PINCH and parvin at

focal adhesions, to transduce ECM signals (Tu et al. 1999, reviewed in Wickström et al. 2010a).

1.7.3 ILK and its role in the skin

Integrin-linked kinase plays a role in cell growth, differentiation, motility, and attachment (reviewed in McDonald et al. 2008). As a scaffold, ILK serves as a linker between integrins and the actin cytoskeleton (Wu & Dedhar 2001; Blumbach et al. 2010). ILK expression is essential during embryogenesis, as ILK-null embryos fail to implant, due to impaired actin cytoskeleton organization and polarization (Sakai et al. 2003). Additionally, ILK modulates front-rear cell polarity, adhesion and migration of epidermal keratinocyte, and it is required for hair follicle morphogenesis (Lorenz et al. 2007, Nakrieko et al. 2008a). ILK forms a complex with engulfment and cell motility 2 (ELMO2) and RhoG, and this complex mediates EGF-induced keratinocyte polarization (Ho et al. 2009, Ho & Dagnino 2012). ILK-deficient keratinocytes also display reduced levels of active Rac1 when stimulated to migrate, which is crucial for the formation of a leading edge in motile cells (Nakrieko et al. 2008a). This underlines the importance of ILK in wound healing. Mice with targeted inactivation of the *Ilk* gene in the epidermis have fragile skin, blisters, abnormal hair follicles, and epidermal detachment from the basement membrane (Nakrieko et al. 2008a, Lorenz et al. 2007). Targeted *Ilk* gene inactivation in keratin-15-expressing keratinocyte hair follicle stem cells resulted in altered wound healing, due to delayed re-epithelialization (Nakrieko et al. 2011). Fibroblast-restricted *Ilk* gene inactivation leads to decreased myofibroblast differentiation

in vitro and *in vivo*, and number of myofibroblasts at the wound site *in vivo*, ultimately resulting in reduced wound closure rates (Blumbach et al. 2010, Vi et al. 2011).

1.8 Rationale and hypothesis

Our laboratory has previously demonstrated that ILK is abundant throughout the dermis (Nakrieko et al. 2008a) and is required for normal TGF-β1-induced dermal myofibroblast differentiation in culture (Vi et al. 2011). ILK-deficient dermal fibroblasts display decreased α-SMA expression and SMAD2 phosphorylation in response to TGF-β1 stimulation (Vi et al. 2011). These observations suggest a key modulatory role for ILK in TβR signalling and for proper wound healing. Moreover, dermis-restricted *Ilk* gene inactivation in mice results in abnormal healing of full-thickness wounds due to reduced levels of TGF-β1, impaired myofibroblast differentiation, and reduced number of myofibroblasts in the wound (Blumbach et al. 2010). ILK-deficient fibroblasts also show impaired cell migration due in part, to increased activity of RhoA, which is associated with cell contractility, and accompanying decrease in active Rac1 (Vi et al. 2011, Blumbach et al. 2010). In addition, ILK interacts with various proteins for mediating signal transduction and it possesses multiple protein-protein interaction domains.

The above observations led me to hypothesize that ILK interacts with TβRII and promotes TβR signalling. To test this hypothesis, my specific objectives were:

1. To investigate if ILK and TβRII associate in protein complexes.

2. To determine if ILK modulates signalling and /or turnover of TβR.

Chapter 2 – Materials and Methods

2.1 Reagents and materials

Reagents and their sources are as follows:

Table 1: Reagents and materials

Reagents and materials	Source	Catalogue number
HyQ-Dulbecco's Modified Eagle Medium-Reduced Serum (HyQ-DMEM-RS)	Hyclone/Thermo Scientific, Logan, UT	SH3056501
Fetal bovine serum (FBS)	Gibco, Burlington, ON	12483
0.25% trypsin with ethylenediaminetetraacetic acid (EDTA)	Gibco, Burlington, ON	25200-056
Ca^{2+}-free Eagle's minimum essential medium (EMEM)	Lonza, Walkersville, MD	06-174G
FBS for keratinocytes	Lonza, Walkersville, MD	14-561F
Chelex 100 chelating resin (sodium form, 200–400 dry mesh size)	Bio-Rad, Mississauga, ON	142-2842
Penicillin and streptomycin solution (10000 U/ml penicillin and 10000 μg/ml streptomycin)	Gibco, Burlington, ON	15140
Hydrocortisone	Sigma, St. Louis, MO	H4001
Insulin	Sigma, St. Louis, MO	I6634
Cholera toxin	List Biological Laboratories Inc, Burlington, ON	100
Epidermal growth factor (EGF)	Sigma, St. Louis, MO	E4127

Triiodothyronine	Sigma, St. Louis, MO	T6397
2.5% trypsin	Gibco, Burlington, ON	15090-046
Type I collagenase	Worthington, Lakewood, NJ	LS004196
Polyethyleneimine (PEI, 25 kDa linear)	Polysciences, Warrington, PA	23966
Primaria™ culture dishes	BD, Mississauga, ON	CA25482-701
24-well Falcon™ cell culture plates	BD, Mississauga, ON	353226
15-ml Falcon™ conical tubes	BD, Mississauga, ON	352097
50-ml Falcon™ conical tubes	BD, Mississauga, ON	352098
70-µm pore size Falcon™ cell strainer	BD, Mississauga, ON	352350
100-µm pore size Falcon™ cell strainer	BD, Mississauga, ON	352360
Phospho Safe extraction reagent	Novagen, San Diego, CA	71296-3
Phenylmethylsulfonylfluoride (PMSF)	Bioshop, Burlington, ON	PMS123
Na_3VO_4	BioShop, Burlington, ON	SOV664
NaF	Sigma, St. Louis, MO	S7920
Aprotinin	BioShop, Burlington, ON	APR200
Pepstatin	BioShop, Burlington, ON	PEP605
Leupeptin	BioShop, Burlington, ON	LEU001
Bradford protein quantification solution	Bio-Rad, Mississauga, ON	500-0006
Pierce protein A/G magnetic beads	Thermo Scientific, Burlington, ON	88803
Dithiothreitol (DTT)	BioShop, Burlington, ON	DTT001
Polyvinylidene fluoride membranes (PVDF)	Millipore, Billerica, MA	IPVH00010

Amersham ECL Prime Western blotting detection reagent	GE Healthcare, Mississauga, ON	RPN2232
UltraCruz autoradiography film	Santa Cruz Biotechnology, Santa Cruz, CA	SC-201697
Rat tail collagen I	BD Biosciences, Bedford, MA	354236
Paraformaldehyde (PFA)	Fisher Scientific, Whitby, ON	AC416780030
Triton X-100	EMD, Darmstadt, Germany	CATX 1568
Hoechst 33342	Life Technologies, Burlington, ON	H1399
Immu-mount mounting medium	Thermo Scientific, Pittsburgh, PA	9990402
Recombinant human transforming growth factor-beta 1 (TGF-β1)	Peprotech, Rocky Hill, NJ	100-21
SB431542	Sigma, St. Louis, MO	54317-5MG
Nystatin	Sigma, St. Louis, MO	N4014

2.2 Antibodies

Antibodies and their sources are as follows:

Table 2: Antibodies

Antibodies	Source	Catalogue number
Anti-HA (Y-11)	Santa Cruz Biotechnology, Santa Cruz, CA	SC-805
Anti-type II TGF-β receptor (TβRII, C-16)	Santa Cruz Biotechnology, Santa Cruz, CA	SC-220
Mouse monoclonal anti-ILK	BD Transduction Laboratories, Lexington, KY	611802
Anti-γ-tubulin	Sigma, St. Louis, MO	T6557
Anti-V5	Invitrogen, Carlsbad, CA	R960.25
Anti-Glyceraldehyde 3-phosphate dehydrogenase (GAPDH)	Assay Designs, Ann Arbor, MI	CSA-335
Anti-phosphorylated SMAD2 (pSMAD2)	Chemicon/Millipore, Temecula, CA	AV3849
Anti-SMAD2/3	BD, Mississauga, ON	610842
HRP-conjugated goat anti-mouse IgG	Jackson ImmunoResearch, West Grove, PA	115-038-003
HRP-conjugated goat anti-rabbit IgG	Cell Signalling, Pickering, ON	7074
AlexaFluor™ 594 -conjugated goat anti-mouse IgG	Molecular Probes/Invitrogen, Eugene, OR	A11005
AlexaFluor™ 488-conjugated goat anti-rabbit IgG	Molecular Probes/Invitrogen, Eugene, OR	A11008

The hybridoma cells that produce E7 anti-β-tubulin antibody developed by M. Klymkowsky were obtained from the Developmental Studies Hybridoma Bank developed under the auspices of NICHD and maintained by The University of Iowa (Department of Biology, Iowa City, IA 52242). For production of anti-β-tubulin antibodies, hybridoma cells were cultured in RPMI-1640 medium (Gibco, Burlington, ON, 22400) supplemented with 10% FBS, 0.01M 2-mercaptoethanol, 1% non-essential amino acids (Gibco, Burlington, ON, 11140), and 50 μg/ml gentamicin (Gibco, Burlington, ON, 151710-064). Cells were cultured at 37°C in a humidified atmosphere containing 5% CO_2 until the growth medium had turned yellow and most of the cells had lifted off the culture flask (2-3 days). The culture medium containing the β-tubulin monoclonal antibody was collected and centrifuged at 1000 x g, 4°C for 10 minutes to remove cells and cell debris. The supernatant was collected and stored at -20°C.

2.3 Cell isolation and culture

2.3.1 Immortalized mouse dermal fibroblasts

Immortalized mouse dermal fibroblasts (IMDF) are a spontaneously immortalized line of dermal fibroblasts originally isolated from 2-days-old CD-1 mice (Apostolova et al. 2002). They were cultured in HyQ-DMEM-RS, supplemented with 8% FBS at 37°C in a humidified atmosphere containing 5% CO_2. All experiments were conducted with cells that had reached ≤ 80% confluence and that had been passaged for 15 generations or less.

2.3.2 Primary mouse epidermal keratinocytes

Epidermal keratinocytes were isolated from *Ilk*^{tm1Star} mice, in which exons 5 to 12 of both *Ilk* alleles are flanked by loxP sequences (hereafter termed *Ilk*$^{f/f}$ mice) (Terpstra et al. 2003). These mice were sacrificed at 3-days of age by CO_2 inhalation, their skin was harvested, and epidermal keratinocytes were isolated and cultured as previously described (Ho et al. 2009, Dagnino et al. 2010). Briefly, after euthanasia, mice were immersed in 70% ethanol for 10 minutes at 4°C, to sterilize the skin. The skin was then removed and was floated, dermis side down, in freshly diluted 0.25% trypsin, for 16 hours at 4°C. The trypsin was removed by aspiration, and replaced with fresh 0.25% trypsin and incubated at 37°C for 15-30 minutes. The epidermis was mechanically separated from the dermis. The dermis was processed separately to isolate fibroblasts, as described in section 2.3.3. The epidermis was minced with scissors and placed in keratinocyte growth medium (Ca^{2+}-free EMEM supplemented with 8% Chelex resin-treated FBS, 100U/ml penicillin, 100µg/ml streptomycin, 74 ng/ml hydrocortisone, 5 µg/ml insulin, 9.5 ng/ml cholera toxin, 5 ng/ml EGF, and 6.7 ng/ml triiodothyronine). The minced tissues were incubated at 37°C for 20 minutes, with gentle rocking, to obtain a single-cell suspension. The latter was then filtered through a 70-µm cell strainer to remove tissue fragments. The cells were plated onto Primaria™ culture dishes at a density of 1 x 10^5 cells/cm^2. The following day, the growth medium was replaced, and medium changes were conducted every other day thereafter. Keratinocytes were cultured at 37°C in a humidified atmosphere containing 5% CO_2. All experiments were conducted on keratinocytes that had reached ≤ 80% confluence, and that had been cultured 2-3 days.

2.3.3 Primary mouse dermal fibroblasts

Primary fibroblasts were isolated from the dermis of 3 days-old *Ilk*$^{f/f}$ mice (Terpstra et al. 2003). Dermal tissues obtained following mechanical separation from the epidermis (section 2.3.2.) were minced with scissors and incubated in a solution containing 0.35% w/v Type I collagenase, diluted in HyQ-DMEM-RS and supplemented with 100U/ml penicillin and 100μg/ml streptomycin. The minced tissues were incubated at 37°C for 30 minutes with gentle rocking. An equal volume of dermal fibroblast growth medium (HyQ-DMEM-RS supplemented with 8% FBS, 100U/ml penicillin, and 100μg/ml streptomycin) was added and the cell suspension was then filtered through a 100-μm cell strainer. The cells in the filtered suspension were centrifuged at 200 x g at 22°C for 5 minutes, resuspended in fibroblast growth medium, and plated onto culture dishes at a density of 2.5 x 10^4 cells/cm^2. Dermal fibroblasts were cultured at 37°C in a humidified atmosphere containing 5% CO_2. All experiments were conducted on cells that had reached ≤ 80% confluence and that had not been passaged more than 4 times.

2.4 Transient transfections

Primary keratinocytes and IMDF cells were transiently transfected with vectors encoding V5-tagged wild-type and mutant ILK and/or with vectors encoding HA-tagged wild-type and mutant TβRII (Figure 2.1) using PEI as previously described (Dagnino et al. 2010). A PEI stock solution of 1 mg/ml was prepared by dissolving PEI in 18 MΩ water with constant stirring, and adjusted to pH 7.0 with HCl. The solution was then sterilized through a 0.22-μm filter and stored in aliquots at -20°C. For a 10-cm culture dish, 3.5-9

μg of total DNA (1 μg/μl stock), 60 μl of 1 mg/ml PEI solution, and sterile 150 mM NaCl were combined to make a total volume of 500 μl. For a well of a 24-well culture plate, the transfection solution contained 2 μg of total DNA (1 μg/μl stock), 6 μl of 1mg/ml PEI solution, and 92 μl of sterile 150 mM NaCl. The transfection solution was mixed by vortexing and incubated at 22°C for 10 minutes. Transfection solutions were added dropwise to the growth medium in individual culture dishes and thoroughly mixed. The cells were cultured in the presence of the transfection solution for 4 hours. The medium was then replaced with fresh culture medium, and the cells were cultured for 24-48 hours prior to processing for immunoblot analysis or immunofluorescence microscopy.

2.5 Adenovirus amplification

The adenoviruses encoding Cre recombinase and green fluorescent protein (GFP) (Ad-Cre), β-galactosidase and GFP (Ad-βgal), or human ILK and GFP (Ad-hILK) were generated in our laboratory and have been described (Vespa et al. 2003, Vi et al. 2011). High-titer adenovirus stocks (10^8-10^9 virus/ml) were prepared using the human embryonic kidney cell line HEK293 (American Type Culture Collection, Manassas, VA). HEK293 cells were cultured in HyQ-DMEM-RS medium supplemented with 4% FBS in 150-cm^2 cell culture flasks. When the cells had reached 80% confluence, they were gently washed with sterile phosphate-buffered saline (PBS). A solution containing serum-free HyQ-DMEM-RS and adenoviruses at a multiplicity of infection (MOI) of 1 was added to the cells. The cells were incubated for 1 hour at 37°C, to allow infection to proceed. After 1 hour, 10 ml of HyQ-DMEM-RS containing 4% FBS was added, to give a final concentration of 2% FBS. The infected HEK293 cells were cultured at 37°C in a

Figure 2. 1. Schematics of plasmids used in transfections

The vectors encoding V5-tagged wild-type and mutant ILK have a CMV promoter (pCMV), a wild-type or mutant ILK construct with C-terminal V5 tag, and ampicillin resistance gene (Amp). The vectors encoding HA-tagged wild-type and mutant TβRII have a CMV promoter, a wild-type or mutant TβRII construct with C-terminal HA tag, and ampicillin resistance gene (Amp).

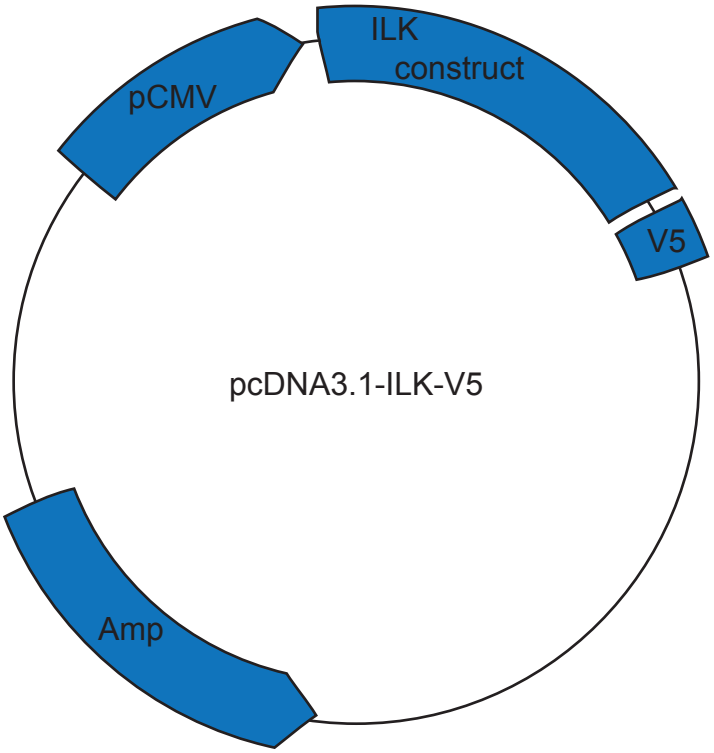
ILK
construct
pCMV
V5
pcDNA3.1-ILK-V5
Amp

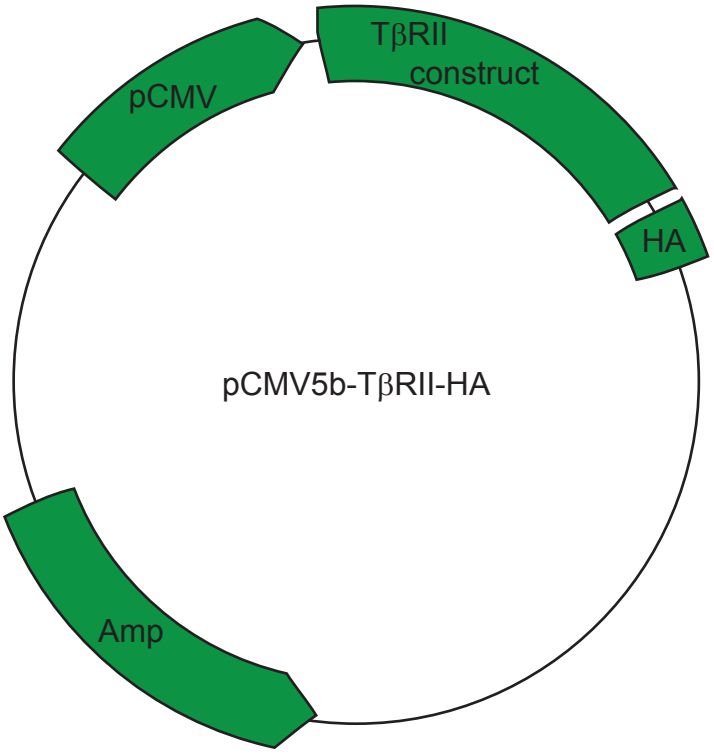
TβRII
construct
pCMV
HA
pCMV5b-TβRII-HA
Amp

humidified atmosphere with 5% CO_2 until 70% of the cells had lifted from the culture flask (7-10 days). The remaining cells were detached from the culture flask by rinsing with culture medium. The cell suspension was transferred to a conical tube and centrifuged at 1800 x g at 22°C for 5 minutes. The culture medium was removed by aspiration, and the cell pellet was resuspended in PBS containing 10% glycerol (300-500 µl per 150-cm^2 culture flask). The cell suspension was subjected to three freeze-thaw cycles using liquid nitrogen and a 37°C water bath. Lysed cells were then centrifuged at 3000 x g at 4°C for 10 minutes and the supernatant containing the adenoviruses was collected and stored in 100-µl aliquots at -80°C until ready to use. Adenovirus stocks were titered by dilution assay, in which HEK293 cells were infected with various dilutions of virus solution for 1 hour and were fixed 24 hours after infection. The cell nuclei were stained using Hoechst 33342 and the percentage of GFP-positive cells was calculated. With the assumption that one viral particle is required to infect one HEK293 cell, the number of infectious viral particles per volume of solution was calculated.

2.6 Adenoviral transduction of primary cells

2.6.1 Dermal fibroblasts

Dermal fibroblasts at 90-95% confluence in 10-cm culture dishes were infected with Ad-Cre, Ad-βgal, or Ad-hILK in 4 ml of serum-free HyQ-DMEM-RS at a MOI of 150. Under these conditions, ≥95% of the cells were infected, as confirmed by GFP fluorescence, with no significant reduction in cell viability. After 4 hours, 4 ml of HyQ-

DMEM-RS with 4% FBS was added to the cells to give a final concentration of 2% FBS. The cells were cultured for 4 days prior to being used for experiments.

For experiments involving two infections, the second infection was conducted 2 days after the first infection with a MOI of 150, and the cells were collected 4 days after the initial infection.

2.6.2 Epidermal keratinocytes

Keratinocytes at 80-95% confluence were infected with Ad-Cre or Ad-βgal in serum-free, Ca^{2+}-free EMEM supplemented with 25 μg/ml BSA at a MOI of 5-20. Under these conditions, ≥95% of the cells were infected, as confirmed by GFP fluorescence, with no significant reduction in cell viability. Five hours after infection, the medium was replaced with keratinocyte growth medium. The cells were cultured for 3 days prior to being used for experiments.

2.7 Preparation of cell lysates and immunoprecipitation

Cells were collected for preparation of lysates 24-48 hours after transfection, or 72-96 hours after infection, as described in individual experiments. The cells were scraped from the culture dishes and centrifuged (200 x g at 4°C, for 10 minutes). The cell pellets were stored at -80°C or processed immediately to prepare lysates.

In experiments in which analyses of phosphorylated proteins were conducted, cells were resuspended in Phospho Safe extraction reagent supplemented with 1 mM PMSF and placed on ice for 30 minutes. The volume of extraction reagent used was approximately

4-fold larger than the estimated size of the cell pellet. The lysates were centrifuged at 18,000 x g, at 4°C, for 10 minutes, and the supernatant was transferred to a new tube. Bradford protein quantification assays were conducted to determine the protein concentration in each lysates sample. To detect endogenous proteins by Western blot analyses, 50 μg of protein per sample were used, whereas 20 μg of protein per sample were used to detect exogenously expressed proteins.

For immunoprecipitation experiments, IMDF cells or dermal fibroblasts were lysed in a modified radioimmunoprecipitation assay (RIPA) buffer (50 mM Tris-HCl pH 7.4, 150 mM NaCl, 1% NP-40, 0.5% sodium deoxycholate, 1 mM PMSF, 10 mM Na_3VO_4, 1 μg/ml NaF, 1 μg/ml aprotinin, 1 μg/ml pepstatin, and 1 μg/ml leupeptin) for 30 minutes on ice. The volume of lysis buffer used was approximately 4-fold larger than the estimated size of the cell pellet. The lysate was centrifuged (18,000 x g, at 4°C for 10 minutes) and the supernatant was transferred to a new tube. Bradford protein quantification assays were conducted to determine the protein concentration in each lysates sample. For immunoprecipitation, lysates (500 μg of protein from IMDF cells or 1 mg of protein from fibroblasts) were incubated with 2 μg of antibodies indicated in specific experiments at 4°C with rocking, for 16 hours. Pierce protein A/G magnetic beads were added to the lysate-antibody mixtures (25 μl per sample), mixed, and incubated for 1 hour at 22°C with gentle rocking. The beads were rinsed 5-8 times with PBS containing 0.02% Tween-20, using 300-500 μl per wash. Antibody/antigen complexes were eluted and denatured by incubating the beads in 1x loading buffer (50 mM Tris-Cl pH 6.8, 2% sodium dodecyl sulphate, 0.1% bromophenol blue, 10%

glycerol) with 10 mM DTT at 22°C for 10 min. The immunecomplexes were resolved by denaturing polyacrylamide gel electrophoresis (SDS-PAGE).

2.8 Denaturing polyacrylamide gel electrophoresis and immunoblotting

Samples of cell lysates or immunoprecipitates were resolved by electrophoresis on SDS-PAGE (5% stacking and 8% resolving polyacrylamide gels). Following electrophoresis, the proteins were transferred to Immobilon-P PVDF transfer membranes. The membranes were blocked with Tris-buffered saline (TBS, 100mM Tris-HCL pH 7.5 and 0.9% NaCl) containing 0.05% Tween-20 and 5% skim milk (TBS-TM), for 1 hour at 22°C, with gentle rocking. The membranes were probed with primary antibodies indicated in individual experiments, diluted in TBS containing 0.05% Tween-20 (TBS-T) or TBS-TM. For antibody probing, the membranes were placed in a 50-ml Falcon^{TM} tube containing 5-7.5 ml of antibody solution, and were fastened to a rotor. The samples were then subjected to rotation at 8 rpm at 22°C for 2 hours or at 4°C for 16 hours. The antibody dilutions and conditions for probing used were: β-tubulin (1:50 v/v in TBS-T), TβRII, ILK, pSMAD2, and HA (1:1000 v/v in TBS-TM), SMAD2/3 (1:1000 v/v in TBS-T), V5 (1:5000 v/v in TBS-T), GAPDH (1:7500 v/v in TBS-T), and γ-tubulin (1:50000 v/v in TBS-T). Following incubation with primary antibody, the membranes were washed with 15 ml of TBS-T three times, for 10-20 minutes per wash, and then incubated with the appropriate HRP-conjugated secondary antibody (1:5000 v/v in TBS-TM) for 1 hour at 22°C. Proteins on the membranes were detected using Amersham ECL Prime Western Blotting Detection Reagent and UltraCruz autoradiography film. All results shown are

representative of at least three experiments. When necessary, PVDF membranes were stripped before being re-probed to detect other proteins, using a guanidine hydrochloride-based stripping solution (6M guanidine hydrochiloride, 0.02% NP-40, 20 mM Tris-HCl pH 7.5, and 0.8% 2-mercaptoethanol) (Yeung & Stanley 2009). To this end, the membranes were incubated with stripping solution for 5 minutes twice, with gentle rocking, at 22°C, and then washed with 15 ml of TBS-T three times, 10 minutes per wash, before being probed with another primary antibody.

2.9 Confocal microscopy

Glass coverslips were submerged in 1M HCl and heated to 50-60°C for 4-16 hours. The solution was allowed to cool and the coverslips were washed extensively with 18 MΩ water. The coverslips were rinsed in ethanol and allowed to air dry. Once dry, the coverslips were coated with 1mg/ml poly-L-lysine (PLL) solution for at least 30 minutes at 22°C, with gentle rocking. PLL-treated coverslips were then washed extensively with 18 MΩ water and allowed to air dry. The PLL-coated coverslips were sterilized by incubating in 70% ethanol for 10 minutes at 22°C, and they were washed with 1ml of sterile PBS three times. IMDF cells were cultured on sterile PLL-coated glass coverslips. For keratinocytes, sterile PLL-coated glass coverslips were further treated with a solution containing 50 µg/ml rat tail collagen I dissolved in 0.02N acetic acid for 4 hours at 37°C. The coverslips were then washed with 1 ml of sterile PBS three times and then keratinocytes were cultured on these coverslips until ready to be processed for microscopy. To this end, the cells were fixed with freshly diluted 4% PFA in PBS for 40 minutes on ice. Cells were then washed for 10 minutes with 1 ml PBS three times, and

permeabilized with 0.1% Triton X-100 in PBS for 30 minutes at 22°C. The samples were then washed for 10 minutes with 1 ml PBS three times, and incubated in PBS containing 1% skim milk and 1% goat serum for 1 hour at 22°C. The samples were washed three times with 1 ml PBS for 10 minutes each, and probed with primary antibodies indicated in individual experiments, with gentle rocking at 22°C for 2 hours or at 4°C for 16 hours. The antibodies were diluted in PBS containing 1% skim milk and 5% goat serum The antibody dilutions used were: HA (1:500 v/v) and V5 (1:1000 v/v). Following incubation with primary antibodies, cells were washed with PBS three times for 10 minutes each, with gentle rocking at 22°C. The samples were then incubated with appropriate AlexaFluor™-conjugated secondary antibodies (1:1000 v/v in PBS with 1% skim milk and 1% goat serum) for 1 hour at 22°C, protected from light. After three 10-minute washes with PBS, coverslips were incubated with Hoechst 33342 (1:10000 v/v, 1μg/ml, final) for 15 minutes, rocking, at 22°C. The glass coverslips were washed three times with 1 ml PBS (10 minutes each) and mounted on microscope slides, using Immu-mount mounting medium and allowed to dry overnight at 22°C, protected from light. A Zeiss LSM5 DUO scanner laser confocal microscope (Jena, Germany) equipped with a 63x/1.4 NA oil immersion lens and ZEN 2009 software (Zeiss, Germany) were used to obtain images.

2.10 Cell treatment with TGF-β1, SB431542, and nystatin

For TGF-β1 treatments, fibroblasts or keratinocytes were incubated, respectively, in serum-free HyQ-DMEM-RS or serum-free Ca^{2+}-free EMEM containing 25 μg/ml BSA, for 4 hours at 37°C. TGF-β1 (10 ng/ml, final) or sterile 18 MΩ water (vehicle) was added

into the medium dropwise and gently mixed. The cells were incubated for 1 hour at 37°C prior to processing. For experiments using SB431452, fibroblasts were incubated in serum-free HyQ-DMEM-RS for 3.5 hours at 37°C. SB431542 (10 μM, final) or sterile dimethyl sulfoxide (DMSO, vehicle, 1:1000 v/v, final) was added directly to the medium dropwise. Thirty minutes after treatment with SB431542 or DMSO, TGF-β1 (10 ng/ml, final) or sterile 18 MΩ water was added to the cell culture medium dropwise and cells were cultured at 37°C for 1 hour. For nystatin treatments, cells were incubated in serum-free HyQ-DMEM-RS supplemented with nystatin (50 μg/ml, final) or sterile DMSO (vehicle, 1:100 v/v, final) for 4 hours at 37°C. TGF-β1 (10 ng/ml, final) or sterile 18 MΩ water (vehicle) was added to the culture medium for one additional hour.

2.11 Densitometric analyses and statistics

ImageJ (Fiji) was used for densitometric analyses (Schindelin et al. 2012). Rectangles of equal sizes were drawn around the bands of interest on scanned images of immunoblots. A profile plot of each band was obtained, which represents the density in the given rectangle. Background values were subtracted, and the densitometric value of each lane was obtained. In order to compare different immunoblots, the pSMAD2 values and SMAD2/3 values of control cells (Ad-βgal-infected cells treated with TGF-β1) were assigned the value of 1 and all other values were adjusted accordingly, resulting in relative density values of the bands. The relative density values of pSMAD2 were then normalized to SMAD2/3 density to obtain adjusted relative values of the bands.

One-way analysis of variance (ANOVA) analyses with Newman-Keuls post-hoc test were conducted to determine significance of the results. GraphPad Prism version 5 was used for statistical analyses and p values less than 0.05 were considered statistically significant.

Chapter 3 – Results

3.1 ILK interacts with TβRII

Our laboratory had previously shown that ILK-deficient primary mouse dermal fibroblasts display abnormal responses to TGF-β1 stimulation (Vi et al. 2011). Thus, I sought to understand the mechanisms whereby ILK modulates TGF-β1 signal transduction pathways in these cells. As an initial step, I investigated if ILK and TβRII associate in primary dermal fibroblasts. To this end, I prepared lysates from cells incubated in the presence or absence of TGF-β1, and isolated TβRII immunoprecipitates. I then analyzed the latter by immunoblot and found the presence of ILK, irrespective of whether or not the cells had been stimulated with TGF-β1 (Figure 3.1).

To investigate whether ILK and TβRII associate in other cell types, I also examined IMDF cells, a spontaneously-immortalized line of dermal fibroblasts previously isolated in our laboratory (Apostolova et al. 2002). Wild-type V5-tagged ILK and wild-type HA-tagged TβRII were exogenously expressed in these cells. I isolated HA immunoprecipitates, and observed the presence of V5-tagged ILK (Figure 3.2). Reciprocally, I observed that TβRII was present in ILK immunecomplexes, indicating that the presence of ILK-TβRII complexes is not limited to primary dermal fibroblasts (Figure 3.2).

Having established the presence of ILK-TβRII complexes in dermal fibroblasts, I next examined the subcellular localization of these two proteins by confocal microscopy. I

Figure 3. 1. Interaction between ILK and TβRII in primary dermal fibroblasts

Primary dermal fibroblasts were incubated in serum-free HyQ-DMEM-RS for 4 hours at 37°C, followed by a 1-hour incubation with TGF-β1 (10 ng/ml) or H_2O (vehicle). Lysates (1 mg protein/sample) were prepared and subjected to immunoprecipitation with antibodies against (A) TβRII or (B) ILK, followed by immunoblotting with the indicated antibodies. Lysates of cells incubated in HyQ-DMEM-RS supplemented with 8% FBS were subjected to immunoprecipitation with antibodies against (A) unrelated rabbit IgG, or (B) unrelated mouse IgG, as control. (C) In parallel, samples of the lysates (50 μg protein/sample) were resolved by SDS-PAGE and transferred to membranes, which were probed with antibodies against TβRII, phosphorylated SMAD2 (pSMAD2), total SMAD2/3, ILK and γ-tubulin, which was used to normalize for protein loading. The results shown are representative of experiments repeated 3 times.

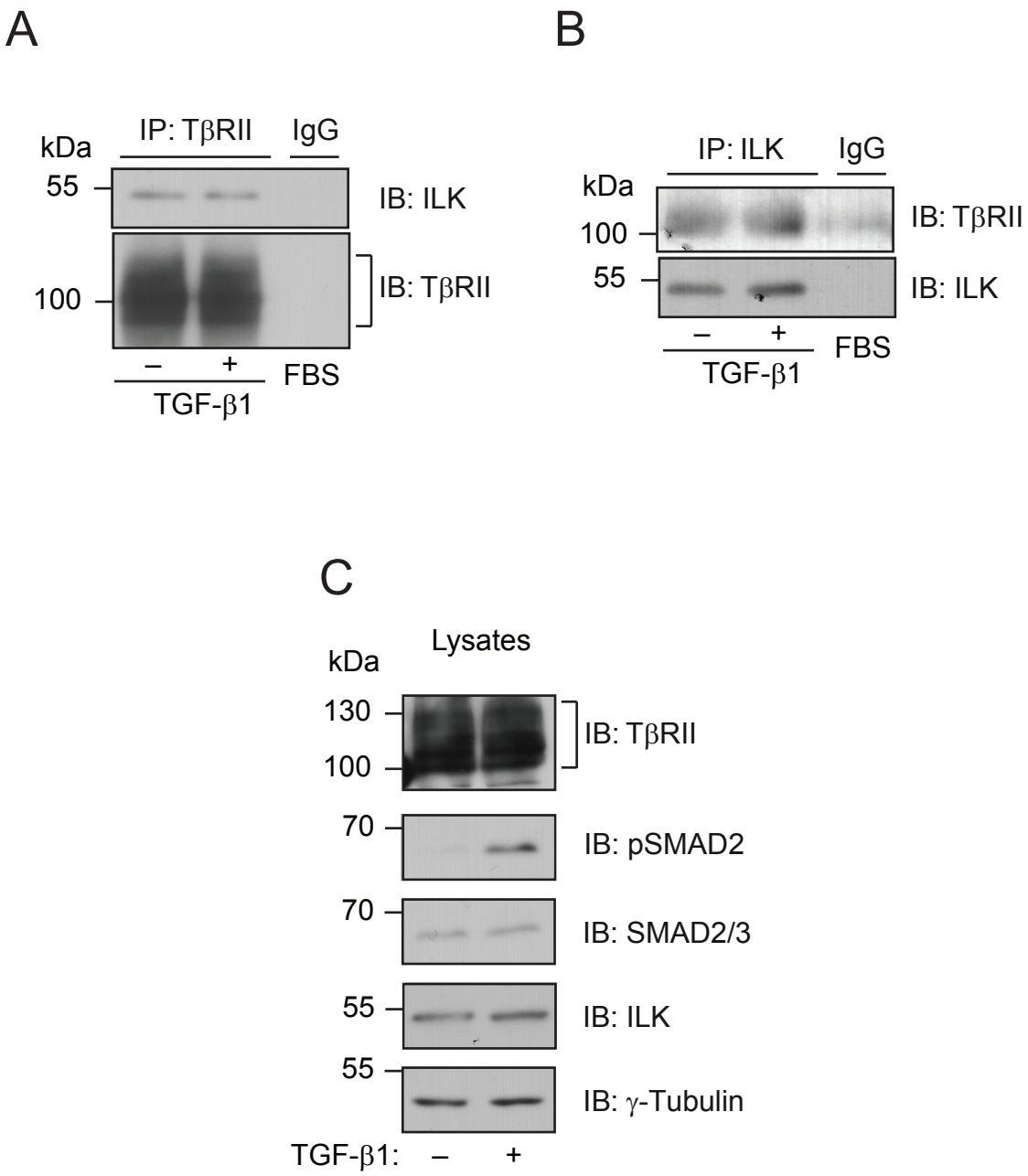
A
kDa
IP: TβRII
IgG
55
IB: ILK
100
IB: TβRII
–
+
FBS
TGF-β1
B
IP: ILK
IgG
kDa
100
IB: TβRII
55
IB: ILK
–
+
FBS
TGF-β1
C
Lysates
kDa
130
100
IB: TβRII
70
IB: pSMAD2
70
IB: SMAD2/3
55
IB: ILK
55
IB: γ-Tubulin
TGF-β1: – +

Figure 3. 2. Interaction between exogenously expressed ILK and TβRII in IMDF cells

IMDF cells were transfected with plasmids encoding V5-tagged ILK and/or HA-tagged TβRII. The negative sign (-) indicates transfection with empty vector. Fourty-eight hours after transfection, cells were lysed and the lysates were subjected to immunoprecipitation with antibodies against (A) V5, or (B) HA (500 μg protein/sample). A sample of the lysates was also subjected to immunoprecipitation with antibodies against unrelated mouse (A) or rabbit (B) IgG, as control. In parallel, aliquots of the lysates (50 μg protein/sample) were resolved by SDS-PAGE and transferred to membranes, which were probed with antibodies against HA, V5, and γ-tubulin, which was used to normalize for protein loading. The results shown are representative of three experiments.

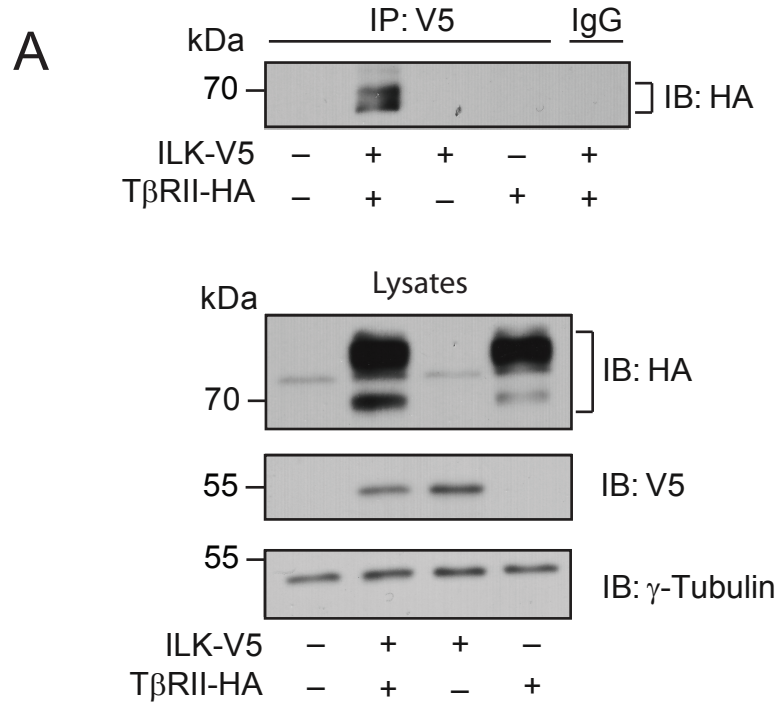
A
kDa
IP: V5
IgG
70
IB: HA
ILK-V5 – + + – +
TβRII-HA – + – + +
kDa
Lysates
70
IB: HA
55
IB: V5
55
IB: γ-Tubulin
ILK-V5 – + + –
TβRII-HA – + – +

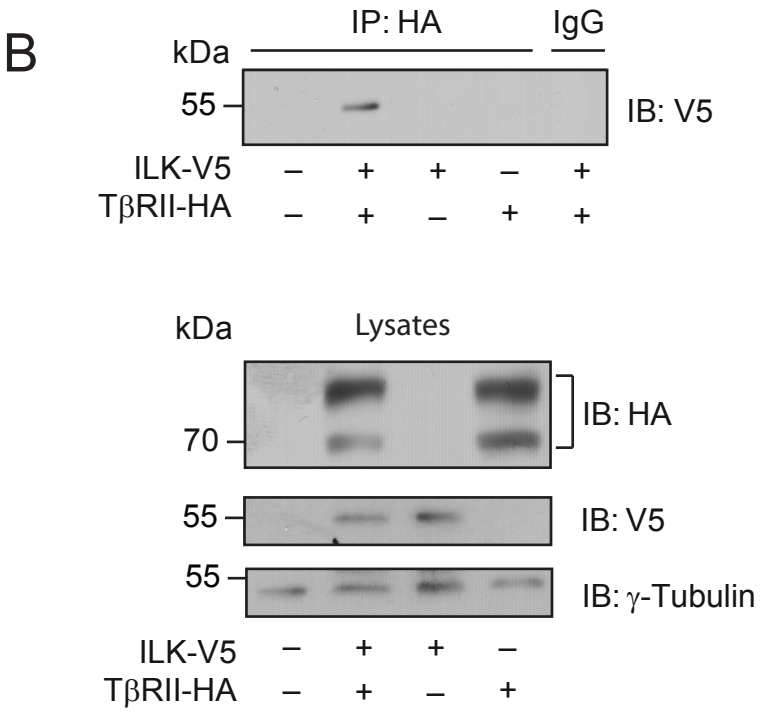
B
kDa
IP: HA
IgG
55
IB: V5
ILK-V5 – + + – +
TβRII-HA – + – + +
kDa
Lysates
70
IB: HA
55
IB: V5
55
IB: γ-Tubulin
ILK-V5 – + + –
TβRII-HA – + – +

transfected IMDF cells with vectors encoding wild-type V5-tagged ILK and wild-type HA-tagged TβRII. Transfected cells were then incubated in the presence or absence of TGF-β1 for 1 hour, and were then processed for microscopy. I observed ILK immunoreactivity throughout the cytoplasm and at the cell edges, in agreement with previous reports in other cell types (Ho et al. 2009) (Figure 3.3). In these cells, I also observed TβRII immunoreactivity in intracellular vesicles, and at the cell membrane. Significantly, ILK and TβRII appeared to colocalize at the cell periphery and in a fraction of intracellular vesicles. This pattern of colocalization was similar in the presence and absence of TGF-β1, indicating that it does not require a TGF-β1 stimulus (Figure 3.3).

3.2 ILK-TβRII colocalization is observed in keratinocytes

As mentioned in section 1.1.4, TβR complexes are endocytosed *via* caveolae or *via* clathrin-coated pits. However, incubation at 4°C without TGF-β1 stimulation results in inhibition of endocytic trafficking, under these conditions, and TβR complexes are predominantly observed at the cell membrane (Figure 3.4 A). At this temperature, all trafficking is halted, including constitutive endocytosis of TβRII (Ehrlich et al. 2001). In addition, it has been reported that no association between TβR and markers of internalization (caveolin-1 for lipid-raft/caveolae-mediated endocytosis, and clathrin for clathrin-mediated endocytosis) occurs under these conditions (Mitchell et al. 2004). Together, these observations suggest that steady state levels of TβRII complexes are mostly observed at the cell surface at 4°C. With TGF-β1 stimulation, cells incubated at 37°C show an increase in TβRI/TβRII complex formation (Figure 3.4 B) and in internalization of TβR complexes into endosomes and caveolae (Figure 3.4 C). Over

Figure 3. 3. Co-localization of ILK and TβRII in IMDF cells

IMDF cells were transfected with plasmids encoding V5-tagged ILK and HA-tagged TβRII. Fourty-eight hours after transfection, cells were cultured in serum-free HyQ-DMEM-RS for 4 hours, followed by treatment with TGF-β1 (10 ng/ml) or H_2O (vehicle) for 1 hour. The cells were processed for confocal microscopy using antibodies against V5 and HA to visualize ILK and TβRII, respectively. Boxed areas in micrographs c, g, k, and o are shown at higher magnification in micrographs d, h, l, and p, respectively. Arrows indicate areas of ILK and TβRII colocalization. Scale bar = 10 μm.

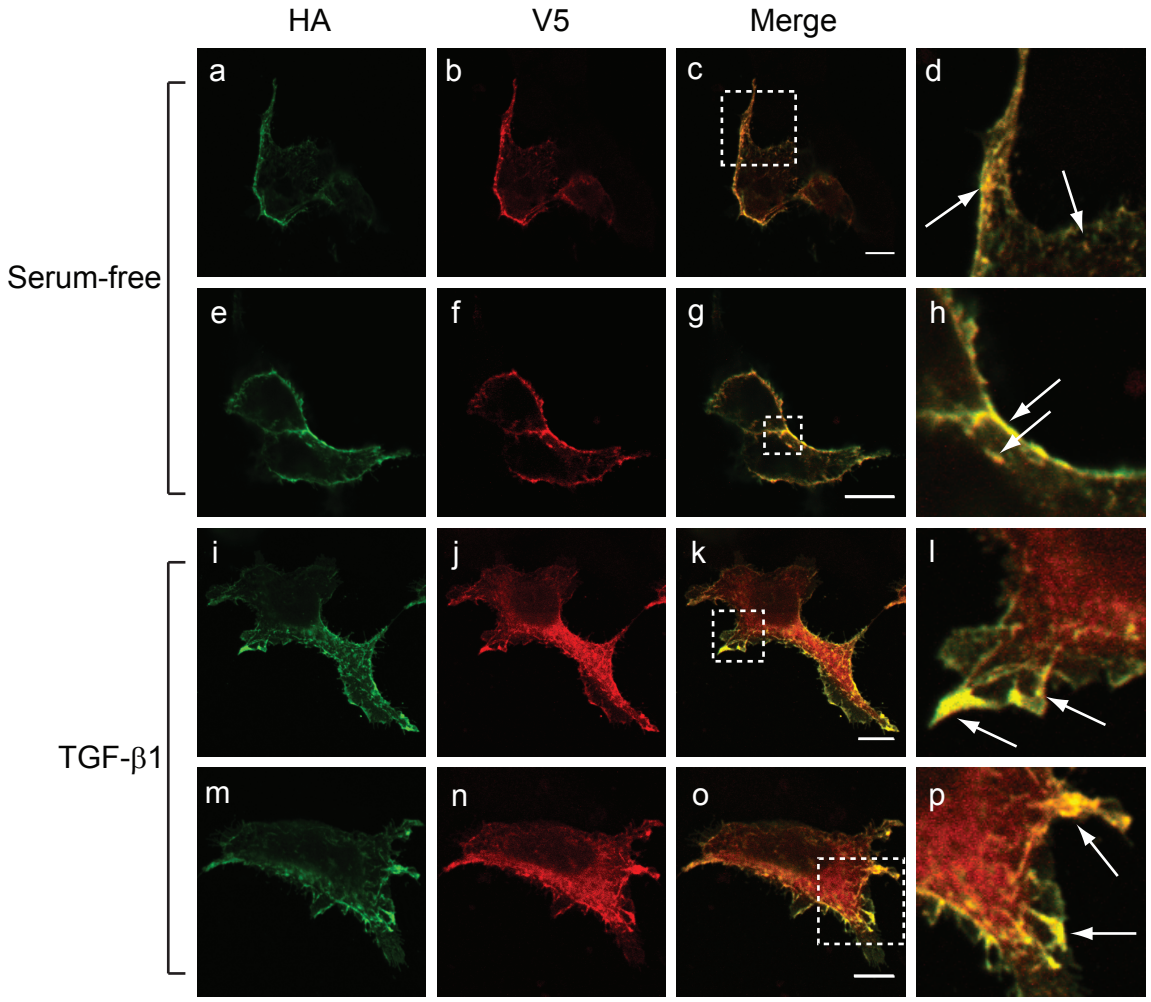
HA
V5
Merge
Serum-free
TGF-β1
a
b
c
d
e
f
g
h
i
j
k
l
m
n
o
p

time, TβR complexes in endosomes are sorted for signalling, recycling, or lysosomal degradation, whereas those TβR complexes in caveolae will be targeted for degradation in proteasomes or lysosomes (Figure 3.4 D).

To determine if ILK and TβRII show areas of colocalization in other cell types, I analyzed primary mouse epidermal keratinocytes, as a model of epithelial cells. In addition, I examined the subcellular localization of TβRII and ILK following ligand binding. Primary epidermal keratinocytes were transfected with wild-type V5-tagged ILK and wild-type HA-tagged TβRII. Twenty-four hours after transfection, the cells were incubated at 4°C for 30 minutes in serum- and TGF-β1-free medium, to impair receptor endocytosis and trafficking. After incubation at 4°C, the cells were stimulated with TGF-β1, and incubated at 37°C for 0, 15, 30, or 60 minutes, and processed for confocal microscopy. In keratinocytes cultured in serum-free medium without TGF-β1 stimulation, I observed ILK-TβRII colocalization in vesicles within the cytosol, as well as at the cell membrane (Figure 3.5 A). This indicates that lack of stimulation by the ligand or inhibition of TβRII internalization by low temperature does not interfere with ILK-TβRII colocalization. Fifteen minutes after TGF-β1 addition to the culture medium, colocalization of ILK and TβRII occurred at the cell membrane, as well as in vesicles (Figure 3.5 B). Cells stimulated with TGF-β1 showed an apparent increase in colocalization along the cell membrane, in agreement with previous reports that TGF-β1 stimulation leads to increased recruitment of receptors and formation of TβR complexes at the cell membrane (Rechtman et al. 2009). Similarly, after 30 and 60 minutes of TGF-β1 treatment, colocalization between ILK and TβRII was observed at the cell membrane,

Figure 3. 4. Schematic representation of the internalization routes of TβR complexes

TβR complexes containing TβRII and TβRI form at the cell membrane upon ligand binding to TβRII. These complexes can be internalized by two different pathways: clathrin-mediated and caveolin-mediated endocytosis. (A) TβRI and TβRII can be found at the cell membrane as monomers, homodimers, and heterodimers. (B) The formation of heterodimeric complexes greatly increases with the binding of TGF-β1 to TβRII. (C) TGF-β1 stimulation increases internalization of the receptor complexes through clathrin-coated pits to form endosomes, or through lipid-rafts to form caveolae/caveolin-positive vesicles. (D) Endosomal TβR complexes are sorted, targeted to signalling endosomes, and recycled back to the cell membrane. They can also be targeted for degradation by the late endosome/lysosome. Alternatively, TβR complexes in caveolae are targeted for degradation by proteasomes and/or lysosomes.

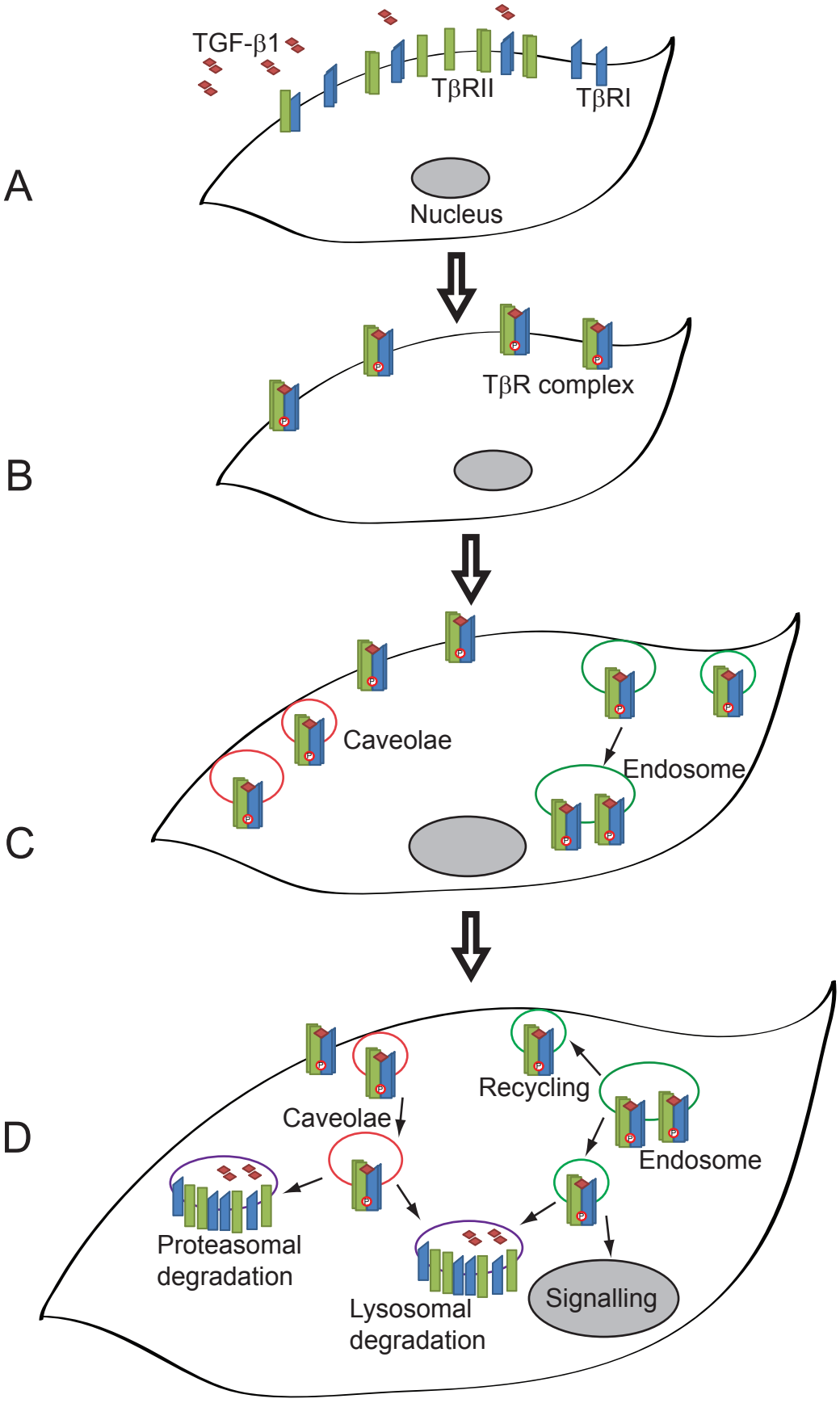
A
TGF-β1
TβRII
TβRI
Nucleus
B
TβR complex
C
Caveolae
Endosome
D
Caveolae
Recycling
Endosome
Proteasomal degradation
Lysosomal degradation
Signalling

in what appeared to be pseudopodia (Figure 3.5 C, D). Thus, ILK and TβRII show areas of colocalization in epidermal keratinocytes at the cell membrane and in intracellular vesicles. In cells cultured without TGF-β1 for 1 hour, ILK- TβRII colocalization was also observed at the cell membrane and in vesicles (Figure 3.5 E). A similar pattern of colocalization was also observed in cells treated with TGF-β1 and continuously incubated at 37°C, without cooling (Figure 3.5 F). Thus, ILK-TβRII colocalization and interaction are not appreciably altered in the presence of TGF-β1 (Figures 3.1 and 3.3).

Another observation to note is that TβRII does not colocalize with ILK at areas that appear to be focal adhesions (Figure 3.5 A, B), suggesting the possibility that a separate pool of ILK that localizes to focal adhesions to transduce ECM signals, but not necessarily TβR signalling, may exist in cells.

3.3 Mapping of protein regions implicated in the ILK-TβRII interaction

To determine the regions in ILK and in TβRII necessary for the interaction between these two proteins, I exogenously expressed various ILK and TβRII mutants in IMDF cells. The ILK mutants I tested included ILK E359K and several deletion mutants (amino acids 67-452, 191-452, 1-300, 1-250, and 1-192) (Figure 3.6 A). ILK E359K is unable to bind many proteins that localize to focal adhesions, such as paxillin, α-parvin, and β-parvin, and does not localize to focal adhesions (Wu & Dedhar 2001, Nikolopoulos & Turner 2002). ILK 67-452 is missing its first two ankyrin repeats, and thus is unable to bind to PINCH (Tu et al. 1999, Li et al. 1999, Vespa et al. 2005), and it also fails to localize to

Figure 3. 5. Colocalization of ILK and TβRII in keratinocytes

Epidermal keratinocytes were transfected with plasmids encoding V5-tagged ILK and HA-tagged TβRII. Fourty-eight hours after transfection, cells were cultured in serum- and Ca^{2+}-free EMEM for 4 hours, followed by (A) incubation on ice for 30 minutes, (B-E) incubation on ice for 30 minutes, then treatment with TGF-β1 (10 ng/ml) or H_2O (vehicle) for the indicated times, or (F) treatment with TGF-β1 (10 ng/ml) for 1 hour at 37°C. After these treatments, the cells were processed for confocal microscopy, using antibodies against V5 and HA to visualize ILK and TβRII, respectively. Boxed areas in micrographs c, g, k, o, s, and w are shown at higher magnification in micrographs d, h, i, p, t, and x, respectively. Arrows indicate areas of ILK and TβRII colocalization. Scale bar = 10 μm.

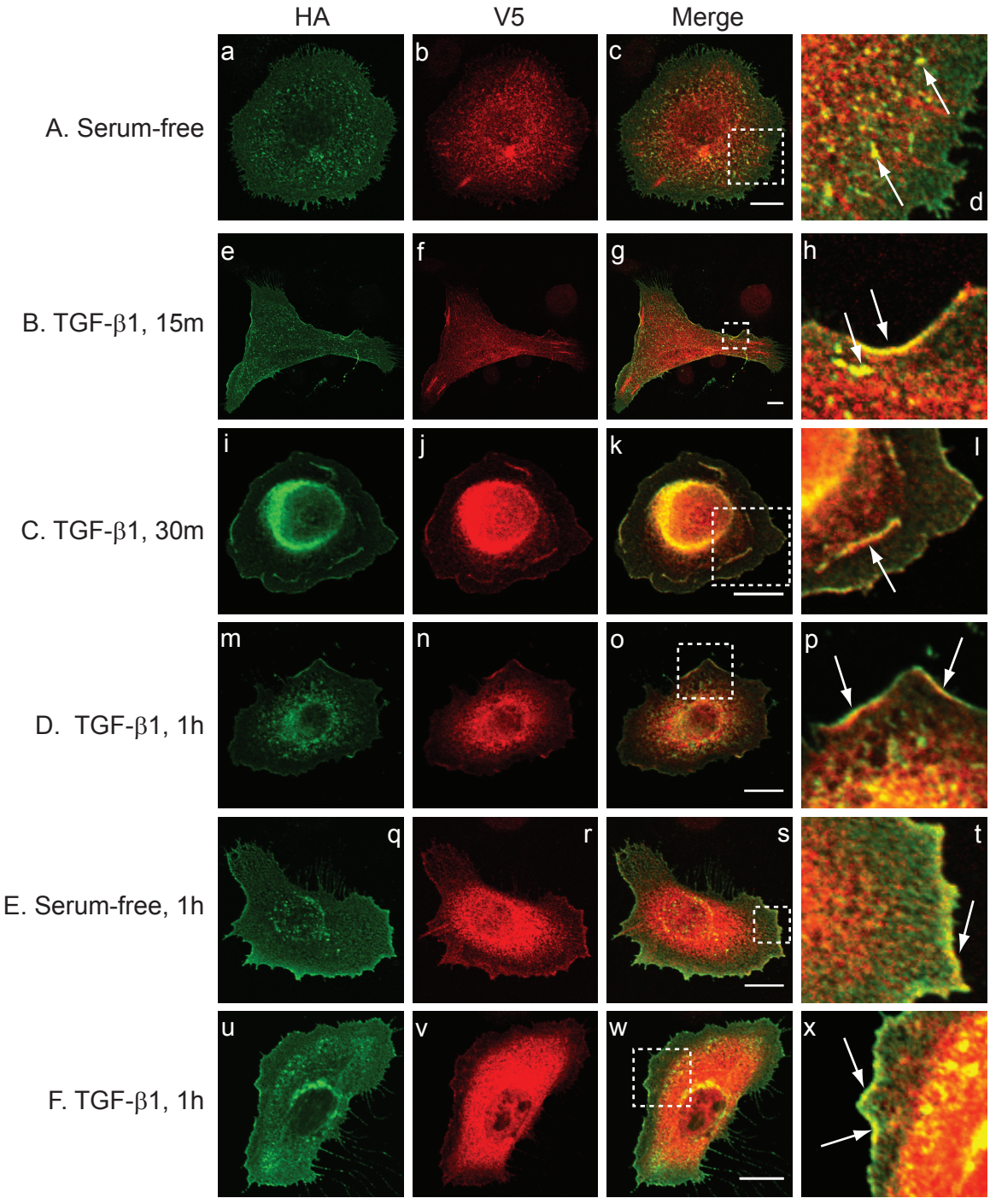
HA
V5
Merge
A. Serum-free
B. TGF-β1, 15m
C. TGF-β1, 30m
D. TGF-β1, 1h
E. Serum-free, 1h
F. TGF-β1, 1h
a
b
c
d
e
f
g
h
i
j
k
l
m
n
o
p
q
r
s
t
u
v
w
x

focal adhesions (Li et al. 1999), cell borders (Vespa et al. 2005), or the nucleus (Nakrieko et al. 2008b). The ILK 191-452 mutant lacks all ankyrin repeats. The ILK 1-300 and 1-250 mutants lack part of the kinase-like domain, including the amino acid residues predicted to mediate interactions with β1 integrin (293-451) (Hannigan et al. 1996). Lastly, ILK 1-192 lacks the kinase-like domain and cannot interact with focal adhesion-associated proteins, such as paxillin, α-parvin, and β-parvin, and is unable to localize to focal adhesions (Wu & Dedhar 2001), similar to ILK E359K.

Vectors encoding V5-tagged ILK mutants were transiently transfected in IMDF cells, together with wild-type HA-tagged TβRII. Cell lysates from transfected cells were prepared for immunoprecipitation. I observed that all of the V5-tagged ILK mutants were present in HA immunecomplexes (Figure 3.6 B, C). These results suggest that ILK may be able to bind TβRII through multiple sites. These data also indicate that direct binding of ILK with paxillin, parvins, PINCH, or β1 integrin is dispensable for its interaction with TβRII. Thus, the disruption in the ability of ILK to localize to focal adhesion does not affect its capacity to interact with TβRII.

To complete the mapping of regions important for ILK-TβRII interaction, TβRII truncation mutants (Figure 3.7 A) were transiently transfected into IMDF cells, together with wild-type V5-tagged ILK. The HA-tagged TβRII mutants used were TβRII K277R, which lacks kinase activity, and two truncation mutants: TβRII 155-567, which lacks most of the extracellular domain, and TβRII 1-199, which lacks most of the intracellular kinase domain. The last two mutants contain the transmembrane domain.

Figure 3. 6. Regions of ILK involved in the ILK-TβRII interaction

(A) Schematic diagram of the V5-tagged human ILK mutants used. Wild-type ILK includes 5 ankyrin repeats, a pleckstrin homology-like domain (PH), and a kinase-like domain (KLD). The asterisk indicates mutation of the E residue at position 359 to K. (B) IMDF cells were transfected with plasmids encoding V5-tagged ILK mutants and/or HA-tagged wild-type TβRII. The negative sign (-) indicates transfection with an empty vector. Fourty-eight hours after transfection, lysates (500 μg protein/sample) were prepared and subjected to immunoprecipitation with antibodies against HA or unrelated rabbit IgG, as control, followed by immunoblotting with the indicated antibodies. In parallel, samples of the lysates (20 μg protein/sample) were resolved by SDS-PAGE and transferred to PVDF membranes, which were probed with antibodies against HA, V5, and γ-tubulin, which was used to normalize for protein loading. The results shown are representative of experiments repeated 3 times.

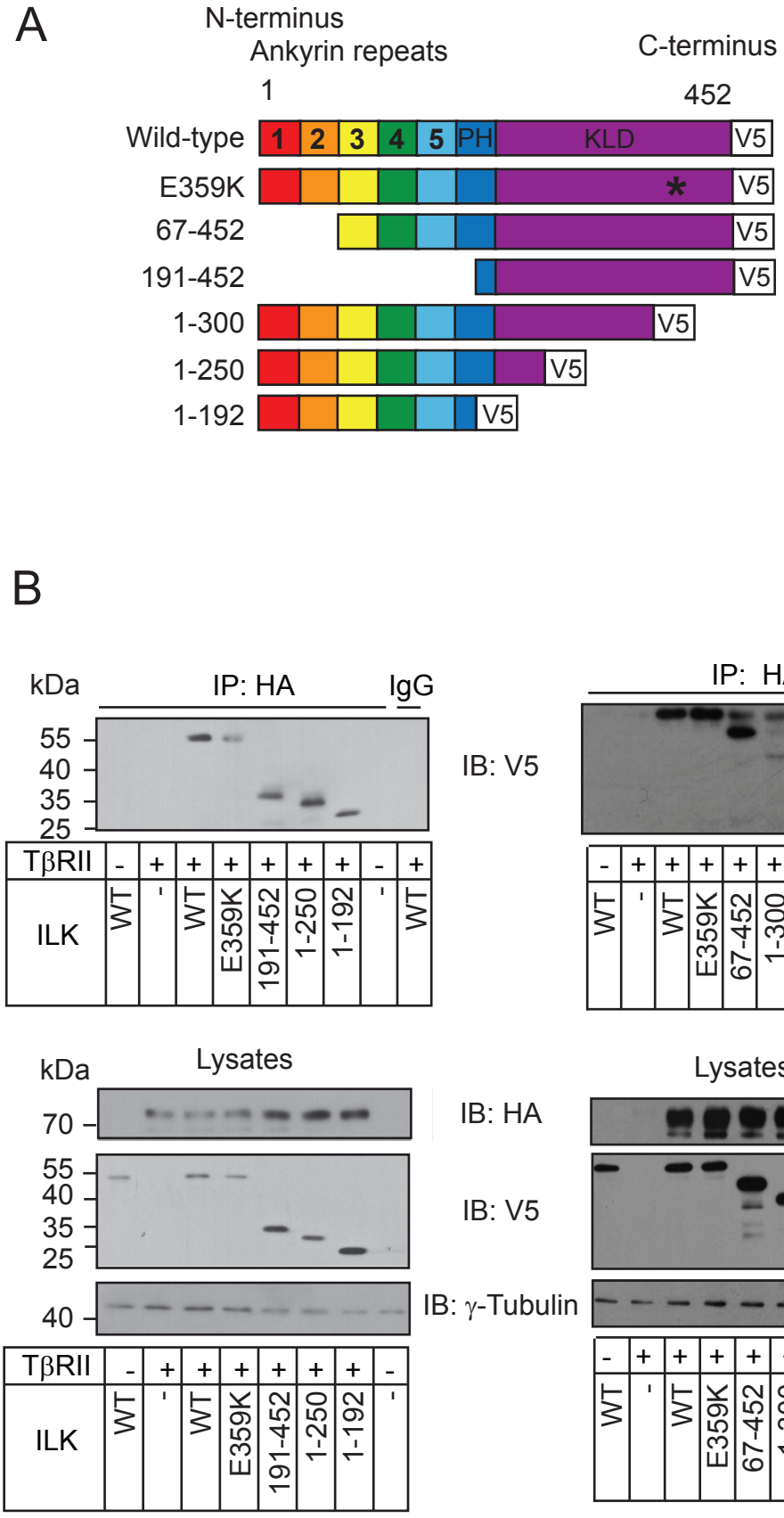
A
N-terminus
Ankyrin repeats
C-terminus
1
452
Wild-type
E359K
67-452
191-452
1-300
1-250
1-192
1
2
3
4
5
PH
KLD
V5
*
B
kDa
IP: HA
IgG
IB: V5
55
40
35
25
TβRII
ILK
WT
E359K
67-452
191-452
1-300
1-250
1-192
Lysates
IB: HA
IB: γ-Tubulin
70
100

Immunoprecipitation experiments showed that wild-type ILK interacts with TβRII K277R and TβRII 155-567 (Figure 3.7 B), indicating that ILK-TβRII interaction does not require either kinase activity of TβRII or its extracellular domain. Notably, ILK and TβRII 1-199 also interact (Figure 3.7 B), suggesting that a small cytoplasmic region on TβRII 1-199 is sufficient for this interaction to occur, or alternatively, that there is an intermediate adaptor protein, possibly with a transmembrane domain, linking ILK and TβRII.

3.4 The kinase activity of TβRI is dispensable for ILK-TβRII complex formation

Given that neither TGF-β1 stimulation nor TβRII kinase activity are required for ILK-TβRII interactions (Figures 3.1 and 3.7B), I sought to determine the role of TβRI kinase activity. Primary dermal fibroblasts were treated with SB-431542, a highly selective TβRI kinase inhibitor, or vehicle, and then incubated with TGF-β1 (or control vehicle). I isolated ILK by immunoprecipitation from these cells, and analyzed them for the presence of TβRII. As previously observed (Figure 3.1), TGF-β1 treatment is not required for ILK-TβRII interaction (Figure 3.8). I also observed the presence of TβRII in ILK immunoprecipitates, irrespective of whether or not cells had been treated with SB-431542 (Figure 3.8). Hence, the kinase function of TβRI and the presence of an activated TβRI-TβRII species are not necessary for ILK-TβRII interactions to occur.

Figure 3. 7. Regions of TβRII involved in the ILK-TβRII interaction

(A) Schematic of the HA-tagged human TβRII mutants used. Wild-type TβRII contains a signal sequence (SS), an extracellular domain (EC), a transmembrane domain (TM), and an intracellular kinase domain. The asterisk indicates mutation of the K residue at position 277 to R. (B) IMDF cells were transfected with plasmids encoding HA-tagged TβRII mutants and V5-tagged wild-type ILK. The negative sign (-) indicates transfection with empty vector. Fourty-eight hours after transfection, the cells were lysed, and the lysates (500 μg protein/sample) were subjected to immunoprecipitation with antibodies against ILK or unrelated mouse IgG, as control, followed by immunoblotting with the indicated antibodies. In parallel, samples of the lysates (20 μg protein/sample) were resolved by SDS-PAGE and transferred to membranes, which were probed with antibodies against HA, V5, and γ-tubulin, which was used to normalize for protein loading. The results shown are representative of experiments repeated 3 times.

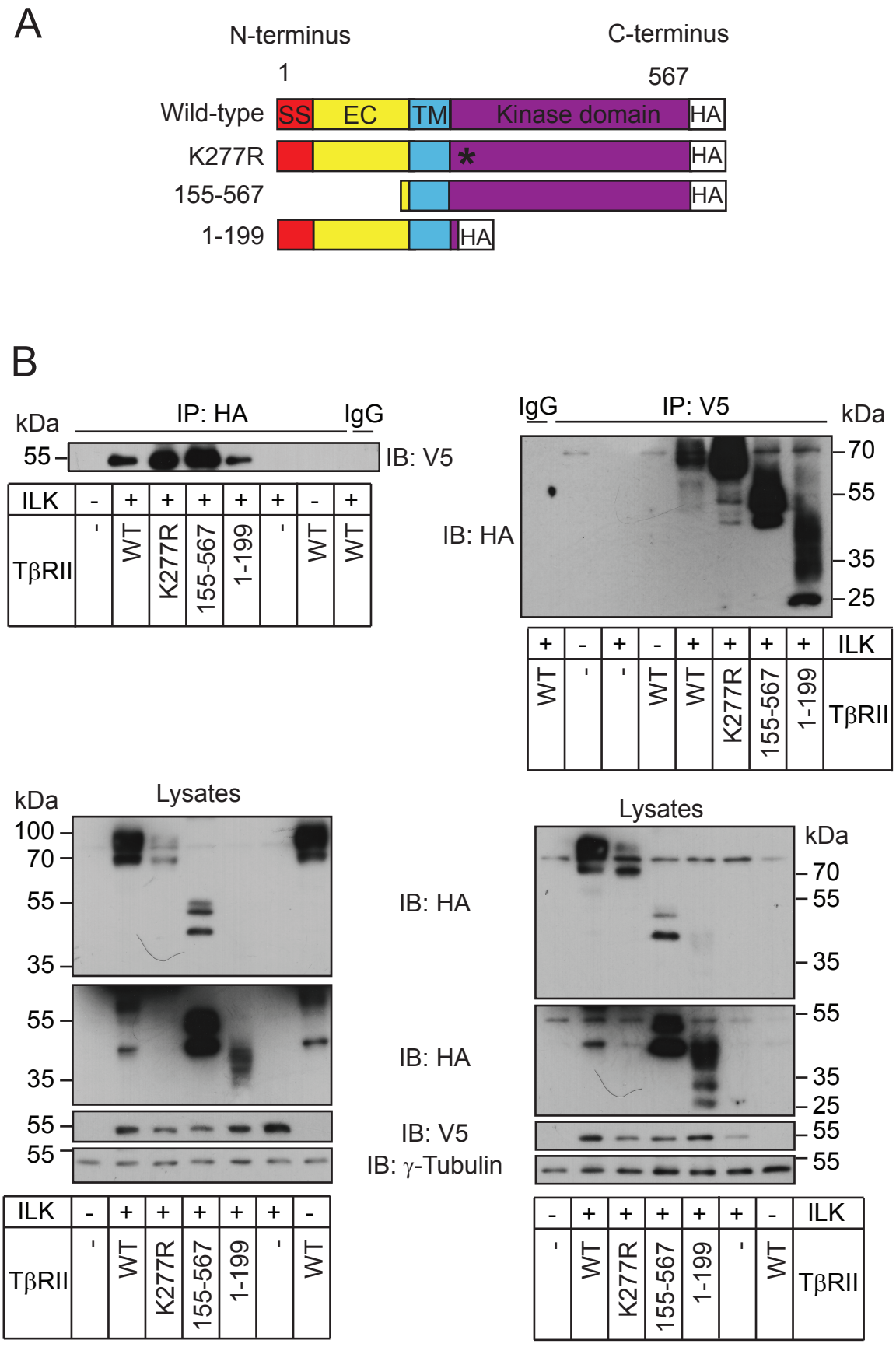
A
N-terminus
C-terminus
1
567
Wild-type
SS
EC
TM
Kinase domain
HA
K277R
*
155-567
1-199
B
kDa
IP: HA
IgG
55
IB: V5
ILK
TβRII
WT
K277R
155-567
1-199
IgG
IP: V5
IB: HA
70
35
25
Lysates
100
IB: HA
IB: V5
IB: γ-Tubulin

Figure 3. 8. Effect of TβRI kinase inhibition on ILK-TβRII interaction

Primary dermal fibroblasts were incubated in serum-free HyQ-DMEM-RS for 3.5 hours at 37°C, treated with SB431542 or DMSO (vehicle) for 0.5 hours, and then treated with TGF-β1 or water (vehicle) for 1 hour. Lysates (1 mg protein/sample) were prepared and subjected to immunoprecipitation with antibodies against ILK or unrelated mouse IgG, as control, followed by immunoblotting with antibodies against TβRII. In parallel, samples of the lysates (50 μg protein/sample) were resolved by SDS-PAGE and transferred to membranes, which were probed with antibodies against pSMAD2, SMAD2/3, ILK, and γ-tubulin, which was used to normalize for protein loading. The results shown are representative of experiments repeated 3 times.

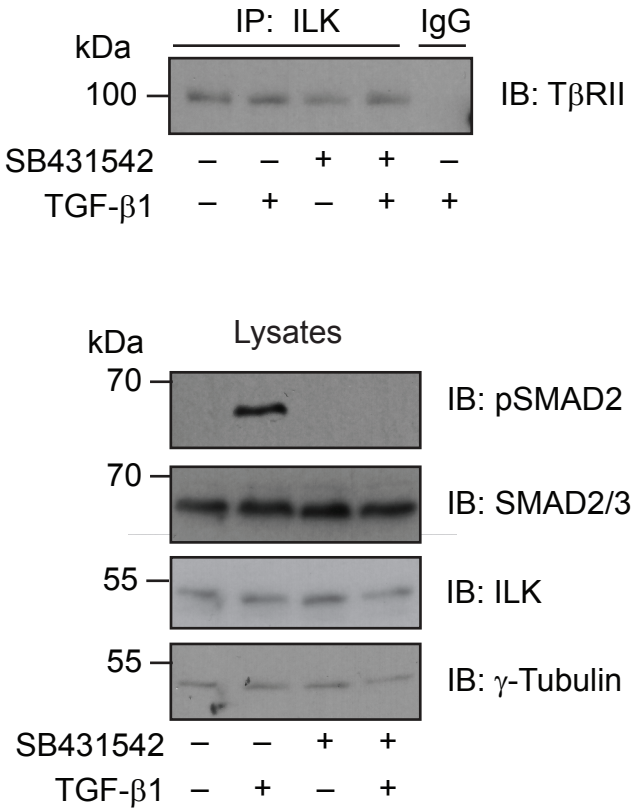
IP: ILK
IgG
kDa
100
IB: TβRII
SB431542 – – + + –
TGF-β1 – + – + +
Lysates
kDa
70
IB: pSMAD2
70
IB: SMAD2/3
55
IB: ILK
55
IB: γ-Tubulin
SB431542 – – + +
TGF-β1 – + – +

3.5 Abrogation of ILK expression results in abnormal responses to TGF-β1

I next studied the effects of inactivating the *Ilk* gene and, consequently, of disrupting the ILK-TβRII interaction, using $Ilk^{f/f}$ dermal fibroblasts. By infecting these cells with adenoviruses encoding Cre-recombinase (Ad-Cre), the *Ilk* gene was inactivated and the levels of ILK decreased by ≥ 90% after a period of four days (Figure 3.9 A). Specifically, there is a substantial decrease in the level of ILK by 72 hours, and by 94 hours after infection, ILK is barely detected. Thus, all experiments using ILK-deficient dermal fibroblasts were conducted between 72 and 94 hours after infection. This experimental system allowed me to address the role of ILK on TβR signalling.

In a first set of experiments, primary dermal fibroblasts were infected with Ad-Cre or a recombinant adenovirus encoding β-galactosidase (Ad-βgal) as control. Four days after infection, the cells were incubated in serum-free medium for 4 hours, and then treated with TGF-β1 or vehicle for 1 hour. The levels of phosphorylated SMAD2 (pSMAD2) were used as an indicator of TβR signalling. In the absence of ILK, I observed attenuated TβR signalling, as evidenced by reduced pSMAD2 levels, relative to those in ILK-expressing cells (Figure 3.9 B), as previously described by Vi et al. (Vi et al. 2011).

To confirm that ILK deficiency is directly linked to abnormal TβR signalling, exogenous expression of wild-type human ILK (hILK) was induced in ILK-deficient fibroblasts. To this end, primary dermal fibroblasts that had already been infected with Ad-Cre or Ad-βgal were infected again 48 hours later with Ad-hILK or Ad-βgal. Four days after the first infection, cells were serum-starved, and then treated with TGF-β1 or vehicle for 1

Figure 3. 9. Effects of *Ilk* gene inactivation on TβR signalling in dermal fibroblasts

(A) Primary $Ilk^{f/f}$ dermal fibroblasts were infected with adenoviruses encoding Cre recombinase (Ad-Cre) at an MOI of 150, and cell lysates were prepared at the indicated times after infection. The cell lysates were analyzed by immunoblot, using anti-ILK antibodies. β-Tubulin was used to normalize for protein loading. All experiments involving *Ilk* gene inactivation were conducted 94 hours after infecting the cells with Ad-Cre. (B) Primary dermal fibroblasts were infected with Ad-Cre (ILK-deficient) or Ad-βgal (ILK-expressing) at an MOI of 150. Ninety-four hours after infection, the cells were incubated in serum-free HyQ-DMEM-RS for 4 hours at 37°C, followed by 1-hour incubation with TGF-β1 (10 ng/ml) or H_2O (vehicle). The cells were lysed, and the lysates (50 μg protein/sample) were analyzed by immunoblotting, using antibodies against pSMAD2, SMAD2/3, ILK, and GAPDH, which was used to normalize for protein loading. The results shown are representative of experiments repeated 3 times.

A

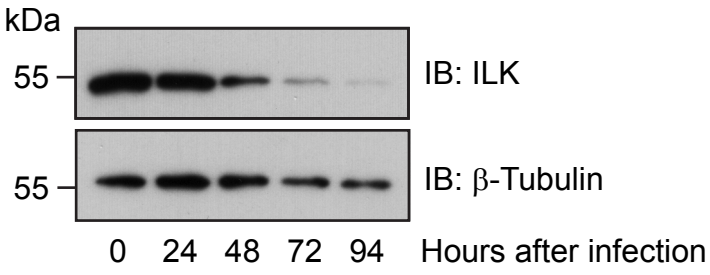
kDa
55
IB: ILK
55
IB: β-Tubulin
0 24 48 72 94
Hours after infection

B

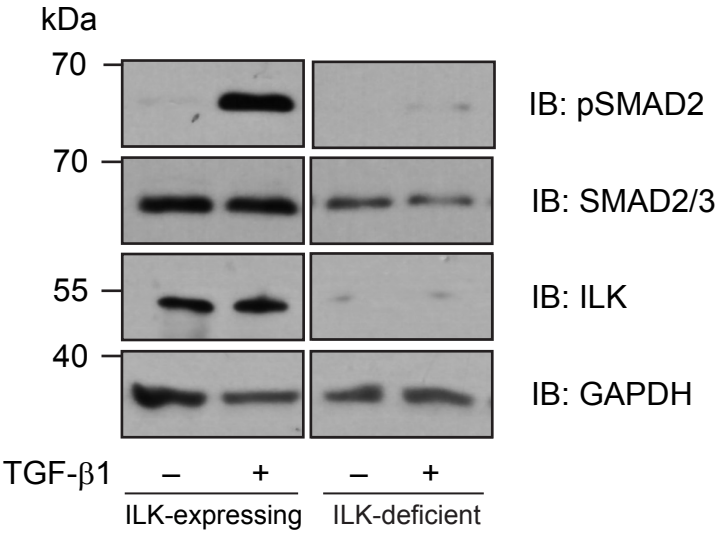
kDa
70
IB: pSMAD2
70
IB: SMAD2/3
55
IB: ILK
40
IB: GAPDH
TGF-β1 – + – +
ILK-expressing
ILK-deficient

hour. I observed that the level of pSMAD2 increased with TGF-β1 stimulation in ILK-expressing cells. In contrast, substantially lower levels of pSMAD2 were observed following TGF-β1 stimulation in ILK-deficient cells (Figure 3.10 A). Significantly, cells deficient in endogenous ILK, but expressing exogenous human ILK showed fully restored levels of pSMAD2 in response to TGF-β1 treatment (Figure 3.10 A, B). This confirms my findings that ILK is essential for normal TβR signalling in primary dermal fibroblasts and that ILK deficiency is directly linked to abnormal TGF-β1 signal transduction. Notably, fibroblasts that express both endogenous and exogenous ILK show somewhat lower levels of pSMAD2 in response to TGF-β1 stimulation (Figure 3.10 A, B). This suggests that optimal ILK levels may be necessary for normal TβR signalling in these cells.

3.6 Ilk gene inactivation results in abnormal TβR signalling in keratinocytes

Given that ILK-TβRII colocalization was observed in keratinocytes (Figure 3.5), I sought to determine whether ILK-deficient keratinocytes display abnormal responses to TGF-β1, similar to ILK-deficient fibroblasts. To address this question, $Ilk^{f/f}$ keratinocytes were infected with Ad-Cre or Ad-βgal. Experiments were conducted 3 days after infection because in these cells, ILK levels decrease by ≥ 90 % over a period of three days (Nakrieko et al. 2008a), and the viability of ILK-deficient keratinocytes decreases 4 days after infection with Ad-Cre. The cells were incubated in serum-free medium, and then treated with TGF-β1 or vehicle for 1 hour. Non-infected, ILK-expressing keratinocytes show significantly higher levels of pSMAD2 with TGF-β1 stimulation, compared to ILK-

Figure 3. 10. Effect of *Ilk* gene inactivation on responses to TGF-β1 stimulation in dermal fibroblasts

(A) Fourty-eight hours after primary $Ilk^{f/f}$ dermal fibroblasts were infected with Ad-Cre (ILK-deficient) or Ad-βgal (ILK-expressing) at an MOI of 150, the cells were infected again with recombinant adenoviruses encoding V5-tagged human ILK (Ad-hILK) or Ad-βgal at an MOI of 150. Ninety-four hours after the first infection, cells were incubated in serum-free HyQ-DMEM-RS for 4 hours, and then treated with TGF-β1 (10 ng/ml) or H_2O (vehicle) for 1 hour. The cells were lysed, and the lysates (50 μg protein/sample) were processed for immunoblotting using antibodies against pSMAD2, SMAD2/3, ILK, and GAPDH, which was used to normalize for protein loading. The arrow indicates exogenously expressed V5-tagged wild-type human ILK, and the arrowhead indicates endogenous wild-type mouse ILK. (B) Densitometric measurements were conducted to quantify the relative abundance of pSMAD2 levels, which were normalized to the total SMAD2/3 levels. The results are expressed as the mean + SEM. The asterisks indicate $p<0.05$ (ANOVA, Newman-Keuls post-hoc test, n = 4).

A

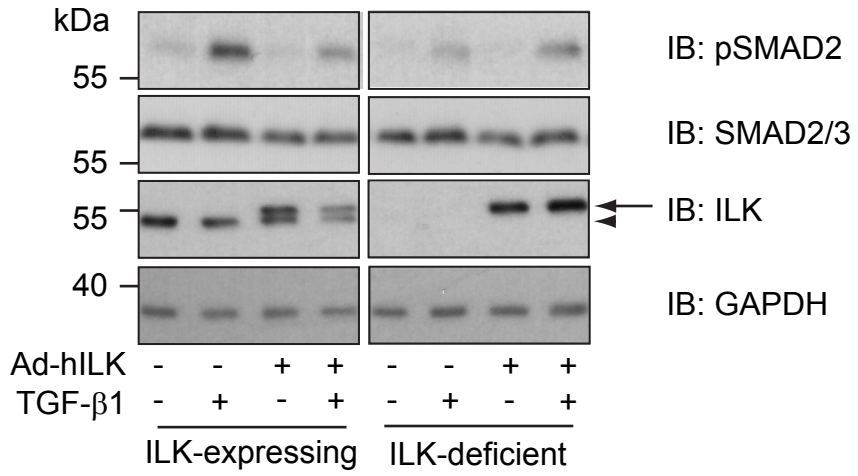
kDa
55
55
55
40
IB: pSMAD2
IB: SMAD2/3
IB: ILK
IB: GAPDH
Ad-hILK - - + + - - + +
TGF-β1 - + - + - + - +
ILK-expressing
ILK-deficient

B

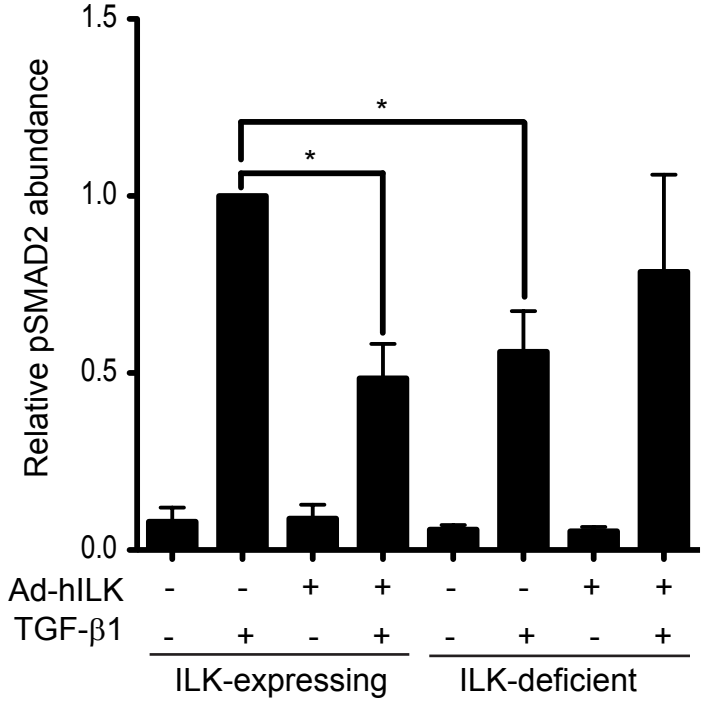
Relative pSMAD2 abundance
1.5
1.0
0.5
0.0
*
*
Ad-hILK - - + + - - + +
TGF-β1 - + - + - + - +
ILK-expressing
ILK-deficient

deficient cells (Figure 3.11 A, B). The levels of pSMAD2 in ILK-deficient cells treated with TGF-β1 are also significantly lower those in Ad-βgal-infected cells treated with TGF-β1 (Figure 3.11 A, B). Thus, ILK-deficient keratinocytes display abnormal TβR signalling, similar to ILK-deficient fibroblasts, and ILK appears to play a crucial role in modulating TβR signalling in cultured keratinocytes, as well as in fibroblasts.

3.7 Inhibition of lipid-raft formation results in restoration of TβR signalling in ILK-deficient fibroblasts

Given that ILK-deficient fibroblasts display abnormal TβR signalling, we had previously assessed if TβR levels are altered in ILK-deficient fibroblasts, and we observed that steady-state levels of TβRII, but not TβRI, are decreased in the absence of ILK (Appendix A; L Vi, S Boo & L Dagnino, unpublished data). We further determined that the decrease in TβRII levels was associated with increased TβRII ubiquitination, suggesting increased proteasomal degradation of TβRII in ILK-deficient dermal fibroblasts (Appendix B; L Vi, S Boo & L Dagnino, unpublished data). Thus, we used MG132, a proteasomal inhibitor, to determine whether inhibition of TβRII proteasomal degradation could restore the abnormal responses to TGF-β1 stimulation in ILK-deficient fibroblasts. For these experiments, primary dermal fibroblasts were infected with Ad-βgal or Ad-Cre. Four days after infection, cells were treated with MG132 or vehicle, and then treated with TGF-β1. We observed that ILK-deficient fibroblasts displayed lower levels of pSMAD2 compared to ILK-expressing cells, when treated with TGF-β1 (Appendix C). More importantly, MG132-treated ILK-deficient fibroblasts displayed similar levels of pSMAD2 to TGF-β1-treated, ILK-expressing fibroblasts (Appendix C). This suggests

Figure 3. 11. Effects of *Ilk* gene inactivation on TβR signalling in epidermal keratinocytes

(A) Primary epidermal keratinocytes were infected with Ad-Cre (ILK-deficient) at MOI of 20, or with Ad-βgal (ILK-expressing) at MOI of 5. Seventy-two hours after infection, the cells were incubated in serum-and Ca^{2+}-free EMEM for 4 hours at 37°C, and then treated with TGF-β1 (10 ng/ml) or H_2O (vehicle) for 1 hour. Lysates were prepared (50 μg protein/sample) and processed for immunoblotting using antibodies against pSMAD2, SMAD2/3, ILK, and γ-tubulin, which was used to normalize for protein loading. (B) Densitometric measurements were conducted to quantify the relative abundance of pSMAD2 levels, which were normalized to the total SMAD2/3 levels. The results are expressed as mean + SEM. The asterisks indicate $p<0.05$ (ANOVA, Newman-Keuls post-hoc test, $n = 4$).

A

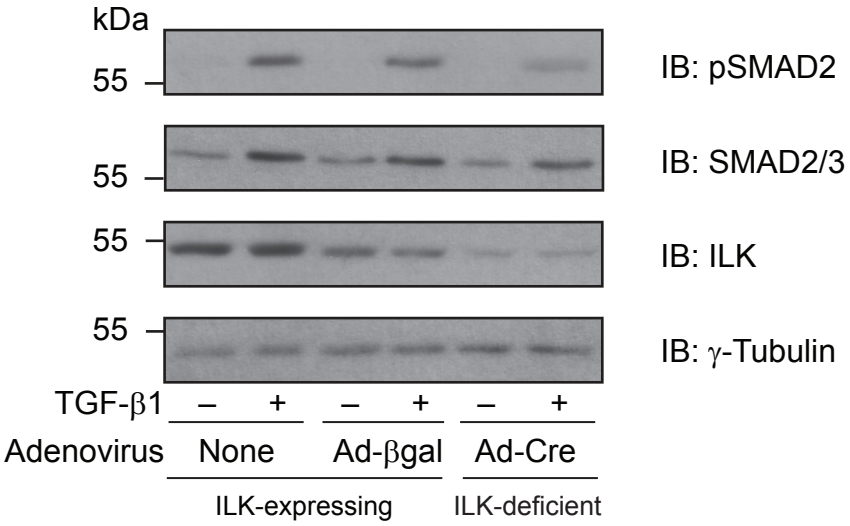
kDa
55
55
55
55
IB: pSMAD2
IB: SMAD2/3
IB: ILK
IB: γ-Tubulin
TGF-β1 – + – + – +
Adenovirus None Ad-βgal Ad-Cre
ILK-expressing
ILK-deficient

B

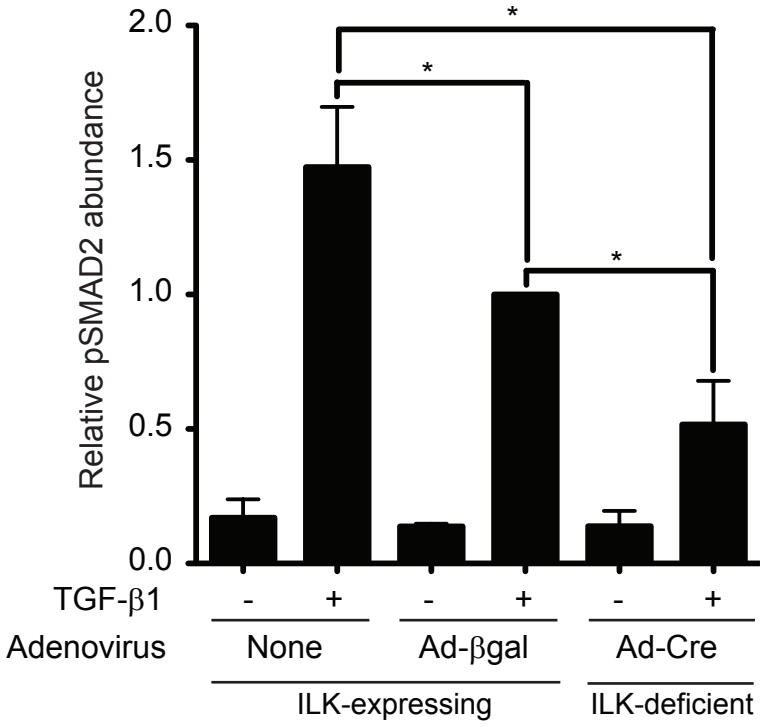
Relative pSMAD2 abundance
2.0
1.5
1.0
0.5
0.0
*
*
*
TGF-β1 - + - + - +
Adenovirus None Ad-βgal Ad-Cre
ILK-expressing
ILK-deficient

that, by inhibiting proteasomal degradation of TβRII, the TGF-β signalling pathway was restored in ILK-deficient fibroblasts. To further validate this finding, I examined the effects of nystatin on TβR signalling in ILK-deficient fibroblasts. Nystatin is a cholesterol sequestering agent that inhibits the formation of lipid-rafts, which are important for formation of caveolin-positive vesicles (Figure 1.3). TGF-β receptor complexes in caveolin-positive vesicles are ubiquitinated and targeted for proteasomal degradation. By inhibiting formation of lipid rafts, subsequent proteasomal degradation of receptor complexes is hindered (Di Guglielmo et al. 2003).

Thus, I generated ILK-expressing and ILK-deficient cells by adenoviral infection with Ad-βgal and Ad-Cre, as described above. These cultures were then treated with nystatin or vehicle in serum-free medium for 4 hours. TGF-β1 or vehicle was then added to the growth medium, and cells were incubated for 1 additional hour. ILK-expressing fibroblasts showed increased pSMAD2 levels with TGF-β1 stimulation, and these levels were not affected by nystatin treatment (Figure 3.12 A, B). As previously observed, ILK-deficient fibroblasts displayed lower levels of pSMAD2 when treated with TGF-β1 (Figure 3.12 A). In contrast, when ILK-deficient cells were treated with nystatin and TGF-β1, there was a marked increase in pSMAD2 levels (Figure 3.12 A, B). Thus, abnormal TβR signalling in ILK-deficient fibroblasts is also restored with nystatin treatment, possibly through inhibition of TβR delivery to caveolin-positive vesicles. The effects of nystatin treatment in ILK-deficient fibroblasts were similar to those observed in our previous experiment using MG132 (Appendix C). These results show that inhibition of TβRII degradation pathways, either by interfering with formation of lipid-

Figure 3. 12. Effects of nystatin treatment in ILK-deficient dermal fibroblasts

(A) Ninety-four hours after primary dermal fibroblasts were infected with Ad-Cre (ILK-deficient) or Ad-βgal (ILK-expressing) at an MOI of 150, cells were incubated in serum-free HyQ-DMEM-RS supplemented with nystatin (50 μg/ml) or DMSO (vehicle) for 4 hours at 37°C, and then treated with TGF-β1 (10 ng/ml) or H_2O (vehicle) for 1 hour. The cells were lysed, and the lysates were processed for immunoblotting using antibodies against pSMAD2, SMAD2/3, ILK, and GAPDH, which was used to normalize for protein loading. (B) Densitometric measurements were conducted to quantify the relative abundance of pSMAD2, which was normalized to the total SMAD2/3 levels. The results are expressed as mean + SEM. The asterisk indicates $p<0.05$ (ANOVA, Newman-Keuls post-hoc test, $n = 5$).

A

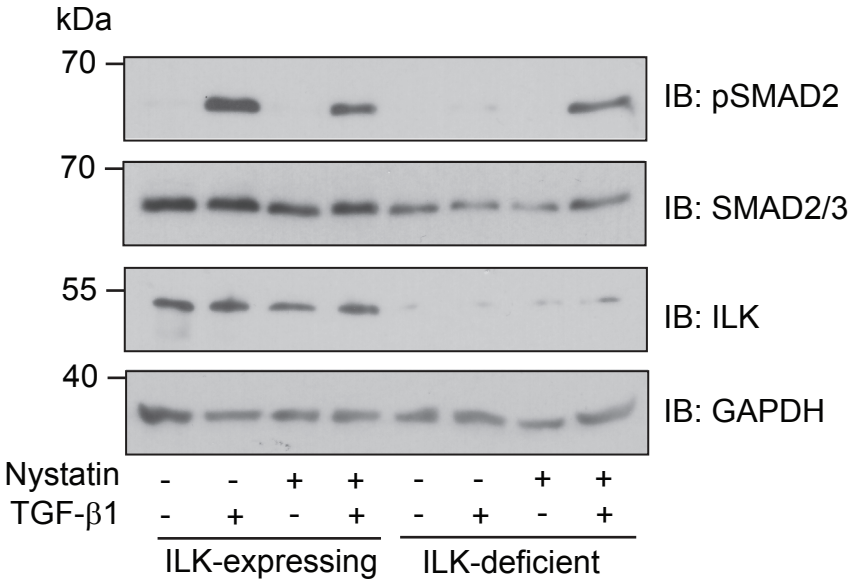
kDa
70
70
55
40
IB: pSMAD2
IB: SMAD2/3
IB: ILK
IB: GAPDH
Nystatin - - + + - - + +
TGF-β1 - + - + - + - +
ILK-expressing
ILK-deficient

B

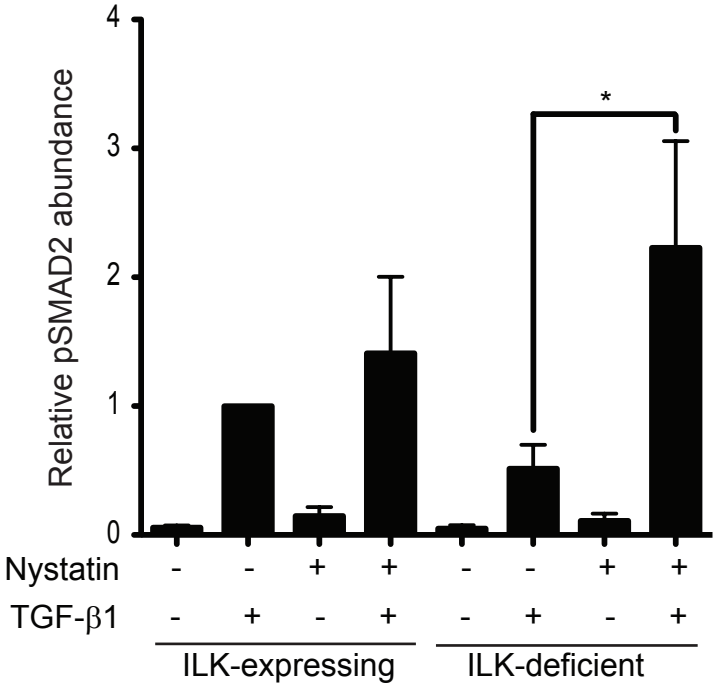
Relative pSMAD2 abundance
0
1
2
3
4
*
Nystatin - - + + - - + +
TGF-β1 - + - + - + - +
ILK-expressing
ILK-deficient

rafts or by preventing proteasomal degradation of TβRII, can restore impaired TβR signalling associated with loss of ILK.

Chapter 4 – Discussion

4.1 Summary and general discussion

Myofibroblast differentiation requires normal TβR signalling as well as mechanotransduction from ECM signals (reviewed in Hinz 2010). We have previously shown that ILK, a scaffolding protein, plays an important role in TβR signalling and in myofibroblast differentiation (Vi et al. 2011), as well as in transduction of integrin signalling (Vi et al. 2011, reviewed in Wickström et al. 2010a). I have elucidated a possible mechanism of action for ILK in modulating TβR signalling.

4.1.1 Interaction between ILK and TβRII

As a scaffold protein, ILK interacts with various proteins associated with the actin cytoskeleton and with focal adhesion proteins to transduce ECM signals (Wu & Dedhar 2001, reviewed in Qin & Wu 2012). I showed that ILK and TβRII associate in primary dermal fibroblasts and in IMDF cells, which constitute a novel interaction for these two proteins. ILK and TβRII colocalize in some intracellular vesicles, and also at the cell membrane. The interaction between ILK and TβRII does not require TGF-β1 stimulation or the kinase function of either TβRI or TβRII.

My mapping experiments show that ILK E359K interacts with TβRII. ILK E359K is a mutant with impaired ability to bind several focal adhesion proteins, such as α-parvin, β-parvin, and paxillin. As a result, this mutant also fails to localize to focal adhesions. The

observation that this mutant can be found in association with TβRII demonstrates that the interaction of ILK and TβRII does not likely occur with focal adhesion involvement, and does not require the presence of paxillin, parvins, or PINCH. Consistent with this proposal, I observed ILK, but not TβRII, immunoreactivity in structures that appeared to be mature focal adhesions, suggesting that the ILK pools involved in focal adhesion assembly and/or function are different from those that associate with TβRII. Additional experiments are needed to confirm this proposal.

A deletion mutant containing only the intracellular domain of TβRII associates with ILK, which indicates that the extracellular domain of TβRII is dispensable for this interaction. Interestingly, a mutant TβRII protein lacking most of the cytoplasmic domain (TβRII 1-199) also interacts with ILK. This suggests that there may be an intermediate protein with a transmembrane domain that interacts with both ILK and the extracellular domain of TβRII, serving as a linker between these two proteins.

4.1.2 Modulatory role of ILK in TβR signalling

Previously, our laboratory showed that ILK-deficient dermal fibroblasts exhibit attenuated responses to stimulation by TGF-β1 (Vi et al. 2011). We now show that this effect is directly linked to loss of ILK expression, since expression of exogenous human ILK into ILK-deficient mouse dermal fibroblasts result in restoration of pSMAD2 levels in response to TGF-β1. It is interesting to note that human ILK, which only differs by two amino acids from mouse ILK, was able to restore TβR signalling in ILK-deficient mouse dermal fibroblast. However, cells expressing both endogenous ILK and exogenous

human ILK show statistically significantly lower levels of TGF-β1-induced pSMAD2 levels. This signifies that an optimal level of ILK may be required for normal cell signalling, a phenomenon often observed with other scaffolding proteins (Witzel et al. 2012).

The disruption of ILK-TβRII complexes by *Ilk* gene inactivation diminishes TβR signalling in the context of generation of pSMAD2. However, the significance of the ILK-TβRII interaction needs to be further explored, since this approach does not address the possibility that ILK may also modulate TβR signalling by mechanisms independent of its ability to form complexes with this receptor. To this end, ILK-TβRII interaction must be disrupted without changing the levels of ILK and TβRII, and then any changes in TβR signalling must be studied. This may be achieved by identifying and expressing an ILK mutant that is unable to interact with TβRII. An alternate approach would be to determine the specific site required for the interaction between ILK and TβRII, and then designing a small molecule inhibitor to abrogate their interaction.

My observations that *Ilk* gene inactivation resulted in reduced pSMAD2 levels and decreased myofibroblast differentiation in response to TGF-β1 are consistent with previous findings by others (Vi et al. 2011, Blumbach et al. 2010). However, Blumbach et al. also showed that exogenous TGF-β1 restored myofibroblast differentiation in cultured ILK-deficient fibroblasts generated from a different mouse strain, as demonstrated by increased pSMAD2 and α-SMA levels in ILK-deficient fibroblasts treated with this cytokine (Blumbach et al. 2010). These seemingly contrasting results may be explained by the different methods used to create ILK-deficient fibroblasts. In my

study, primary dermal fibroblasts were isolated from 3-day-old *Ilk*$^{f/f}$ mice. The fibroblasts were cultured and an acute loss of ILK was induced by adenoviral infection. However, in the study by Blumbach et al., transgenic mice with floxed *Ilk* gene were crossed with mice with tamoxifen-regulated Cre recombinase expressed under the control of the collagen I promoter, which regulates transcription specifically in fibroblasts. Cre-mediated recombination was induced in 12-day-old mice by tamoxifen administration for 5 days and the primary dermal fibroblasts were isolated after tamoxifen induction. Thus, fibroblast-restricted *Ilk* gene inactivation *in vivo* may have created a more chronic condition, where compensatory mechanisms may be triggered in order to maintain homeostasis (Blumbach et al. 2010). To summarize, there are a few differences that may explain the different observations between the two studies: the strain of mice, the age of mice when sacrificed for fibroblast isolation, and the method of *Ilk* gene inactivation.

4.1.2.1 Modulatory role of ILK in TβRII degradation and trafficking

ILK-deficient dermal fibroblasts display abnormal responses to TGF-β1, likely due, at least in part, to decreased steady-state levels of TβRII and increased ubiquitination and degradation of TβRII (Appendix A, B; L Vi, S Boo & L Dagnino, unpublished data). This decrease in TβRII level was abrogated by proteasomal inhibition, which also restored pSMAD2 levels in ILK-deficient fibroblasts stimulated with TGF-β1 (Appendix C; L Vi, S Boo & L Dagnino, unpublished data). I also observed that disruption of lipid-raft formation with nystatin, which is necessary to direct TβRII towards the degradation pathway, also resulted in restoration of pSMAD2 levels in TGF-β1-treated ILK-deficient fibroblasts. Thus, loss of *Ilk* expression results in increased ubiquitination and

degradation of TβRII. This suggests the possibility that ILK may play a role in modulation of TβRII trafficking. Only a few proteins have been identified to interact with TβRs and regulate TGF-β signalling. For example, as described in chapter 1, SARA interacts with SMAD2 and TβR complexes to promote SMAD2 phosphorylation and TβR signalling (Tsukazaki et al. 1998), and the interaction between SMAD7 and TβRI leads to inhibition of TβR signalling *via* abrogation of SMAD2/SMAD4 complex formation (Hayashi et al. 1997). More recently, disintegrin and metalloproteinase 12 (ADAM12) has been identified as a binding partner for TβRII, and this interaction promotes clathrin-dependent TβR signalling and inhibits TβRII degradation (Atfi et al. 2007). Discs large homolog 5 (DLG5) has been also shown to interact with TβRI and TβRII, promoting proteasomal degradation of TβRI (Sezaki et al. 2013). The identification of an interaction between ILK and TβRII and the role ILK plays in promoting TβR signalling is novel and an important step to elucidate the mechanisms involved in TβR signalling and, possibly, trafficking.

The notion that ILK participates in plasma membrane organization and trafficking has been presented previously. In ILK-expressing mice, caveolin-1 is observed in basal keratinocytes, along the basal aspect of the plasma membrane (Wickström et al. 2010b). However, ILK-deficient mice showed caveolin-1 expression in basal and suprabasal keratinocytes and caveolin-1 showed cytoplasmic distribution, rather than exclusive association with the basal aspect of the plasma membrane (Wickström et al. 2010b). The abnormal caveolin-1 distribution in ILK-deficient keratinocytes is caused by microtubule instability, suggesting that ILK promotes microtubule stability and modulates

internalization by caveolae (Wickström et al. 2010b). Furthermore, ILK-deficient endothelial cells showed impaired caveolin-1 dynamics and abnormal distribution of caveolin-1 within the cell due to disturbed organization of microtubules and actin filaments, demonstrating the modulatory role of ILK in the process of endocytosis and trafficking (Malan et al. 2013). These studies show that ILK promotes caveolae-mediated endocytosis in keratinocytes and endothelial cells. This is different from the model I have proposed based on my observations, that ILK either promotes clathrin-mediated endocytosis of TβR and/or negatively regulates caveolae-mediated endocytosis in dermal fibroblasts (Figure 4.1). Given that different systems were used to conduct these experiments, it is plausible that ILK may play a different role in dermal fibroblasts, compared to keratinocytes or endothelial cells, and that ILK promotes clathrin-mediated TβR signalling and myofibroblast differentiation by negatively regulating TβR internalization *via* caveolae.

4.2 Significance

TGF-β1 signalling pathway is one of the fundamental signalling pathways involved in many biological and pathological processes, including wound healing and cancer progression. TβR signalling leads to different outcomes, depending on the cell type. For example, TGF-β1 causes attenuation of cell proliferation in epidermal keratinocytes, but proliferation and differentiation of dermal fibroblasts (Matsumoto et al. 1990, Pietenpol et al. 1990, reviewed in Hinz 2007). This pathway has been implicated in pathogenesis of various disorders, such as fibrosis, impaired wound healing, and cancer, and thus, better

Figure 4. 1. Model of TβR signalling modulation by ILK

ILK-deficient dermal fibroblasts show increased degradation of TβR, suggesting that ILK may play a role in modulation of TβRII trafficking. ILK may promote clathrin-mediated endocytosis of TβRII and TβR signalling and negatively regulate caveolae-mediated endocytosis of TβRII and degradation of TβRs.

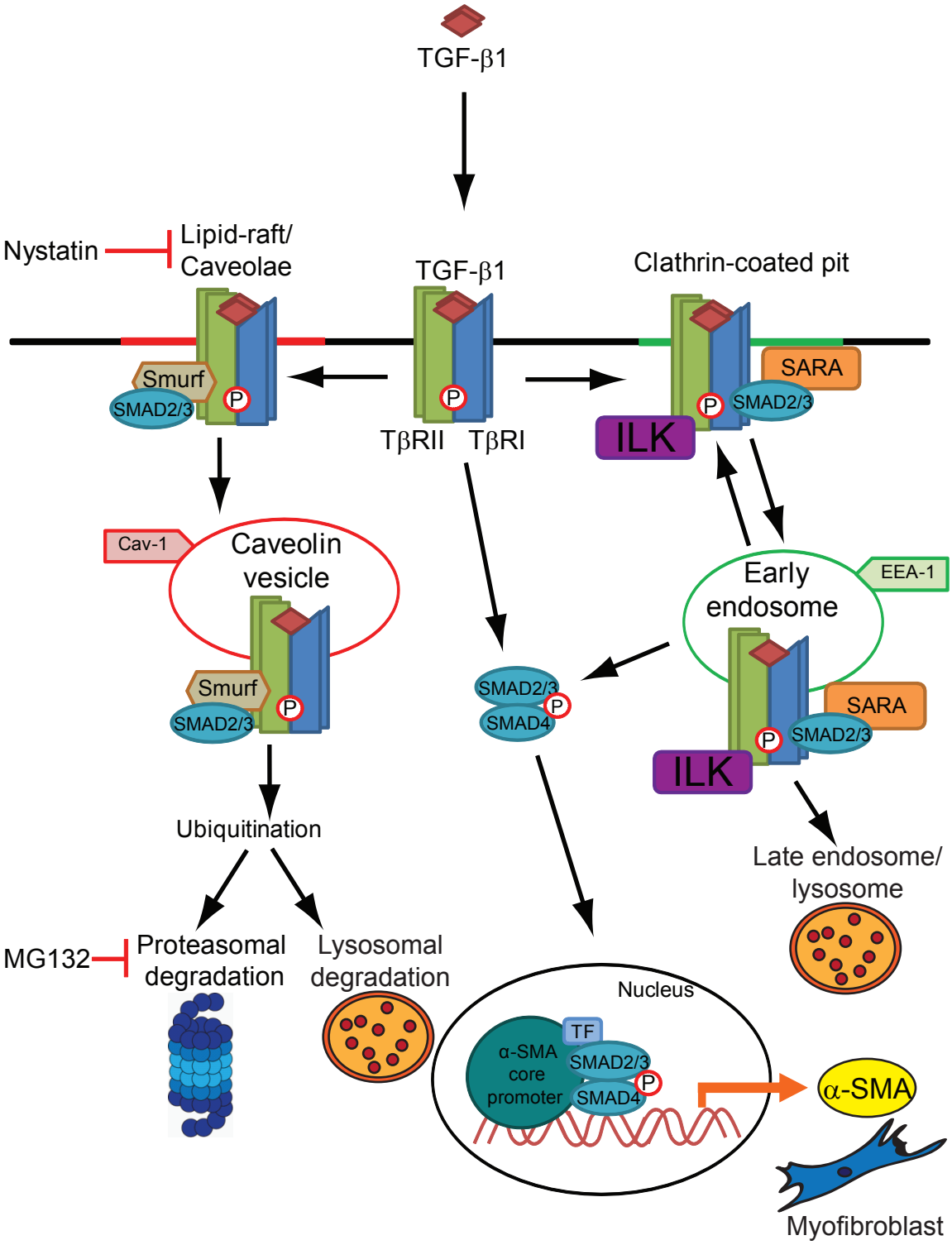
TGF-β1
Nystatin
Lipid-raft/
Caveolae
TGF-β1
Clathrin-coated pit
Smurf
SMAD2/3
P
TβRII
TβRI
SARA
ILK
Cav-1
Caveolin
vesicle
Early
endosome
EEA-1
SMAD4
Ubiquitination
Late endosome/
lysosome
MG132
Proteasomal
degradation
Lysosomal
degradation
Nucleus
TF
α-SMA
core
promoter
α-SMA
Myofibroblast

understanding of the signalling events associated with TβR stimulation would be beneficial for developing therapies to treat a variety of disorders.

There exist many levels of cross modulation of different pathways involved in fibrosis, wound healing, and oncogenesis. Based on findings from our laboratory and others, ILK seems to be a common downstream effector of the TβR signalling pathway and integrin-mediated pathways, and thus ILK could potentially be an effective therapeutic target for incomplete wound healing, excessive scar formation, and/or cancer.

The previously unappreciated role of ILK in modulating TβR signalling I have demonstrated in dermal fibroblasts and epidermal keratinocytes opens doors to potential therapies targeting ILK to modulate TβR signalling in skin diseases with aberrant TβR signalling.

My findings can have potential implications in the treatment of fibrosis, excess scar tissue formation, and cancer biology. High levels of ILK expression and TβR signalling have been implicated in the progression of various fibrotic disorders (reviewed in McDonald et al. 2008). Unfortunately, current treatments for excessive skin scarring are not fully effective or in early phases of clinical trials (reviewed in Tziotzios et al. 2012). Recent potential therapies that show promising preliminary results involve attenuation of TβR signalling by inhibiting TGF-β1 and/or TGF-β2, or by treatment with avotermin (human recombinant TGF-β3), which has been shown to reduce scar tissue formation (reviewed in Tziotzios et al. 2012, So et al. 2011). TGF-β also plays various roles in cancer progression (reviewed in Massagué 2008). Some clinical studies for treating cancer involve targeting the TGF-β pathway, and include approaches for inhibition of TGF-β

production, and the use of anti-TGF-β antibodies and small-molecule inhibitors of TβRs (reviewed in Massagué 2008). Thus, ILK, which also modulates TβR signalling, may be a therapeutic target for treating abnormal wound healing disorders or cancers associated with aberrant responses to TGF-β.

4.3 Future directions

My work and the work of others (Vi et al. 2011, Blumbach et al. 2010) show that ILK deficiency results in abrogation of TβR signalling. However, it has yet to be determined if TβR trafficking is regulated by ILK. Thus, a comparison of TβR distribution and internalization in ILK-expressing and ILK-deficient fibroblasts using endocytic markers, such as EEA-1, for early endosome, and Cav-1, for caveolae, would help elucidate the role ILK may play on TβR trafficking. I also showed that ILK-TβRII colocalization occurs in intracellular vesicles. However, the exact nature of these vesicles remains to be determined. Thus, trafficking experiments using biotinylated TGF-β1 and markers of signalling and degradatory pathway could be conducted to reveal the internalization pathway of ILK-TβRII complexes as a function of time. The process of endocytosis, sorting of receptor complexes, and recycling or degradation can occur in as little as 10 minutes (Maxfield & McGraw 2004). Thus, it would be interesting to see the distribution of ILK and TβRII in cells treated with TGF-β1 for a shorter period of time than I used in my experiments. The use of markers for early endosomes, late endosomes, recycling endosomes, and caveolae would also be useful in determining where ILK-TβRII complexes reside at different times after TGF-β1 stimulation.

In my experiments showing colocalization between ILK and TβRII, I noted ILK, but not TβRII, in what appeared to be mature focal adhesions. Using antibodies against vinculin or paxillin, focal adhesions can be identified, and this would help in determining whether ILK proteins participating in focal adhesion-mediated signalling are distinct from ILK proteins modulating TβR pathway.

Finally, the interaction between ILK and TβRII on TβR signalling needs to be further analysed. Using bacterially-produced ILK and TβRII, it can be determined whether the interaction between these proteins is direct or indirect. Finding a mutant ILK that is unable to interact with TβRII would be important in determining the significance of this interaction on TβR signalling. By introducing this mutant in ILK-deficient fibroblasts, it can be determined whether ILK-TβRII interaction is crucial in promoting TβR signalling, or if expression of ILK is sufficient for mediating TβR signalling. Alternatively, a mutant TβRII that is unable to interact with ILK can be expressed in TβRII-deficient fibroblasts, and then the TβR signalling can be studied. A small molecular inhibitor, which impedes ILK-TβRII interaction, may also be used.

References

Apostolova MD, Ivanova IA, Dagnino C, D'Souza SJ & Dagnino L (2002). Active nuclear import and export pathways regulate E2F-5 subcellular localization. *J Biol Chem* **277**, 344471-344479.

Asano Y, Ihn H, Yamane K, Jinnin M & Tamaki K (2006a). Increased expression of integrin alphavbeta5 induces the myofibroblastic differentiation of dermal fibroblasts. *Am J Pathol* **168**, 499-510.

Asano Y, Ihn H, Jinnin M, Mimura Y & Tamaki K (2006b). Involvement of alphavbeta5 integrin in the establishment of autocrine TGF-beta signaling in dermal fibroblasts derived from localized scleroderma. *J Invest Dermatol* **126**, 1761-1769.

Ashcroft GS, Yang X, Glick AB, Weinstein M, Letterio JL, Mizel DE, Anzano M, Greenwell-Wild T, Wahl SM, Deng C & Roberts AB (1999). Mice lacking Smad3 show accelerated wound healing and an impaired local inflammatory response. *Nat Cell Biol* **1**, 260-266.

Atfi A, Dumont E, Colland F, Bonnier D, L'helgoualc'h A, Prunier C, Ferrand N, Clement B, Wewer UM & Theret N (2007). The disintegrin and metalloproteinase ADAM12 contributes to TGF-beta signaling through interaction with the type II receptor. *J Cell Biol* **178**, 201-208.

Bierie B & Moses HL (2006). Tumour microenvironment: TGFbeta: the molecular Jekyll and Hyde of cancer. *Nat Rev Cancer* **6**, 506-520.

Blumbach K, Zweers MC, Brunner G, Peters AS, Schmitz M, Schulz JN, Schild A, Denton CP, Sakai T, Fässler R, Krieg T & Eckes B (2010). Defective granulation tissue formation in mice with specific ablation of integrin-linked kinase in fibroblasts – role of TGFβ1 levels and RhoA activity. *J Cell Sci* **123**, 3872-3883.

Boudeau J, Miranda-Saavedra D, Barton GJ & Alessi DR (2006). Emerging roles of pseudokinases. *Trends Cell Biol* **16**, 443-452.

Brakebusch C, Grose R, Quondamatteo F, Ramirez A, Jorcano JL, Pirro A, Svensson M, Herken R, Sakai T, Timpl R, Werner S & Fässler R (2000). Skin and hair follicle integrity is crucially dependent on β1 integrin expression on keratinocytes. *EMBO J* **19**, 3990-4003.

Breuss JM, Gallo J, DeLisser HM, Klimanskaya IV, Folkesson HG, Pittet JF, Nishimura SL, Aldape K, Landers DV, Carpenter W, Gillett N, Sheppard D, Matthay MA, Albelda SM, Kramer RH & Pytela R (1995). Expression of the β6 integrin subunit in development, neoplasia and tissue repair suggests a role in epithelial remodelling. *J Cell Sci* **108**, 2241-2251.

Carracedo S, Lu N, Popova SN, Jonsson R, Eckes B & Gullberg D (2010). The fibroblast integrin alpha11beta1 is induced in a mechanosensitive manner involving activin A and regulates myofibroblast differentiation. *J Biol Chem* **285**, 10434-10445.

Chin GS, Liu W, Peled Z, Lee TY, Steinbrech DS, Hsu M & Longaker MT (2000). Differential expression of transforming growth factor-β receptors I and II and activation of Smad 3 in keloid fibroblasts. *Plast Reconstr Surg* **108**, 423-429.

Chiswell BP, Zhang R, Murphy JW, Boggon TJ & Calderwood DA (2008). The structural basis of integrin-linked kinase-PINCH interactions. *Proc Natl Acad Sci U S A* **105**, 20677-20682.

Choma DP, Milano V, Pumiglia KM & DiPersio CM (2007). Integrin α3β1-dependent activation of FAK/Src regulates Rac1-mediated keratinocyte polarization on laminin-5. *J Invest Dermatol* **127**, 31-40.

Chu H, Thievessen I, Sixt M, Lammermann T, Waisman A, Braun A, Noegel AA & Fässler R (2006). Gamma-Parvin is dispensable for hematopoiesis, leukocyte trafficking, and T-cell-dependent antibody response. *Mol Cell Biol* **26**, 1817-1825.

Dagnino L, Ho E & Chang WY (2010). Expression and analysis of exogenous proteins in epidermal cells. *Methods Mol Biol* **585**, 93-105.

Deng JT, Sutherland C, Brautigan DL, Eto M & Walsh MP (2002). Phosphorylation of the myosin phosphatase inhibitors, CPI-17 and PHI-1, by integrin-linked kinase. *Biochem J* **367**, 517-524.

Desmoulière A, Geinoz A, Gabbiani F & Gabbiani G (1993). Transforming growth factor-beta 1 induces alpha-smooth muscle actin expression in granulation tissue myofibroblasts and in quiescent and growing cultured fibroblasts. *J Cell Biol* **122**, 103-111.

Desmoulière A, Chaponnier C & Gabbiani G (2005). Tissue repair, contraction, and the myofibroblasts. *Wound Repair Regen* **13**, 7-12.

Dünker N & Krieglstein K (2000). Targeted mutations of transforming growth factor-β genes reveal important roles in mouse development and adult homeostasis. *Eur J Biochem* **267**, 6982-6988.

Edlund S, Bu S, Schuster N, Aspenstrom P, Heuchel R, Heldin NE, ten Dijke P, Helding CH & Landstrom M (2003). Transforming growth factor-beta1 (TGF-beta)-induced apoptosis of prostate cancer cells involves Smad7-dependent activation of p38 by TGF-beta-activated kinase 1 and mitogen-activated protein kinase kinase 3. *Mol Biol Cell* **14**, 529-544.

Ehrlich M, Shmuely A & Henis YI (2001). A single internalization signal from the di-leucine family is critical for constitutive endocytosis of the type II TGF-beta receptor. *J Cell Sci* **114**, 1777-1786.

Eswaran J, Patnaik D, Filippakopoulos P, Wang F, Stein RL, Murray JW, Higgins JM & Knapp S (2009). Structure and functional characterization of the atypical human kinase haspin. *Proc Natl Acad Sci U S A* **106**, 20198-20203.

Flanders KC, Sullivan CD, Fujii M, Sowers A, Anzano MA, Arabshahi A, Major C, Deng C, Russo A, Mitchell JB & Roberts AB (2002). Mice lacking Smad3 are protected against cutaneous injury induced by ionizing radiation. *Am J Pathol* **160**, 1057-1068.

Flanders KC (2004). Smad3 as a mediator of the fibrotic response. *Int J Exp Pathol* **85**, 47-64.

Fukuda K, Gupta S, Chen K, Wu C & Qin J (2009). The pseudokinase site of ILK is essential for its binding to alpha-Parvin and localization to focal adhesions. *Mol Cell* **36**, 819-830.

Fukuda K, Knight JD, Piszczek G, Kothary R & Qin J (2011). Biochemical, proteomic, structural, and thermodynamic characterizations of integrin-linked kinase (ILK): cross-validation of the pseudokinase. *J Biol Chem* **286**, 21886-21895.

Gailit J, Welch MP & Clark RA (1994). TGF-beta 1 stimulates expression of keratinocyte integrins during re-epithelialization of cutaneous wounds. *J Invest Dermatol* **103**, 221-227.

Geiger B, Spatz JP & Bershadsky AD (2009). Environmental sensing through focal adhesions. *Nat Rev Mol Cell Biol* **10**, 21-33.

Gilboa L, Wells RG, Lodish HF & Henis YI (1998). Oligomeric structure of type I and type II transforming growth factor beta receptors: homodimers form in the ER and persist at the plasma membrane. *J Cell Biol* **140**, 767-777.

Grashoff C, Aszodi A, Sakai T, Hunziker EB & Fässler R (2003). Integrin-linked kinase regulates chondrocyte shape and proliferation. *EMBO Rep* **4**, 432-438.

Grose R, Hutter C, Bloch W, Thorey I, Watt FM, Fässler R, Brakebusch C & Werner S (2002). A crucial role of beta 1 integrins for keratinocyte migration in vitro and during cutaneous wound repair. *Development* **129**, 2303-2315.

Hannigan GE, Leung-Hagesteijn C, Fitz-Gibbon L, Coppolino MG, Radeva G, Filmus J, Bell jC & Dedhar S (1996). Regulation of cell adhesion and anchorage-dependent growth by a new beta 1-integrin-linked protein kinase. *Nature* **379**, 91-96.

Hayashi H, Abdollah S, Qiu Y, Cai J, Xu YY, Grinnel BW, Richardson MA, Topper JN, Gimbrone MA Jr., Wrana JL & Falb D (1997). The MAD-related protein Smad7 associates with the TGFbeta receptor and functions as an antagonist of TGFbeta signaling. *Cell* **89**, 1165-1173.

He W, Cao T, Smith DA, Myers TE & Wang XJ (2001). Smads mediate signaling of the TGFbeta superfamily in normal keratinocytes but are lost during skin chemical carcinogenesis. *Oncogene* **20**, 471-483.

He W, Li AG, Wang D, Han S, Zheng B, Goumans MJ, ten Dijke P & Wang XJ (2002). Overexpression of Smad7 results in severe pathological alterations in multiple epithelial tissues. *EMBO J* **21**, 2580-2590.

Henis YI, Moustakas A, Lin HY & Lodish HF (1994). The types II and III transforming growth factor-beta receptors form homo-oligomers. *J Cell Biol* **126**,, 139-154.

Hinz B (2007). Formation and function of the myofibroblast during tissue repair. *J Invest Dermatol* **127**, 526-537.

Hinz B (2010). The myofibroblast: paradigm for a mechanically active cell. *J Biomech* **43**, 146-155.

Ho E, Irvine T, Vilk GJ, Lajoie G, Ravichandran KS, D'Souza SJ & Dagnino L (2009). Integrin-linked kinase interactions with ELMO2 modulate cell polarity. *Mol Biol Cell* **20**, 3033-3043.

Ho E & Dagnino L (2012). Epidermal growth factor induction of front-rear polarity and migration in keratinocytes is mediated by integrin-linked kinase and ELMO2. *Mol Biol Cell* **23**, 492-502.

Ito Y, Sarkar P, Mi Q, Wu N, Bringas P Jr, Liu Y, Reddy S, Maxson R, Deng C & Chai Y (2001). Overexpression of Smad2 reveals its concerted action with Smad4 in regulating TGF-beta-mediated epidermal homeostasis. *Dev Biol* **236**, 181-194.

Kavsak P, Rasmussen RK, Causing CG, Bonni S, Zhu H, Thomsen GH & Wrana JL (2000). Smad7 binds to Smurf2 to form an E3 ubiquitin ligase that targets the TGF beta receptor for degradation. *Mol Cell* **6**, 1365-1376.

Lange A, Wickström SA, Jakobson M, Zent R, Sainio K & Fässler R (2009). Integrin-linked kinase is an adaptor with essential functions during mouse development. *Nature* **461**, 1002-1006.

Le Roy C & Wrana JL (2005). Clathrin- and non-clathrin-mediated endocytic regulation of cell signalling. *Nat Rev Mol Cell Biol* **6**, 112-126.

Levy L & Hill CS (2005). Smad4 dependency defines two classes of transforming growth factor {beta} (TGF-{beta}) target genes and distinguishes TGF-{beta}-induced epithelial-mesenchymal transition from its antiproliferative and migratory responses. *Mol Cell Biol*, **25**, 8108-8125.

Li F, Zhang Y & Wu C (1999). Integrin-linked kinase is localized to cell-matrix focal adhesions but not cell-cell adhesion sites and the focal adhesion localization of integrin-linked kinase is regulated by the PINCH-binding ANK repeats. *J Cell Sci* **112**, 4589-4599.

Liu S, Kapoor M, Denton CP, Abraham DJ & Leask A (2009). Loss of beta1 integrin in mouse fibroblasts results in resistance to skin scleroderma in a mouse model. *Arthritis Rheum* **60**, 2817-2821.

Liu S, Xu SW, Blumbach K, Eastwood M, Denton CP, Eckes B, Krieg T, Abraham DJ & Leask A (2010). Expression of integrin beta1 by fibroblasts is required for tissue repair in vivo. *J Cell Sci* **123**, 3674-3682.

Liu S & Leask A (2013). Integrin β1 is required for dermal homeostasis. *J Invest Dermatol* **133**, 899-906.

Liu X, Wen FQ, Kobayashi T, Abe S, Fang Q, Piek E, Bottinger EP, Roberts AB & Rennard SI (2003). Smad3 mediates the TGF-beta-induced contraction of type I collagen gels by mouse embryo fibroblasts. *Cell Motil Cytoskeleton* **54**, 248, 253.

Lopez-Casillas F, Wrana JL & Massagué J (1993). Betaglycan presents ligand to the TGF beta signaling recepteor. *Cell* **73**, 1435-1444.

Lorenz K, Grashoff C, Torka R, Sakai T, Langbein L, Bloch W, Aumailley M & Fässler R (2007). Integrin-linked kinase is required for epidermal and hair follicle morphogenesis. *J Cell Biol* **177**, 501-513.

Mackinnon AC, Qadota H, Norman KR, Moerman DG & Williams BD (2002). C. elegans PAT-4/ILK functions as an adaptor protein withint integrin adhesion complexes. *Curr Biol* **12**, 787-797.

Malan D, Elischer A, Hesse M, Wickström SA, Fleischmann BK & Bloch W (2013). Deletion of integrin linked kinase in endothelial cells results in defective RTK signaling caused by caveolin1 mislocalization. *Development* **140**, 987-995.

Margadant C & Sonnenberg A (2010). Integrin-TGF-beta crosstalk in fibrosis, cancer and wound healing. *EMBO Rep* **11**, 97-105.

Margadant C, Charafeddine RA & Sonnenberg A (2010). Unique and redundant functions of integrins in the epidermis. *FASEB J* **24**, 4133-4152.

Martin P (1997). Wound healing—aiming for perfect skin regeneration. *Science* **276**, 75-81.

Martinez-Ferrer M, Afshar-Sherif AR, Uwamariya C, de Crombrugghe B, Davidson JM & Bhowmick NA (2010). Dermal transforming growth factor-beta responsiveness mediates wound contraction and epithelial closure. *Am J Pathol* **176**, 98-107.

Massagué J (2008). TGFbeta in cancer. *Cell* **134**, 215-230.

Matsumoto K, Hashimoto K, Hashiro M, Yoshimasa H & Yoshikawa K (1990). Modulation of growth and differentiation in normal human keratinocytes by transforming growth factor-beta. *J Cell Physiol* **145**, 95-101.

Maxfield FR & McGraw TE (2004). Endocytic recycling. *Nat Rev Mol Cell Biol* **5**, 121-132.

Maydan M, McDonald PC, Sanghera J, Yan J, Rallis C, Pinchin S, Hannigan GE, Foster LJ, Ish-Horowicz D, Walsh MP & Dedhar S (2010). Integrin-linked kinase is functional Mn2+-dependent protein kinase that regulates glycogen synthase kinase-3β (GSK-3beta) phosphorylation. *PLoS One* **5**, e12356.

McDonald PC, Fielding AB & Dedhar S (2008). Integrin-linked kinase—essential roles in physiology and cancer biology. *J Cell Sci* **121**, 3121-3132.

Mitchell H, Choudhury A, Pagano RE & Leof EB (2004). Ligand-dependent and –independent transforming growth factor-beta receptor recycling regulated by clathrin-mediated endocytosis and Rab11. *Mol Biol Cell* **15**, 4166-4178.

Miyazono K, Olofsson A, Colosetti P & Heldin CH (1991). A role of the latent TGF-beta-1-binding protein in the assembly and secretion of TGF-beta 1. *EMBO J* **10**, 1091-1101.

Miyazono K, ten Dijke P & Heldin CH (2000). TGF-beta signaling by Smad proteins. *Adv Immunol* **75**, 115-157.

Mu D, Cambier S, Fjellbirkeland L, Baron JL, Münger JS, Kawakatsu H, Sheppard D, Broaddus VC & Nishimura SL (2002). The integrin alpha(v)beta8 mediates epithelial homeostasis through MT1-MMP-dependent activation of TGF-beta1. *J Cell Biol* **157**, 493-507.

Mucsi I, Skorecki KL & Goldberg HJ (1996). Extracellular signal-regulated kinase and the small GTP-binding protein, Rac, contribute to the effects of transforming growth factor-beta1 on gene expression. *J Biol Chem* **271**, 16567-16572.

Mukherjee K, Sharma M, Urlaub H, Bourenkov GP, Jahn R, Sudhof TC & Wahl MC (2008). CASK functions as a MG2+-independent neurexin kinase. *Cell* **133**, 328-339.

Münger JS, Harpel JG, Giancotti FG & Rifkin DB (1998). Interactions between growth factors and integrins: latent forms of transforming growth factor-beta are ligands for the integrin alphavbeta1. *Mol Biol Cell* **9**, 2627-2638.

Münger JS, Huang X, Kawakatsu H, Griffiths MJD, Dalton SL, Wu J, Pittet JF, Kaminski N, Garat C, Matthay MA, Rifkin DB & Sheppard D (1999). The integrin alpha v beta 6 binds and activates latent TGF beta 1: a mechanism for regulating pulmonary inflammation and fibrosis. *Cell* **96**, 319-328.

Nakrieko KA, Welch I, Dupuis H, Bryce D, Pajak A, St Arnaud R, Dedhar S, D'Souza SJ & Dagnino L (2008a). Impaired hair follicle morphogenesis and polarized keratinocyte movement upon conditional inactivation of integrin-linked kinase in the epidermis. *Mol Biol Cell* **19**, 1462-1473.

Nakrieko KA, Vespa A, Mason D, Irvine TS, D'Souza SJ & Dagnino L (2008b). Modulation of integrin-linked kinase nucleo-cytoplasmic shuttling by ILKAP and CRM1. *Cell Cycle* **7**, 2157-2166.

Nakrieko KA, Rudkouskaya A, Irvine TS, D'Souza SJ & Dagnino L (2011). Targeted inactivation of integrin-linked kinase in hair follicle stem cells reveals an important modulatory role in skin repair after injury. *Mol Biol Cell* **22**, 2532-2540.

Nikolopoulos SN & Turner CE (2002). Molecular dissection of actopaxin-integrin-linked kinase-Paxillin interactions and their role in subcellular localization. *J Biol Chem* **277**, 1568-1575.

Owens DM, Romero MR, Gardner C & Watt FM (2003). Suprabasal alpha6beta4 integrin expression in epidermis results in enhanced tumourigenesis and disruption of TGFbeta signalling. *J Cell Sci* **116**, 3783-3791.

Persad S, Attwell S, Gray V, Mawji N, Deng JT, Leung D, Yan J, Sanghera J, Walsh MP & Dedhar S (2001). Regulation of protein kinase B/Akt-serine 473 phosphorylation by integrin-linked kinase: critical roles for kinase activity and aino acids arginine 211 and serine 343. *J Biol Chem* **276**, 27462-27469.

Pietenpol JA, Hold JT, Stein RW & Moses HL (1990). Transforming growth factor beta 1 suppression of c-myc gene transcription: role in inhibition of keratinocyte proliferation. *Proc Natl Acad Sci U S A* **87**, 3758-3762.

Pircher E, Jullien P & Lawrence DA (1986). Beta-transforming growth factor is stored in human blood platelets as a latent high molecular weight complex. *Biochem Biophys Res Commun* **136**, 30-37.

Prud'homme GJ & Piccirillo CA (2000). The inhibitory effects of transforming growth factor-beta-1 (TGF-beta1) in autoimmune diseases. *J Autoimmun* **14**, 23-42.

Qiao W, Li AG, Owens P, Xu X, Wang XJ & Deng CX (2006). Hair forllicle defects and squamous cell carcinoma formation in Smad4 conditional knockout mouse skin. *Oncogene* **25**, 207-217.

Qin J & Wu C (2012). ILK: a pseudokinase in the center stage of cell-matrix adhesion and signaling. *Curr Opin Cell Biol* **24**, 607-613.

Raghavan S, Bauer C, Mundschau G, Li Q & Fuchs E (2000). Conditional ablation of beta1 integrin in skin. Severe defects in epidermal proliferation, basement membrane formation, and hair follicle invagiation. *J Cell Biol* **150**, 1149-1160.

Rechtman MM, Nakaryakov A, Shapira KE, Ehrlich M & Henis YI (2009). Different domains regulate homomeric and heteromeric complex formation among type I and type II transforming growth factor-beta receptors. *J Biol Chem* **284**, 7843-7852.

Reynolds LE, Conti FJ, Lucas M, Grose R, Robinson S, Stone M, Saunders G, Dickson C, Hynes RO, Lacy-Hulbert A & Hodivala-Dilke K (2005). Accelerated re-epithelialization in beta3-integrin-deficient-mice is associated with enhanced TGF-beta1 signaling. *Nat Med* **11**, 167-174.

Reynolds LE, Conti FJ, Silva R, Robinson SD, Iyer V, Rudling R, Cross B, Nye E, Hart IR, Dipersio CM & Hodivala-Dilke KM (2008). Alpha3beta1 integrin-controlled Smad7 regulates reepithelialization during wound healing in mice. *J Clin Invest* **118**, 965-974.

Runyan CE, Schnaper HW & Poncelet AC (2005). The role of internalization in transforming growth factor beta1-induced Smad2 association with Smad anchor for receptor activation (SARA) and Smad2-dependent signaling in human mesangial cells. *J Biol Chem* **280**, 8300-8308.

Sakai T, Li S, Docheva D, Grashoff C, Sakai K, Kostka G, Braun A, Pfeifer A, Yurchenco PD & Fässler R (2003) Integrin-linked kinase (ILK) is required for polarizing the epiblast, cell adhesion, and controlling actin accumulation. *Genes Dev* **17**, 926-940.

Schindelin J, Arganda-Carreras I, Frise E, Kaynig V, Longair M, Pietzsch T, Preibisch S, Rueden C, Saalfeld S, Schmid B, Tinevez JY, White DJ, Hartenstein V, Eliceiri K, Tomancak P & Cardona A (2012). Fiji: an open-source platform for biological-image analysis. *Nat Methods* **9**, 676-682.

Sezaki T, Tomiyama L, Kimura Y, Ueda K & Kioka N (2013). Dlg5 interacts with the TGF-β receptor and promotes its degradation. *FEBS Lett* **587**, 1624-1629.

Shi Y & Massagué J (2003). Mechanisms of TGF-beta signalling from cell membrane to the nucleus. *Cell* **113**, 685-700.

Silver FH, Siperko LM & Seehra GP (2003). Mechanobiology of force transduction in dermal tissue. *Skin Res Technol* **9**, 3-23.

Simmons K & Toomre D (2000). Lipid rafts and signal transduction. *Nat Rev Mol Cell Biol* **1**, 31-39.

Singer AJ & Clark RA (1999). Cutaneous wound healing. *N Engl J Med* **341**, 738-746.

Sirard C, de la Pompa JL, Elia A, Itie A, Mirtosos C, Cheung A, Hahn S, Wakeham A, Schwartz L, Kern SE, Rossant J & Mak TW (1998). The tumor suppressor gene Smad4/Dpc4 is required for gastrulation and later for anterior development of the mouse embryo. *Genes Dev* **12**, 107-119.

So K, McGrouther DA, Bush JA, Durani P, Taylor L, Skotny G, Mason T, Metcalfe A, O'kane S & Ferguson MW (2011). Avotermin for scar improvement following scar revision surgery: a randomized, double-blind, within-patient, placebo-controlled, phase II clinical trial. *Plast Reconstr Surg* **128**, 163-172.

Sumiyoshi K, Nakao A, Setoguchi Y, Okumura K, Tsuboi R & Ogawa H (2003). Smads regulate collagen gel contraction by human dermal fibroblasts. *Br J Dermatol* **149**, 464-470.

Terpstra L, Prud'homme J, Arabian A, Takeda S, Karsenty G, Dedhar S & St Arnaud R (2003). Reduced chondrocyte proliferation and chondrodysplasia in mice lacking the integrin-linked kinase in chondrocytes. *J Cell Biol* **162**, 139-148.

Tomasek JJ, Gabbiani G, Hinz B, Chaponnier C & Brown RA (2002). Myofibroblasts and mechano-regulation of connective tissue remodeling. *Nat Rev Mol Cell Biol* **3**, 349-363.

Tredget EE (1999). Pathophysiology and treatment of fibroproliferative disorders following thermal injury. *Ann N Y Acad Sci* **888**, 165-182.

Tsukazaki T, Chiang TA, Davison AF, Attisano L & Wrana JL (1998). SARA, a FYVE domain protein that recruits Smad2 to the TGFbeta receptor. *Cell* **95**, 779-791.

Tu Y, Li F, Goicoechea S & Wu C (1999). The LIM-only protein PINCH directly interacts with integrin-linked kinase and is recruited to integrin-rich sites in spreading cells. *Mol Cell Biol* **19**, 2425-2434.

Tu Y, Huang Y, Zhang Y, Hua Y & Wu C (2001). A new focal adhesion protein that interacts with integrin-linked kinase and regulates cell adhesion and spreading. *J Cell Biol* **153**, 585-598.

Tuan TL & Nichter LS (1998). The molecular basis of keloid and hypertrophic scar formation. *Mol Med Today* **4**, 19-24.

Tziotzios C, Profyris C & Sterling J (2012). Cutaneous scarring: Pathophysiology, molecular mechanisms, and scar reduction therapeutics Part II. Strategies to reduce scar formation after dermatologic procedures. *J Am Acad Dermatol* **66**, 13-24.

Vespa A, Darmon AJ, Turner CE, D'Souza SJ & Dagnino L (2003). Ca^{2+}-dependent localization of integrin-linked kinase to cell junctions in differentiating keratinocytes. *J Biol Chem* **278**, 11528-115235.

Vespa A, D'Souza SJ & Dagnino L (2005). A novel role for integrin-linked kinase in epithelial sheet morphogenesis. *Mol Biol Cell* **16**, 4084-4095.

Vi L, de Lasa C, DiGuglielmo GM & Dagnino L (2011). Integrin-linked kinase is required for TGF-β1 induction of dermal myofibroblast differentiation. *J Invest Dermatol* **131**, 586-593.

Wahl SM (1994). Transforming growth factor beta: the good, the bad, and the ugly. *J Exp Med* **180**, 1587-1590.

Watt FM (2002). Role of integrins in regulating epidermal adhesion, growth and differentiation. *EMBO J* **21**, 3919-3926.

Wickström SA, Lang A, Montanex E & Fässler R (2010a). The ILK/PINCH/parvin complex: the kinase is dead, long live the pseudokinase! *EMBO J* **29**, 281-291.

Wickström SA, Lange A, Hess MW, Polleux J, Spatz JP, Pfaller K, Lambacher A, Bloch W, Mann M, Huber LA & Fässler R (2010b). Integrin-linked kinase controls microtubule dynamics required for plasma membrane targeting of caveolae. *Dev Cell* **19**, 574-588.

Witzel F, Maddison L & Bluthgen N (2012). How scaffolds shape MAPK signaling: what we know and opportunities for systems approaches. *Front Physiol* **3**, 475

Wrana JL, Attisano L, Wieser R, Ventura F & Massagué J (1994). Mechanism of activation of the TGF-beta receptor. *Nature* **370**, 341-347.

Wu C & Dedhar S (2001). Integrin-linked kinase (ILK) and its interactors: a new paradigm for the coupling of extracellular matrix to actin cytoskeleton and signaling complexes. *J Cell Biol* **155**, 505-510.

Yamaji S, Suzuki A, Sugiyama Y, Koide Y, Yoshida M, Kanamori H, Mohri H, Ohno S & Ishigatsubo Y (2001). A novel integrin-linked kinase-binding protein, affixin, is involved in the early stage of cell-substrate interaction. *J Cell Biol* **153**, 1251-1264.

Yang L, Mao C, Teng Y, Li W, Zhang J, Cheng X, Li X, Han X, Xia Z, Deng H & Yang X (2005). Targeted disruption of Smad4 in mouse epidermis results in failure of hair follicle cycling and formation of skin tumors. *Cancer Res* **65**, 8671-8678.

Yang L, Li W, Wang S, Wang L, Li Y, Yang X & Peng R (2012). Smad4 disruption accelerates keratinocyte reepithelialisation in murine cutaneous wound repair. *Histochem Cell Biol* **138**, 573-582.

Yang X, Letterio JJ, Lechleider RJ, Chen L, Hayman R, Gu H, Roberts AB & Deng D (1999). Targeted disruption of SMAD3 results in impaired mucosal immunity and diminished T cell responsiveness to TGF-beta. *EMBO J* **18**, 1280-1291.

Yang X, Chen L, Xu X, Li C, Huang C & Deng CX (2001). TGF-beta/Smad3 signals repress chondrocyte hypertrophic differentiation and are required for maintaining articular cartilage. *J Cell Biol* **153**, 35-46.

Yang Z, Mu Z, Dabovic B, Jurukovski V, Yu D, Sung J, Xiong X & Münger JS (2007). Absence of integrin-mediated TGFbeta1 activation in vivo recapitulates the phenotype of TGFbeta1-null mice. *J Cell Biol* **176**, 787-793.

Yeung YG & Stanley ER (2009). A solution for stripping antibodies from polyvinylidene fluoride immunoblots for multiple reprobing. *Anal Biochem* **389**, 89-91.

Yu H, Bock O, Bayat A, Ferguson MW & Mrowietz U (2006). Decreased expression of inhibitory SMAD6 and SMAD7 in keloid scarring. *J Plast Reconstr Aesthet Surg* **59**, 221-229.

Yu L, Hebert MC & Zhang YE (2002). TGF-beta receptor-activated p38 MAP kinase mediates Smad-independent TGF-beta responses. *EMBO J* **21**, 3749-3759.

Yu Q & Stamenkovic I (2000). Cell surface-localized matrix metalloproteinase-9 proteolytically activates TGF-beta and promotes tumor invasion and angiogenesis. *Genes Dev* **14**, 163-176.

Zambruno G, Marchisio PC, Marconi A, Vaschieri C, Melchiori A, Giannetti A & De Luca M (1995). Transforming growth factor-beta 1 modulates beta 1 and beta 5 integrin receptors and induces de novo expression of the alpha v beta 6 heterodimer in normal human keratinocytes: implications for wound healing. *J Cell Biol* **129**, 853-865.

Zervas CG, Gregory SL & Brown NH (2001). Drosophila integrin-linked kinase is required at sites of integrin adhesion to link the cytoskeleton to the plasma membrane. *J Cell Biol* **152**, 1007-1018.

Appendices

Appendix A: ILK deficiency results in decreased levels of TβRII but not TβRI

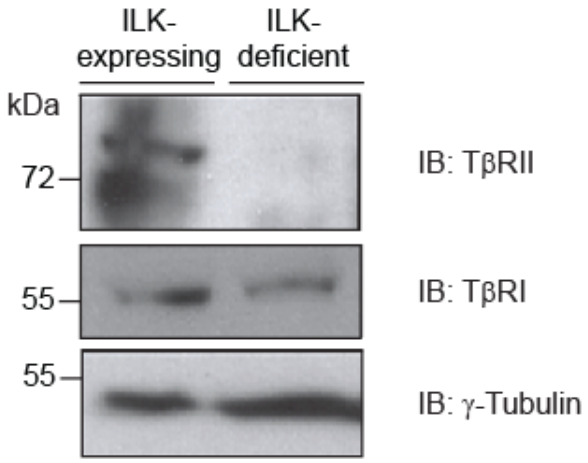

Primary *Ilk*$^{f/f}$ dermal fibroblasts were infected with Ad-Cre (ILK-deficient) or Ad-βgal (ILK-expressing) at a MOI of 150. Four days after infection, lysates were prepared (100 μg protein/sample) and processed for immunoblotting, using antibodies against TβRII, TβRI, and γ-tubulin, which was used to normalize for protein loading. The level of TβRI is comparable in ILK-expressing and ILK-deficient cells, but the level of TβRII is reduced in ILK-deficient fibroblasts compared to ILK-expressing fibroblasts.

Appendix B: ILK deficiency results in increased ubiquitination of TβRII

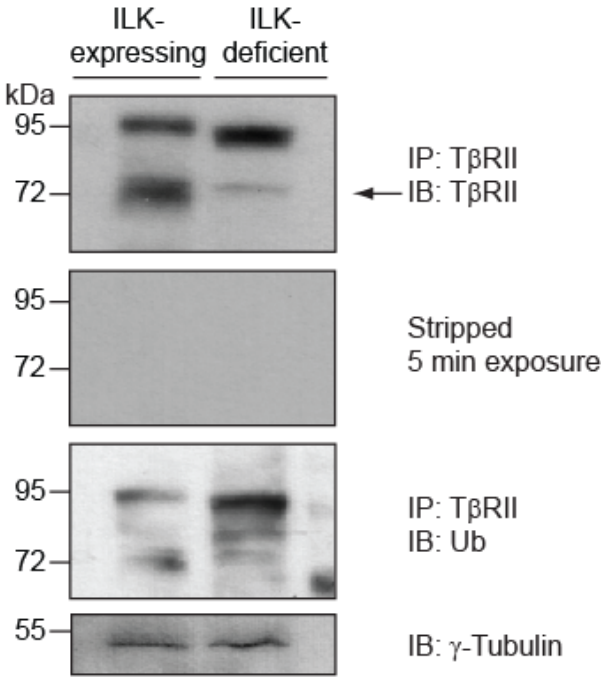

Primary dermal fibroblasts were infected with Ad-Cre (ILK-deficient) or Ad-βgal (ILK-expressing). Lysates (2 mg protein/sample) were prepared and subjected to immunoprecipitation with antibodies against TβRII or unrelated rabbit IgG, as control, followed by immunoblotting with TβRII or ubiquitin (Ub). In parallel, samples of lysates (20 μg protein/sample) were resolved by SDS-PAGE and transferred to a membrane, which was probed with antibodies against γ-tubulin, which was used to normalize for protein loading. The results shown are representative of experiments repeated 3 times. The level of TβRI is comparable in ILK-expressing and ILK-deficient cells, but the level of TβRII is reduced in ILK-deficient fibroblasts compared to ILK-expressing fibroblasts.

Appendix C: MG132 treatment restores pSMAD2 levels upon TGF-β1 stimulation

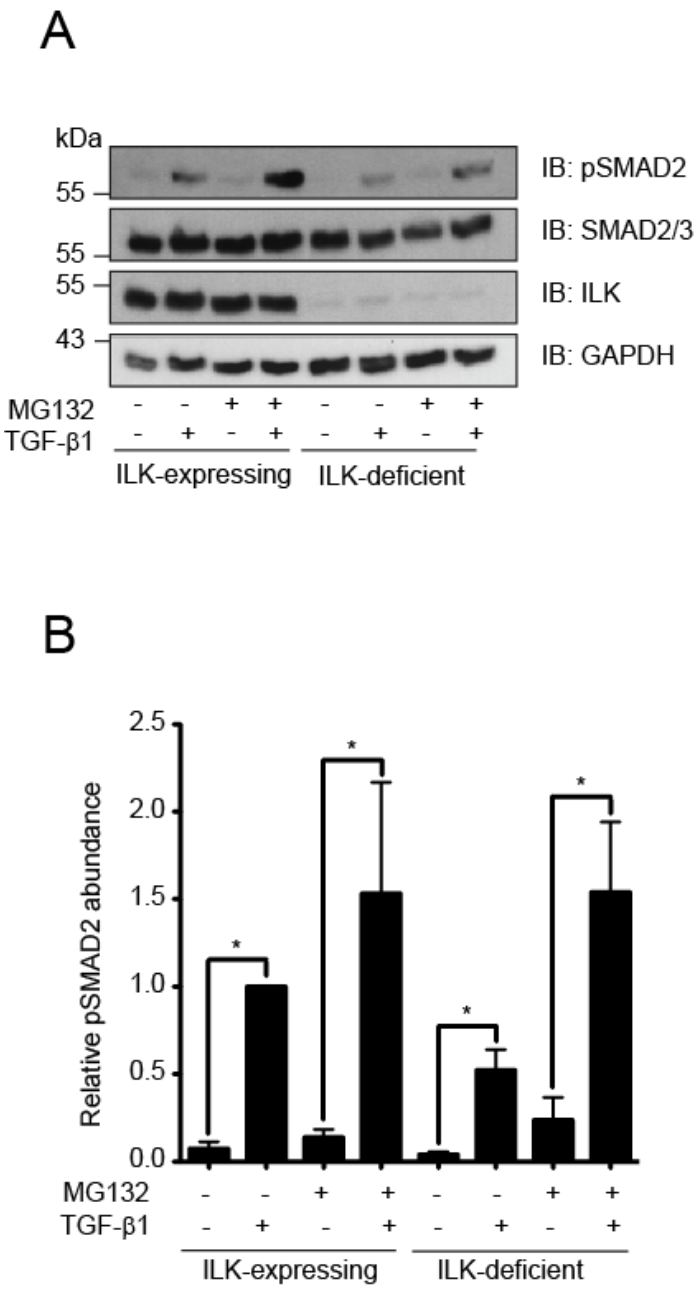

(A) Four days after primary dermal fibroblasts were infected with Ad-Cre (ILK-deficient) or Ad-βgal (ILK-expressing), they were incubated in serum-free media supplemented with 0.1% FBS, 0.05% bovine serum albumin with MG132 (10 μM, final) or DMSO

(vehicle) for 8 hours and then treated with TGF-β1 or vehicle for 1 hour. Cells were lysed and processed for immunoblotting using antibodies against indicated proteins. GAPDH was used as a loading control. The level of pSMAD2 is reduced in ILK-deficient fibroblasts compared to ILK-expressing fibroblasts and this decrease is restored by MG132 treatment. (B) Densitometry of four experiments was conducted to quantify the relative abundance of pSMAD2 levels, which were normalized to the SMAD2/3 levels. Results are expressed as mean + SEM. Asterisk indicates significant difference ($p<0.05$, ANOVA, Newman-Keuls post-hoc test). There is a decrease in the level of pSMAD2 in ILK-deficient fibroblasts compared to ILK-expressing fibroblasts, and this is increased with MG132 treatment. There is no significant difference in pSMAD2 levels between ILK-deficient cells treated with MG132 and ILK-expressing cells treated with vehicle.

Curriculum Vitae

Name:	Stellar Hyeeun Boo
Post-secondary Education and Degrees:	University of Western Ontario London, Ontario, Canada 2011-2013 M. Sc.
	The University of Western Ontario London, Ontario, Canada 2007-2011 B.MSc.
Honours and Awards:	Ontario Graduate Scholarship September 2012-August 2013
	Western Graduate Research Scholarship September 2012-August 2013, September 2011-August 2012
	Schulich Graduate Scholarship September 2012-August 2013, September 2011-August 2012
	Mobility, Musculoskeletal Health and Arthritis Undergraduate Research Award Canadian Institute of Health Research June 2011-August 2011
	Western Scholars Award University of Western Ontario June 2011
	Strategic Training Program in Cancer Research and Technology Transfer Undergraduate Research Scholarship Canadian Institute of Health Research May 2010-August 2010
	Dean’s Honor List University of Western Ontario 2011, 2010, 2009, 2008

The Scholar's Program Scholarship
University of Western Ontario
September 2008

Christina A. MacKerracher Admission Scholarship
University of Western Ontario
September 2007

Related Work Experience

Teaching Assistant (Physiology 3130Y)
University of Western Ontario
September 2012-April 2013, January 2012-April 2012

Undergraduate Research Student
Supervisor: Dr. Lina Dagnino
June 2011-August 2011, May 2010-August 2010

Peer-Reviewed Publications:

Boo S, Dagnino L (2013). Integrins as modulators of transforming growth factor beta signaling in dermal fibroblasts during skin regeneration after injury. Advances in Wound Care, 2(5), 238-246.

Non Peer-Reviewed Publications:

Vi L, **Boo S**, Dagnino L (2011). Integrin-linked kinase (ILK) is required for TGF- receptor type II signaling in dermal myofibroblasts. Clinical and Investigative Medicine, 34(6S), 40.

Presentations: (*denotes oral presentation)

Boo S, Vi L, Dagnino L. ILK modulates TβRII turnover and TGF-β1/Smad signalling in dermal fibroblasts. CIHR-STP CaRTT Department of Oncology Research and Education Day, June 21, 2013, London, ON, Canada

***Boo S**, Vi L, Dagnino L. ILK modulates TGF-β receptor turnover and TGF-β1/Smad signalling in dermal fibroblasts. Mostly Mammals in Montreal, March 21-23, 2013, Montreal, QC, Canada

Dagnino L, **Boo S**, Vi L. ILK modulates TβRII turnover and TGF-β1/Smad signalling in dermal fibroblasts. 51st Annual American Society for Cell Biology Meeting, December 15-19, 2012, San Francisco, CA, U.S.A.

Boo S, Vi L, Dagnino L. ILK modulates TβRII turnover and TGF-β1/Smad signalling in dermal fibroblasts. UWO Physiology Pharmacology Research Day, November 6, 2012, London, ON, Canada

***Boo S**, Vi L, Dagnino L. ILK modulates TβRII turnover and TGF-β1/Smad signalling in dermal fibroblasts. CIHR-STP CaRTT Department of Oncology Research and Education Day, June 22, 2012, London, ON, Canada

Boo S, Vi L, Dagnino L. ILK modulates TβRII turnover and TGF-β1/Smad signalling in dermal fibroblasts. Great Lakes Mammalian Development Meeting, April 12-14, 2012, Toronto, ON, Canada

Boo S, Vi L, Dagnino L. ILK modulates TβRII turnover and TGF-β1/Smad signalling in dermal fibroblasts. Lawson Research Day, March 20, 2012, London, ON, Canada

Boo S, Vi L, Dagnino L. ILK modulates TβRII turnover and TGF-β1/Smad signalling in dermal fibroblasts. UWO Physiology Pharmacology Research Day, November 8, 2011, London, ON, Canada

Vi L, **Boo S**, Dagnino L. Integrin-linked kinase is required for TGF-β receptor II signalling in dermal myofibroblasts. Canadian Society for Clinical Investigation/CIHR Young Investigator Forum, September 13, 2011, Ottawa, ON, Canada

Vi L, **Boo S**, Dagnino L. Integrin-linked kinase is required for TGF-β receptor II signalling in dermal myofibroblasts. Developmental Biology Research Day, May 31, 2011, London, ON, Canada

Vi L, **Boo S**, Dagnino L. Integrin-linked kinase is required for TGF-beta receptor II signalling. Annual Margaret Moffat Research Day, March 29, 2011, London, ON, Canada

Boo S, Vi L, Dagnino L. ILK interacts with TGF-β receptor type II to modulate TGF-β1/Smad signalling in dermal fibroblasts. Lawson Research Day, March 22, 2011, London, ON, Canada

Vi L, **Boo S**, Dagnino L. Integrin-linked kinase is required for TGF-β receptor type II stability and signalling. Great Lakes Mammalian Development Meeting, March 3-5, 2011, Toronto, ON, Canada

Boo S, Vi L, Dagnino L. ILK interacts with TGF-β receptor type II to modulate TGF-β1/Smad signalling in dermal fibroblasts. Annual Pathology and Toxicology Research Day, March 2, 2011, London, ON, Canada

Vi L, **Boo S**, Dagnino L. Integrin-linked kinase is required for TGF-beta 1 induction of dermal fibroblast differentiation to myofibroblasts. 50th Annual American Society for Cell Biology Meeting, December 11-15, 2010, Philadelphia, PA, U.S.A.